



Early Opening of Portland Cement Concrete (PCC) Pavements to Traffic

SPR# 0092-01-04

**James A. Croveti
Department of Civil and Environmental Engineering
Marquette University
Lev Khazanovich
University of Minnesota**

September 2005

WHRP 05-13

WISCONSIN HIGHWAY RESEARCH PROGRAM #0092-01-04

**EARLY OPENING OF PORTLAND CEMENT
CONCRETE (PCC) PAVEMENTS TO TRAFFIC**

FINAL REPORT

by

James Crovetti, Ph.D., Principal Investigator
Marquette University
Department of Civil & Environmental Engineering
P.O. Box 1881
Milwaukee, WI 53201-1881

Lev Khazonovich, Ph.D.
University of Minnesota
Department of Civil Engineering
500 Pillsbury Drive S.E.
Minneapolis, MN 55455

Submitted to:

WISCONSIN DEPARTMENT OF TRANSPORTATION

September 2005

DISCLAIMER

This research was funded through the Wisconsin Highway Research Program by the Wisconsin Department of Transportation and the Federal Highway Administration under Project # 0092-01-04. The contents of this report reflect the views of the authors who are responsible for the facts and the accuracy of the data presented herein. The contents do not necessarily reflect the official views of the Wisconsin Department of Transportation or the Federal Highway Administration at the time of publication.

This document is disseminated under the sponsorship of the Department of Transportation in the interest of information exchange. The United States Government assumes no liability for its contents or use thereof. This report does not constitute a standard, specification or regulation.

The United States Government does not endorse products or manufacturers. Trade and manufacturers' names appear in this report only because they are considered essential to the object of the document.

ACKNOWLEDGEMENTS

The authors greatly appreciate the support, advice, and technical contributions received from members of the WHRP Rigid Pavement Technical Oversight Committee during the conduct of this study. The authors also acknowledge the support provided by field personnel from Streu Construction Co., Zignego Company Inc. and Collins Engineers Inc. during the conduct of the field study.

Technical Report Documentation Page

1. Report No. WHRP 05-13	2. Government Accession No.	3. Recipient's Catalog No.	
4. Title and Subtitle Early Opening of Portland Cement Concrete (PCC) Pavements to Traffic		5. Report Date September 2005	6. Performing Organization Code
7. Authors James A. Croveti & Lev Khazanovich		8. Performing Organization Report No.	
9. Performing Organization Name and Address Marquette University P.O. Box 1881 Milwaukee, WI 53201-1881		10. Work Unit No. (TRAIS)	
12. Sponsoring Agency Name and Address Wisconsin Department of Transportation Division of Transportation Infrastructure Development Research Coordination Section 4802 Sheboygan Avenue Madison, WI 53707		11. Contract or Grant No. WHRP Project 0092-01-04	
13. Type of Report and Period Covered Final Report, Jun 2001 – Sep 2005		14. Sponsoring Agency Code	
15. Supplementary Notes			
16. Abstract <p>This report presents the results of a detailed stress analysis and a field and laboratory test program which investigated the early-age strength gain for selected PCC paving mixtures used in Wisconsin as well as the effects of early-age loading on doweled pavement joints. A simplified procedure for predicting critical dowel-PCC interface stresses was developed. This procedure was used in conjunction with allowable bearing stresses to establish minimum compressive strength requirements for opening to traffic based on pavement design parameters, including PCC, base, subgrade and dowel material properties. Equations for predicting early-age PCC compressive strength from 7-Day or 28-Day laboratory test results were developed based on maturity readings. The best correlation was observed for estimating the %7-Day early-age strength based on maturity readings of field-cured bagged cylinders. Exposed dowel load and deflection tests were used to investigate the effects of early-age loading on the PCC immediately surrounding the dowel. These tests proved inconclusive with no apparent trends in the data. More research in this area is needed to develop appropriate testing protocol and practical guidelines for implementation</p>			
17. Key Words PCC Pavements, Early Opening, Maturity, Dowel Bar Stress		18. Distribution Statement No restriction. This document is available to the public through the National Technical Information Service, 5285 Port Royal Road, Springfield VA 22161	
19. Security Classif. (of this report) Unclassified	19. Security Classif. (of this page) Unclassified	20. No. of Pages 85	21. Price

Form DOT F 1700.7 (8-72)

Reproduction of completed page authorized

EXECUTIVE SUMMARY

Project Summary

This research study consists of analyzing the impacts of early-age loadings on concrete pavements. Detailed stress analyses were conducted to establish relations between critical dowel-concrete bearing stresses and load placement and to develop criteria for minimum PCC strength requirements. A field study of four PCC paving projects was conducted to test the impacts of dowel loadings during early PCC strength gain. Materials sampled during paving were used to fabricate test specimens to assess the impacts of dowel loadings during periods when the compressive strength of the PCC was significantly below the minimum value currently specified in Wisconsin for opening to traffic. Correlations between various PCC strength measures and between strength and maturity readings were also developed.

Project Background

The current Wisconsin Department of Transportation (WisDOT) Standard Specifications for Highway and Structure Construction establishes the time when newly constructed Portland cement concrete (PCC) pavements may be opened to traffic based on test cylinders or minimum time periods related to atmospheric temperatures. Where test cylinders are used, minimum concrete compressive strengths of 20,700 kPa (3,000 psi) and 24,200 kPa (3,500 psi) are required prior to opening of urban and rural pavements, respectively. When the opening is not controlled by test cylinders, minimum time periods prior to opening are designated based on prevailing temperatures and may range from 7 to

21 days for traditional concrete mixes. The delay period between paving and opening to traffic can pose problems for contractors in terms of the prosecution of work and/or to business and property owners who must find alternate access routes or parking locations.

Various strategies, including the use of high early strength concrete or fast-track paving operations, have been employed to reduce the delay period between paving and minimum required strength gain. While these strategies can be effective in shortening the opening delay period, it must be remembered that increased early strength generally results in a slight reduction in the ultimate strength gain of most concrete mixtures. This strength reduction is not generally considered as detrimental to pavement performance, but in some cases may lead to a reduced fatigue life in the order of 3-5 years. An alternative strategy for reducing the opening delay period is the allowance of earlier trafficking, either unlimited or tiered, to allow more timely access to homes and businesses impacted by construction and perhaps to allow for earlier access by construction equipment.

Process

Literature was reviewed from various national sources detailing the best methods for determining critical dowel bearing stresses. Finite-element modeling of typical PCC pavement structures was completed to develop a simplified procedure for estimating dowel bearing stresses. The results of these analyses were utilized to develop relations between critical loadings and bearing stress ratios. A field study was undertaken to test the validity of the developed procedures and to provide specimens for testing composed of typical PCC paving materials. A comprehensive data analysis was conducted to develop meaningful

relations between PCC strength, maturity, and earl-age loading effects.

Findings

This report presents the results of a detailed stress analysis and a field and laboratory test program which investigated the early-age strength gain for selected PCC paving mixtures used in Wisconsin as well as the effects of early-age loading on doweled pavement joints. The study findings are summarized as:

1. An easy-to-use procedure for predicting critical dowel-PCC interface stresses may be used in conjunction with allowable bearing stresses to establish minimum compressive strength requirements for opening to traffic based on pavement design parameters, including PCC, base, subgrade and dowel material properties.
2. Specific equations for predicting early-age PCC compressive strength from 7-Day or 28-Day laboratory test results were developed for the tested Wisconsin mixtures based on maturity readings. These equations provide a practical means for establishing appropriate times for quality assurance testing. The best correlation was observed for estimating the %7-Day early-age strength based on maturity readings of field-cured bagged cylinders.
3. Comparative cylinder compressive and beam flexural strength tests were used to validate relations between these two important strength measures. These equations provide a practical means for estimating the early-age PCC flexural strength based on simple cylinder compression tests. Using data from the four Wisconsin mixtures tested at ages up to 28 days after placement, the best correlation was observed between flexural strength and compressive strength raised to the $2/3$ power.

4. Exposed dowel load and deflection tests were used to investigate the effects of early-age loading on the PCC immediately surrounding the dowel. These tests proved inconclusive with no apparent trends in the data. More research in this area is needed to develop appropriate testing protocol and practical guidelines for implementation.

Recommendations

Based on the research effort documented in this report, the following recommendations are made:

1. The minimum opening compressive strength requirement to protect against dowel-PCC bearing stresses exceeding allowable values may be readily determined based on key pavement design inputs including slab thickness, subgrade support k-value and dowel bar diameter.
2. For doweled PCC pavements using 1.25 inch dowels, the current minimum opening compressive strength of 3,000 psi appears warranted. For pavements with 1.50 inch dowels, the minimum opening compressive strength may be reduced to the range of 2,300 to 2,750 psi depending on pavement design inputs. Based on the current WisDOT specifications as detailed in Section 14-10-10 of the Facilities Development Manual, this would include all PCC pavements with a constructed thickness of 10 inches or greater.
3. Maturity readings from test cylinders, cured in the field alongside the mainline pavement, may be used to provide an indication of the strength gain of the pavement based on 7-Day or 28-Day laboratory strength measures. For practical

implementation, the 7-Day laboratory strength measure may be more appropriate to allow for test cylinders to be cast with available paving materials combined at the specified PCC mixture proportions.

TABLE OF CONTENTS

DISCLAIMER	ii
ACKNOWLEDGEMENTS	ii
TECHNICAL REPORT DOCUMENTATION PAGE	iii
EXECUTIVE SUMMARY	iv
1.0 INTRODUCTION.....	1
1.1 Background and Problem Statement.....	1
1.2 Critical PCC Stresses	2
1.2.1 Critical Loading Position	3
1.2.2 Tabatabaie-Barenberg Model	4
1.3 Modulus of Dowel Support.....	9
1.4 Load Transferred by the Dowel	16
1.4.1 Load Transfer Efficiency	17
1.4.2 Maximum Free-edge Deflection	25
1.4.3 Critical Dowel Load Verification	26
1.5 Step-by-Step Analysis Procedure	31
1.6 Early Age PCC Bearing Stresses	34
1.7 Early Opening Criteria Used by Other States	39
1.8 Summary of Dowel Bearing Stresses	39
2.0 FIELD STUDY	43
2.1 Introduction.....	43
2.2 Curing Conditions	44
2.3 Summary	52
3.0 LABORATORY STUDY.....	53
3.1 Introduction.....	53
3.2 Compression Test Results.....	53
3.2.1 <i>STH 57 - Fredonia</i>	54
3.2.2 <i>South Whitnall Avenue - Cudahy</i>	57
3.2.3 <i>STH 32 - Racine</i>	57
3.2.4 <i>STH 23 - Fond du Lac</i>	58
3.2.5 <i>Maturity Readings</i>	61
3.3 Flexural Testing	66
3.4 Exposed Dowel Specimens	69
3.4.1 <i>STH 57 - Fredonia</i>	69
3.4.2 <i>South Whitnall Avenue - Cudahy</i>	75
3.4.3 <i>STH 32 - Racine</i>	77
3.4.4 <i>STH 23 - Fond du Lac</i>	79
3.5 Summary of Laboratory Testing	81
4.0 SUMMARY AND RECOMMENDATIONS	82
REFERENCES.....	85

LIST OF FIGURES

Figure 1.2.1 ISALB200 model of a transverse joint	5
Figure 1.2.2 Bearing stresses vs load position for the right critical dowel	5
Figure 1.2.3 Bearing stresses vs load position for the left critical dowel.....	6
Figure 1.2.4 Critical load position for the left critical dowel.....	6
Figure 1.2.5 Tabatabaie and Barenberg model of doweled PCC pavements.....	7
Figure 1.2.6 Pressure exerted on a loaded dowel	7
Figure 1.3.1 Modeling of PCC-dowel interaction	12
Figure 1.3.2 2D finite element mesh of dowel/PCC interaction	12
Figure 1.3.3 2D finite element mesh of dowel/PCC interaction-fragment around dowel.....	13
Figure 1.3.4 Typical contours of vertical displacements	13
Figure 1.3.5 Typical contours of vertical displacements for a fragment around dowel ..	14
Figure 1.3.6 Modulus of Dowel support vs PCC modulus	14
Figure 1.4.1 Comparison of ISLAB200 LTE and LTE from Croveti's Equation (SAL-RWP) ...	21
Figure 1.4.2 Comparison of ISLAB200 LTE and LTE from Croveti's Equation (TAL-RWP) ...	21
Figure 1.4.3 Comparison of ISLAB200 LTE and LTE from Croveti's Equation (SAL-LWP)....	22
Figure 1.4.4 Comparison of ISLAB200 LTE and LTE from Croveti's Equation (TAL-LWP)....	22
Figure 1.4.5 Comparison of ISLAB200 LTE and LTE from modified Croveti's Equation (SAL-RWP) ..	23
Figure 1.4.6 Comparison of ISLAB200 LTE and LTE from modified Croveti's Equation (TAL-RWP) ..	23
Figure 1.4.7 Comparison of ISLAB200 LTE and LTE from modified Croveti's Equation (SAL-LWP) ..	24
Figure 1.4.8 Comparison of ISLAB200 LTE and LTE from modified Croveti's Equation (TAL-LWP) ..	24
Figure 1.4.9 Comparison of ISLAB2000 and predicted free edge deflections (SAL-RWP)	27
Figure 1.4.10 Comparison of ISLAB2000 and predicted free edge deflections (TAL-RWP) ...	27
Figure 1.4.11 Comparison of ISLAB2000 and predicted free edge deflections (SAL-LWP)....	28
Figure 1.4.12 Comparison of ISLAB2000 and predicted free edge deflections (TAL-LWP)	28
Figure 1.4.13 Total load transferred by a critical dowel (SAL-RWP)	29
Figure 1.4.14 Total load transferred by a critical dowel (TAL-RWP)	29
Figure 1.4.15 Total load transferred by a critical dowel (SAL-LWP).....	30
Figure 1.4.16 Total load transferred by a critical dowel (TAL-LWP)	30
Figure 1.6.1 Bearing stresses vs PCC strength (SAL-RWP).....	36
Figure 1.6.2 Bearing stresses vs PCC strength (SAL-LWP)	36
Figure 1.6.3 Bearing stresses vs PCC strength (TAL-RWP)	37
Figure 1.6.4 Bearing stresses vs PCC strength (TAL-LWP).....	37
Figure 1.6.5 Dowel bearing stress ratios (TAL-LWP)	38
Figure 1.6.6 Dowel bearing stress ratios (TAL-LWP)	38
Figure 2.2.1 7-Day post paving temperature profile, STH57-Fredonia	46
Figure 2.2.2 7-Day post paving temperature profile, STH57-Fredonia	46
Figure 2.2.3 7-Day post paving temperature profile, STH57-Fredonia	47
Figure 2.2.4 7-Day post paving temperature profile, STH57-Fredonia	47
Figure 2.2.5 7-Day post paving temperature profile, STH57-Fredonia	48
Figure 2.2.6 7-Day post maturity profile, STH57-Fredonia	48

LIST OF FIGURES (Cont.)

Figure 2.2.7 28-day post paving maturity plot for S Whitnall Ave-Cudahy.....	50
Figure 2.2.8 28-day post paving maturity plot for STH32-Racine.....	50
Figure 2.2.7 28-day post paving maturity plot for STH23-Fond du Lac	51
Figure 3.2.1 Comparative compressive strength results, STH57-Fredonia	56
Figure 3.2.2 Comparative compressive strength results, STH57-Fredonia	56
Figure 3.2.3 Compressive strength results, S Whitnall Ave - Cudahy	59
Figure 3.2.4 Compressive strength results, STH32 - Racine	59
Figure 3.2.5 Compressive strength results, STH23 – Fond du Lac	60
Figure 3.2.6 Project maturity plots using air temperatures	62
Figure 3.2.7 Project maturity plots using bagged cylinder temperatures	62
Figure 3.2.8 Combined maturity plot using air temperatures.....	63
Figure 3.2.9 Combined maturity plot using bagged cylinder temperatures.....	63
Figure 3.2.10 Combined maturity plot using air temperatures.....	65
Figure 3.2.11 Combined maturity plot using bagged cylinder temperatures.....	65
Figure 3.3.1 Portable beam tester	67
Figure 3.3.2 Comparative plot of flexural vs compressive strength	67
Figure 3.3.3 Comparative plot of flexural vs compressive strength	68
Figure 3.3.4 Comparative plot of flexural vs compressive strength	68
Figure 3.4.1 6x6x12 exposed dowel specimen prepared for initial testing	71
Figure 3.4.2 Cracked 6x6x12 exposed dowel specimen	71
Figure 3.4.3 9x12x12 exposed dowel specimen	73
Figure 3.4.4 Exposed dowel deflection results – STH57-Fredonia	76
Figure 3.4.5 Exposed dowel deflection results – STH57-Fredonia	76
Figure 3.4.6 Exposed dowel deflection results – S Whitnall Ave- Cudahy	78
Figure 3.4.7 Exposed dowel deflection results – STH32-Racine	78
Figure 3.4.8 Exposed dowel deflection results – STH23-Fond du Lac	80

LIST OF TABLES

Table 1.3.1 Modulus of Dowel Support Computed by Eq 1.7	10
Table 1.3.2 Calculated Modulus of Dowel Support Values from ABAQUS Analysis	12
Table 1.4.1 Coefficients for Eqs 1.18 and 1.19	25
Table 1.4.2 Coefficients for Eq 1.20	26
Table 1.7.1 Early Opening Criteria Used in the U.S.	41
Table 2.1.1 Project Data.....	43
Table 3.4.1 STH 57 Exposed Dowel Bar Data	74
Table 3.4.2 S Whitnall Avenue Exposed Dowel Bar Data	75
Table 3.4.3 STH32-Racine Exposed Dowel Bar Data	77
Table 3.4.4 STH23-Fond du Lac Exposed Dowel Bar Data	79

CHAPTER 1 INTRODUCTION

1.1 Background and Problem Statement

The current Wisconsin Department of Transportation (WisDOT) Standard Specifications for Highway and Structure Construction establishes the time when newly constructed Portland cement concrete (PCC) pavements may be opened to traffic based on test cylinders or minimum time periods related to atmospheric temperatures. Where test cylinders are used, minimum concrete compressive strengths of 20,700 kPa (3,000 psi) and 24,200 kPa (3,500 psi) are required prior to opening of urban and rural pavements, respectively. When the opening is not controlled by test cylinders, minimum time periods prior to opening are designated based on prevailing temperatures and may range from 7 to 21 days for traditional concrete mixes. The delay period between paving and opening to traffic can pose problems for contractors in terms of the prosecution of work and/or to business and property owners who must find alternate access routes or parking locations.

Various strategies, including the use of high early strength concrete or fast-track paving operations, have been employed to reduce the delay period between paving and minimum required strength gain. While these strategies can be effective in shortening the opening delay period, it must be remembered that increased early strength generally results in a slight reduction in the ultimate strength gain of most concrete mixtures. This strength reduction is not generally considered as detrimental to pavement performance, but in some cases may lead to a reduced fatigue life in the order of 3-5 years. An alternative strategy for reducing the opening delay period is the allowance of earlier trafficking, either unlimited or tiered, to allow more timely access to homes and businesses impacted by

construction and perhaps to allow for earlier access by construction equipment.

This Final Report presents a review of critical PCC stresses as well as research findings based on field and laboratory testing of concrete specimens obtained during construction on selected PCC paving projects in Wisconsin.

1.2 Critical PCC Stresses

One of the possible negative effects of early opening of PCC pavements is development of excessive bearing stress beneath dowels in transverse joints which can lead to micro or macro cracking in the PCC surrounding the dowels. While there may be no visible signs of this cracking on the surface, the load transfer capacity of the joint may be diminished and the performance life of the PCC pavement may be compromised. Therefore, one of the objectives of this study was to develop a practical yet realistic procedure for estimating these stresses to help ensure they are not allowed to exceed corresponding limit stresses.

Dowel – concrete interaction is a complex engineering problem. Although in the recent years significant progress was achieved in development of comprehensive 3D finite element models, there is no widely accepted, theoretically sound, and field-validated model available for predicting these values. Moreover, a 3D finite element analysis is computationally demanding and is not suited for routine analysis.

A more practical approach for determination of the dowel bearing stresses is using specialized finite element programs like ILLISLAB or ISLAB2000 (Tabatabae and Barenberg 1980, Khazanovich et al 1999). Although these programs are not as computationally demanding as 3D finite element programs, nevertheless, a more simple procedure that can be implemented in a spreadsheet and used by Wisconsin DOT in a

routine analysis is desired.

ISLAB2000 was used in this study to determine the effect of early age PCC strength, as defined by the PCC modulus of elasticity, on dowel bearing stresses under a variety of loading conditions. Critical loading positions and corresponding critical dowels were determined and a simplified analytical procedure was developed for estimating critical PCC bearing stresses. This procedure allows for the determination of critical PCC bearing stresses without running a finite element program.

This section presents the development of such procedure, summarizes it in an easy to follow step-by-step form, and discusses the results of the sensitivity study performed for a typical Wisconsin pavement structure.

1.2.1 Critical Loading Position

Critical loading positions were determined for early age loading of a transverse joint of a typical Wisconsin PCC pavement. The following structure was considered:

- 9-in PCC with the modulus of elasticity equal to 2.50×10^6 psi
- 6-in aggregate base thickness, modulus of elasticity is equal to 30 ksi.
- Coefficient of subgrade reaction (k-value) is 100 psi/in
- Passing lane width – 12 ft
- Truck lane width – 14 ft (striped 2 ft off edge)
- Doweled transverse joints
- Joint type – dowel bars
- Dowel diameter – 1.25 in
- Dowel spacing – 12 in, beginning 6 in off the edges
- Steel modulus of elasticity – 2×10^7 psi
- Poisson's ratio of the dowel bar material – 0.2
- Modulus of dowel support - 500,000 psi/in
- Transverse joint spacing – 15 ft
- Longitudinal joints with joint stiffness 12000 psi (approximate LTE=70%)

A standard 34-kips tandem axle load was placed at different distances from the striped edge of the truck lane (24 inches from the slab edge), an example of which is shown in Figure 1.2.1. PCC bearing stresses were determined under each dowel along the joint. It was found that the most loaded dowels in the right and left wheel paths are located 42 inches from the free slab edge and 6 inches from the longitudinal joint, respectively. Figures 1.2.2 and 1.2.3 present the values of bearing stresses for different load positions under the right and left critical dowels, respectively. One can observe that the critical axle location for the right critical dowel is when the outer right wheel of the axle is placed 32 inches from the pavement edge. For the left critical dowel, the critical axle location is when the outer left wheel of the axle is placed right at the longitudinal edge (see Figure 1.2.4).

1.2.2 Tabatabaie-Barenberg Model

A very simple but realistic model for analysis of dowel-PCC interaction was proposed by Tabatabaie and Barenberg (1980). They used Frieberg's analysis (Frieberg 1940) of dowels in rigid pavement which is based upon work presented by Timoshenko (1925). This model treats dowels as beams resting on a spring foundation, illustrated in Figure 1.2.5. The springs model compressibility of the PCC slab which means that dowel pressure on the concrete is proportional to dowel deflection within concrete. The Tabatabaie-Barenberg model assumes that the dowel is long enough so that it can be considered infinite in both directions. This assumption does not introduce significant discrepancies if dowel deflections with respect to concrete vanish close to the PCC joint.

If the total action of concrete on the dowel from one PCC slab is P , as shown in Figure 1.2.6, then deflection of the dowel in the other slab can be presented in the following form (Timoshenko and Lesser 1925):

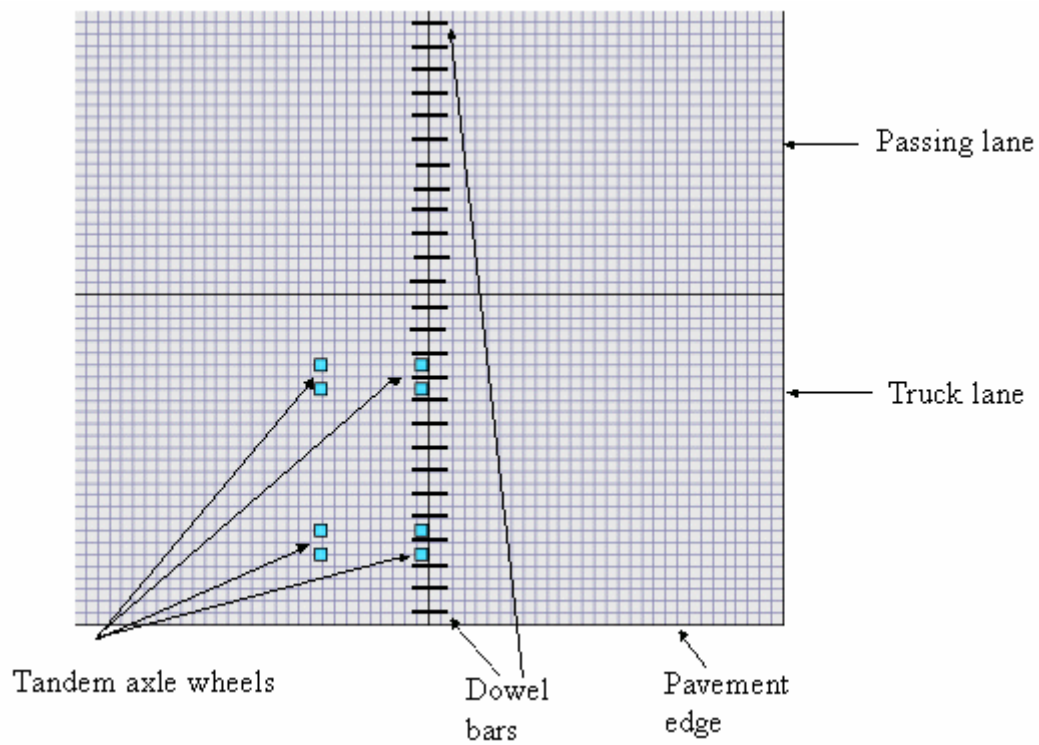


Figure 1.2.1 ISLAB2000 model of a transverse joint

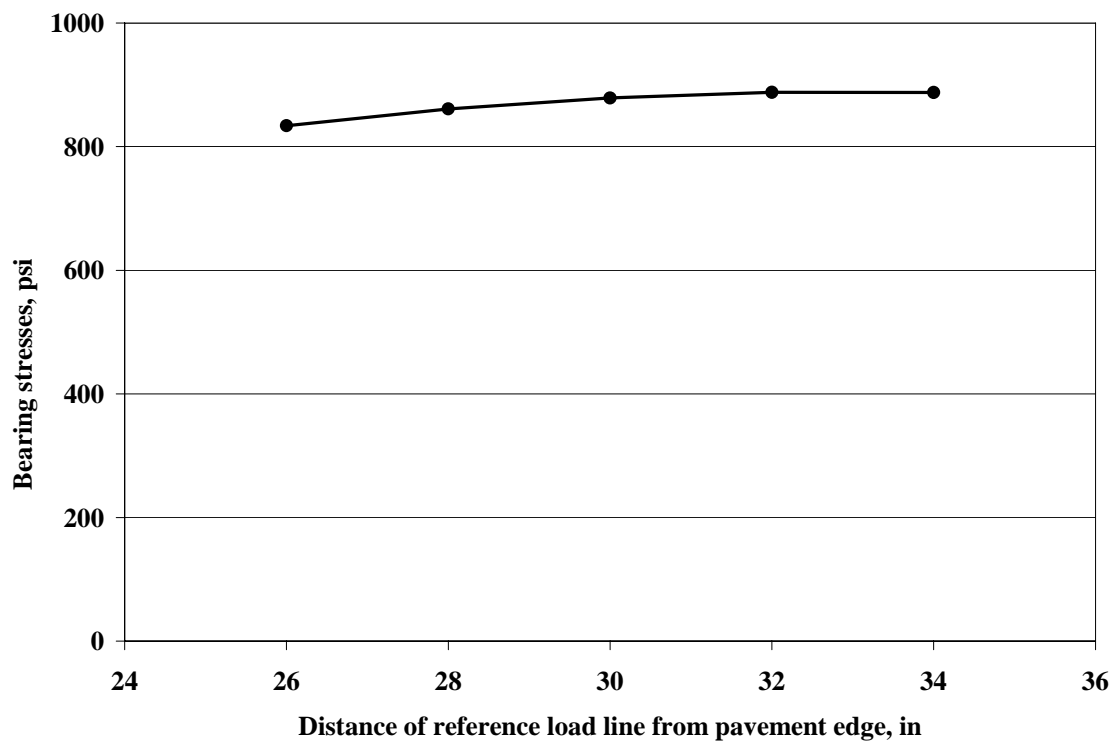


Figure 1.2.2. Bearing stresses vs. load position for the right critical dowel

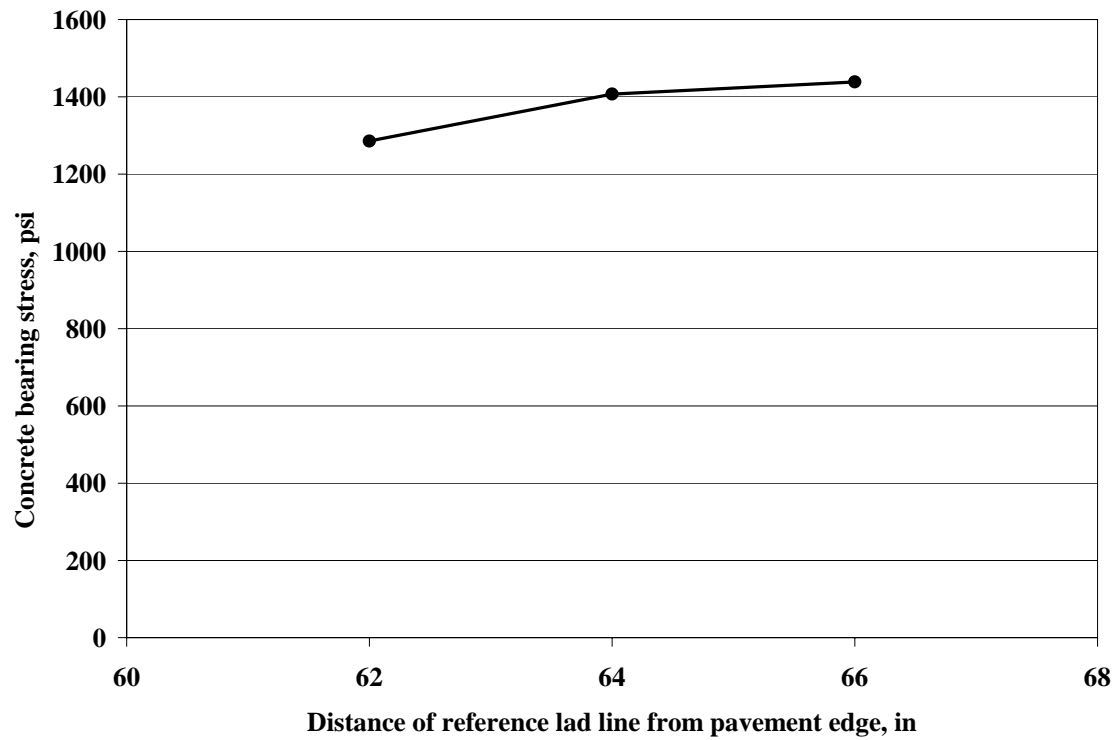


Figure 1.2.3. Bearing stresses vs. load position for the left critical dowel

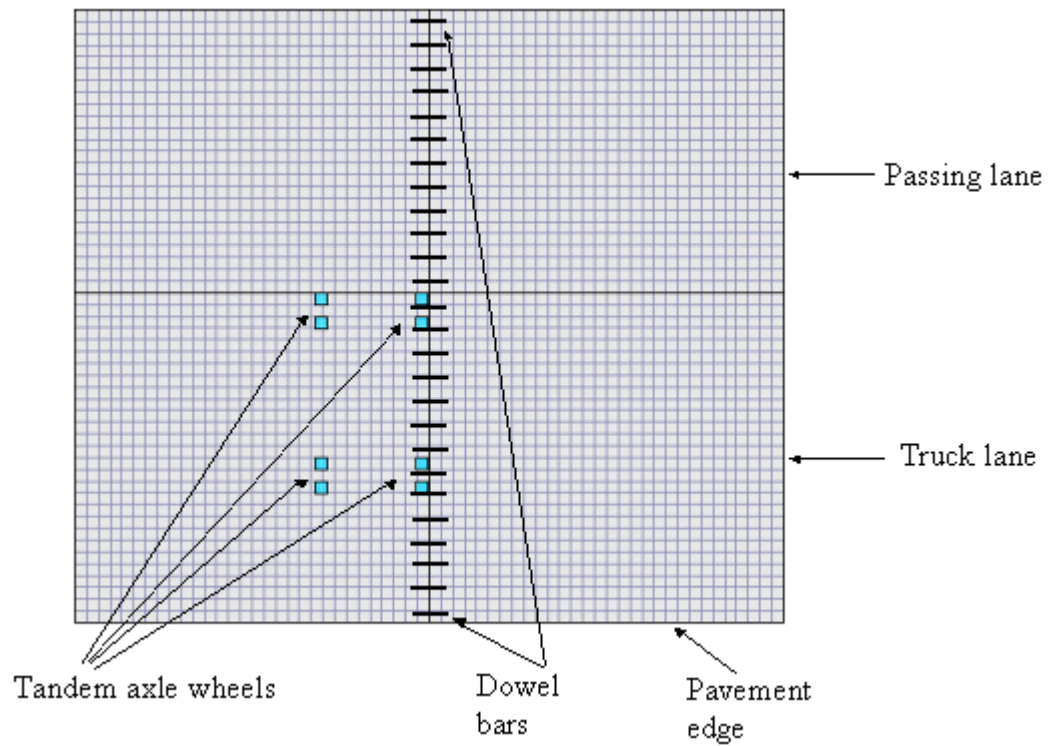


Figure 1.2.4. Critical load position for the left critical dowel

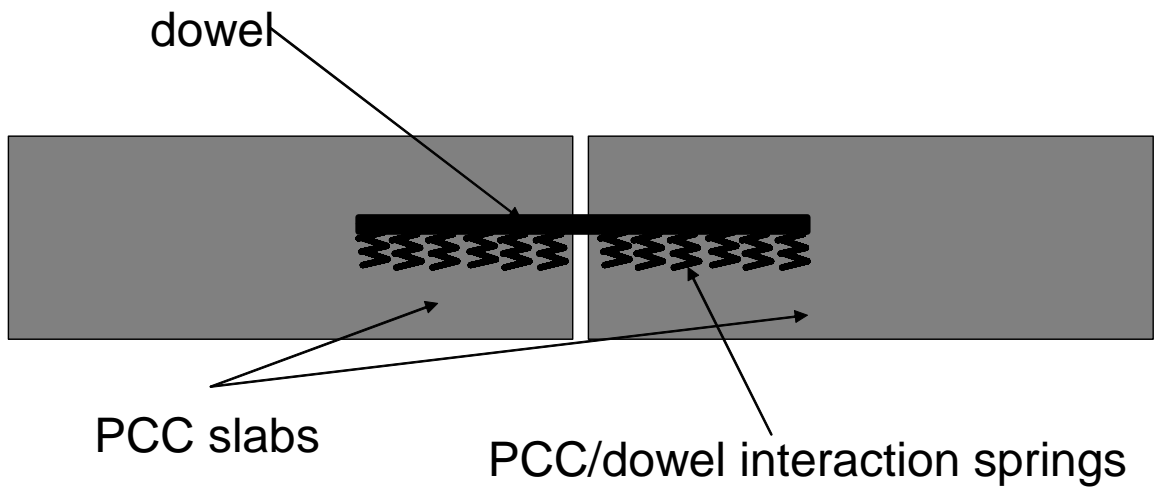


Figure 1.2.5. Tabatabaie and Barenberg model of doweled joints of PCC pavements.

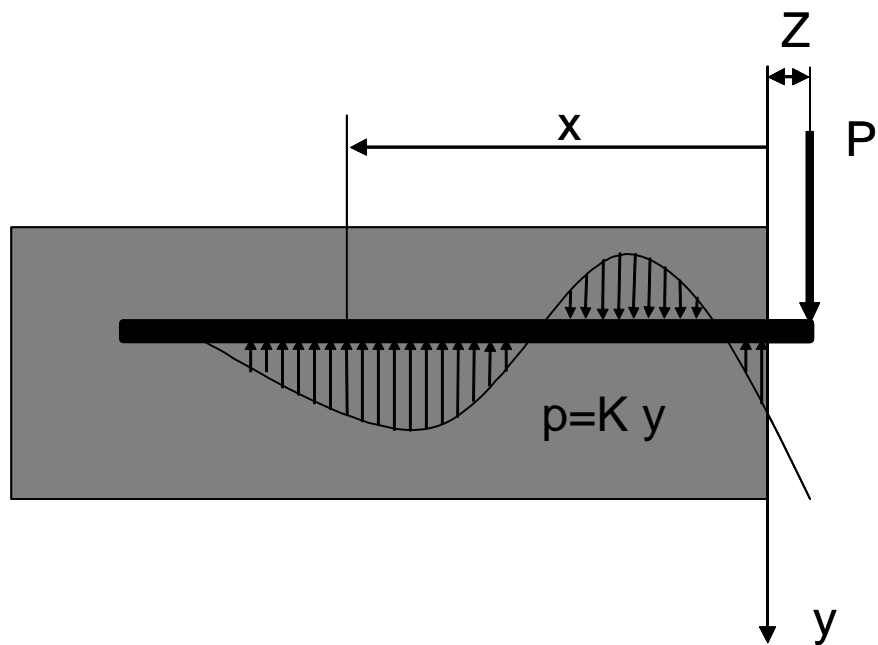


Figure 1.2.6. Pressure exerted on a loaded dowel

$$y = e^{-\beta x} [P \cos \beta x - \beta M_o (\cos \beta x - \sin \beta x)] / 2 \beta^3 E_d I_d \quad \text{Eq 1.1}$$

where: y = vertical deformation of PCC under the dowel
 x = coordinate along dowel from face of concrete
 M_o = bending moment on dowel at face of concrete
 β = the relative stiffness of a dowel bar embedded in concrete
 E_d = elastic modulus of dowel bar material, psi
 I_d = moment of inertia of the dowel

The relative stiffness of a dowel bar embedded in concrete, β , is defined as:

$$\beta = [K d / 4 E_d I_d]^{0.25} \quad \text{Eq. 1.2}$$

where: K = modulus of dowel support, psi/in
 d = dowel diameter, in
 $I_d = \pi d^4 / 64$

If the joint-width opening is designated Z , and considering that the concrete slabs are much stiffer than dowels, the moment at the dowel – concrete interface is as follows:

$$M_o = -PZ / 2 \quad \text{Eq. 1.3}$$

Substituting Eq 1.3 into Eq 1.1 leads to the following expression for the maximum dowel deflection in the concrete:

$$y_o = [P (2 + \beta Z)] / [4 \beta^3 E_d I_d] \quad \text{Eq. 1.4}$$

The maximum bearing pressure on the concrete is defined by:

$$\sigma = K y_o = [K P (2 + \beta Z)] / [4 \beta^3 E_d I_d] \quad \text{Eq. 1.5}$$

One can see that the maximum bearing pressure on concrete depends on the following parameters:

- Total load transferred by the dowel
- Modulus of dowel support
- Joint opening
- Dowel diameter
- Dowel modulus of elasticity

The last two items naturally do not depend on the pavement age. Although joint opening depends of pavement age through magnitude of developed shrinkage, the age effect is usually overshadowed by the effect of joint movement due to temperature variation in the PCC slab. Therefore, only the modulus of dowel support and the magnitude of the load transferred by the dowel considered for further investigation.

1.3 Modulus of Dowel Support

The modulus of dowel support initially proposed by Grinter and Frieberg is defined as the reaction per unit area causing a deflection equal to one

$$K = p / y \quad \text{Eq. 1.6}$$

where: K = modulus of dowel support, psi/in
 p = vertical contact stress between dowel and concrete, psi
 y = vertical deflection of concrete, in

The modulus of dowel support is usually assumed between 300,000 and 1,500,000 psi/in and Tabatabaie recommended the value between 250,000 and 8,000,000 psi/in. Nishizawa et al (1989) developed simple analytical model for estimation of dowel support model and proposed the following equation for K :

$$K = [8 (1 - \mu_c) E_c] / [(1 + \mu_c) (1 - 2\mu_c) (h - d)] \quad \text{Eq. 1.7}$$

where: μ_c = Poisson's ratio of PCC
 E_c = PCC modulus of elasticity, psi
 h = slab thickness, in
 d = dowel diameter, in

Table 1.3.1 presents the values of K calculated according to Eq. 1.7 for a slab thickness $H = 10$ in, dowel diameter $d = 1.25$ in, PCC Poisson's ratio $\mu_c = 0.15$, and a range

of concrete modulus, E_c , from 1,000,000 to 5,000,000 psi. As provided, the K values vary in a wide range depending on PCC modulus, falling within the ranges proposed by Tabatabaie but exceeding recommendations given by Yoder and Witzak.

Table 1.3.1 Modulus of Dowel Support Computed by Eq. 1.7

PCC modulus of Elasticity, E_c , psi	Modulus of Dowel Support, K, psi/in
1,000,000	965,395
1,500,000	1,448,092
2,000,000	1,930,790
2,500,000	2,413,487
3,000,000	2,896,185
3,500,000	3,378,882
4,000,000	3,861,579
4,500,000	4,344,277
5,000,000	4,826,974

Considering importance of the modulus of dowel support for determination of critical PCC bearing stresses, a decision to re-examine relationship between the PCC modulus of elasticity and the K parameter was made.

A finite element model of interaction between a dowel and surrounding concrete of the pavement slab of PCC slab was developed in this study. As in the Friberg model, it was assumed that the interaction for a slice of PCC slab surrounding a dowel depends only on the contact force between the dowel and PCC and does not depend on behaviors of the rest of the pavement system. Therefore, only a thin PCC slice with a height equal to the PCC slab thickness and a width equal to the dowel spacing was modeled, as shown in Figure 1.3.1.

A 2D finite element model of an individual PCC/dowel slice was developed using a commercial finite element package ABAQUS. Figures 1.3.2 and 1.3.3 show the entire finite element mesh and the portion of the model around the dowel, respectively. The contact interface between the PCC slab and dowel was assumed to be frictionless which allows the dowel to separate freely under loading while at the same time the contact pair elements prevent the dowel from penetrating through the concrete. A force of 100 lbs was used to model the force transferred from the dowel slice to the slice of the concrete slab. The bottom of the PCC fragment was restrained from vertical displacements.

A factorial of ABAQUS runs were performed using the following model parameters:

- PCC slab thickness = 10 in
- PCC Poisson ratio = 0.15
- dowel modulus of elasticity = 20×10^6 psi
- dowel Poisson ratio = 0.2
- dowel diameter = 1.25 in
- dowel spacing = 12 in

The PCC modulus of elasticity was varied from 500 ksi to 5Mpsi. Figures 1.3.4 and 1.3.5 present typical distributions of dowel and PCC displacements. One can see that a top portion of the dowel surface separated from the PCC whereas the bottom portion of the dowel remains in the contact. The maximum dowel displacements occur at the bottom of the dowel. Those displacements were used for calculation of the modulus of dowel support using the following equation:

$$K = P / y_d \quad \text{Eq. 1.8}$$

The calculated modulus of dowel support values for the different PCC moduli of elasticity are summarized in Table 1.3.2 and Figure 1.3.6. As expected, an increase in PCC modulus leads to increase in the value of PCC-dowel interaction. The resulting moduli are slightly lower than predicted by the Nishizawa et al model.

Table 1.3.2: Calculated Modulus of Dowel Support Values from ABAQUS Analysis

PCC modulus of elasticity, psi	Modulus of Dowel Support, psi/in
1,000,000	768,492
2,000,000	1,538,462
3,000,000	2,285,714
4,000,000	3,076,923
5,000,000	3,809,524

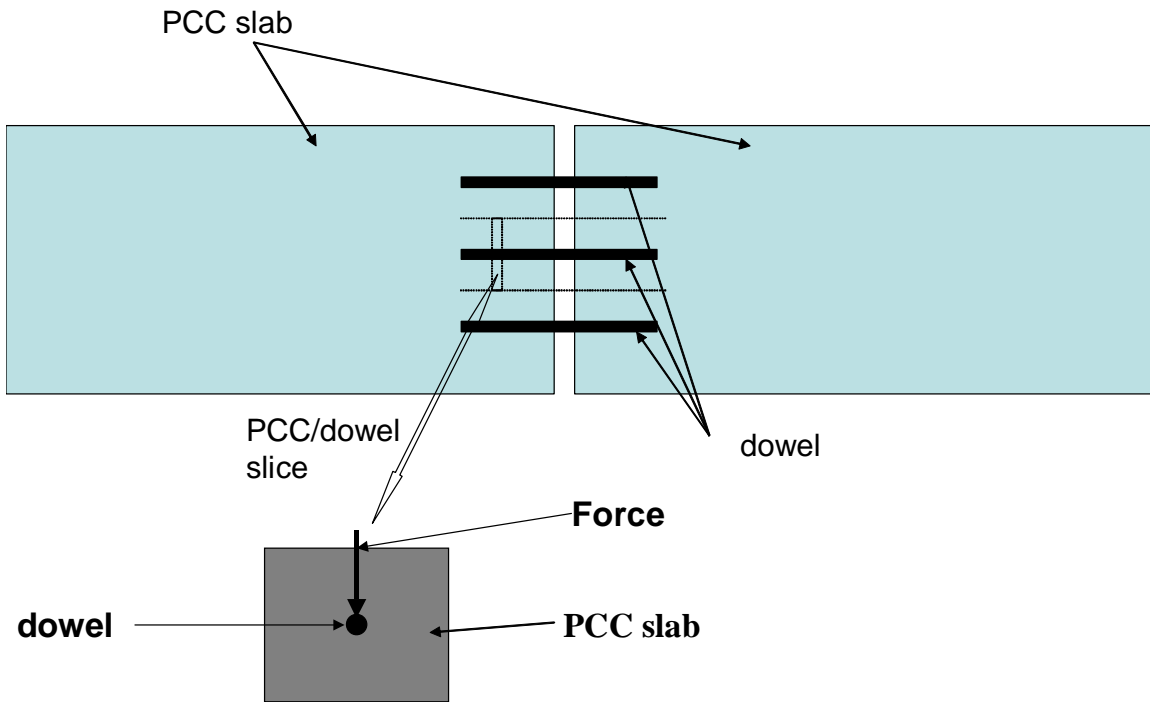


Figure 1.3.1. Modeling of PCC- dowel interaction

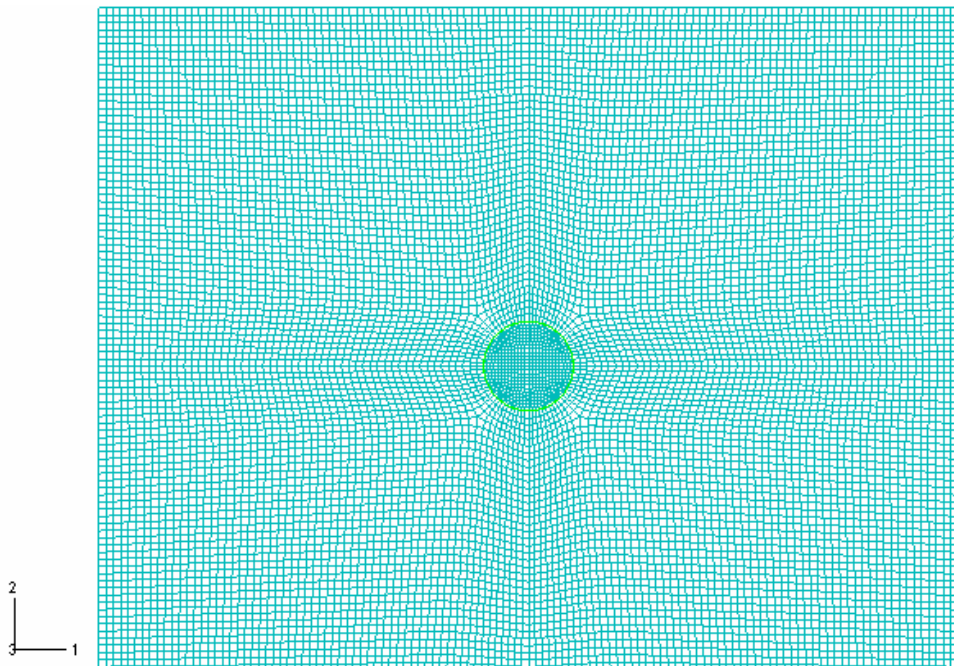
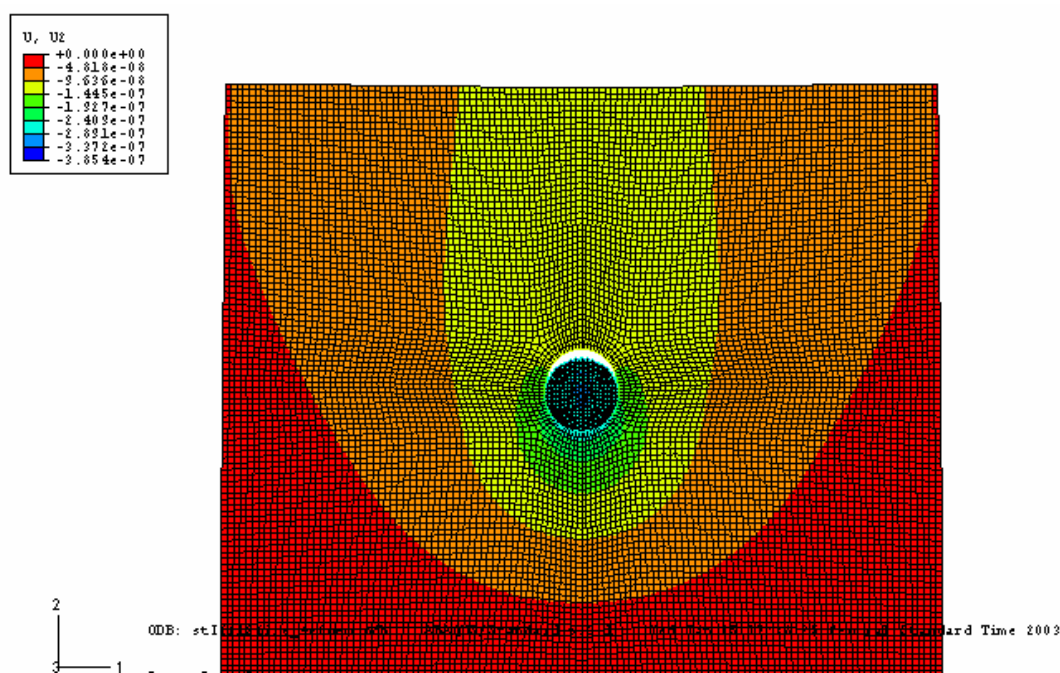
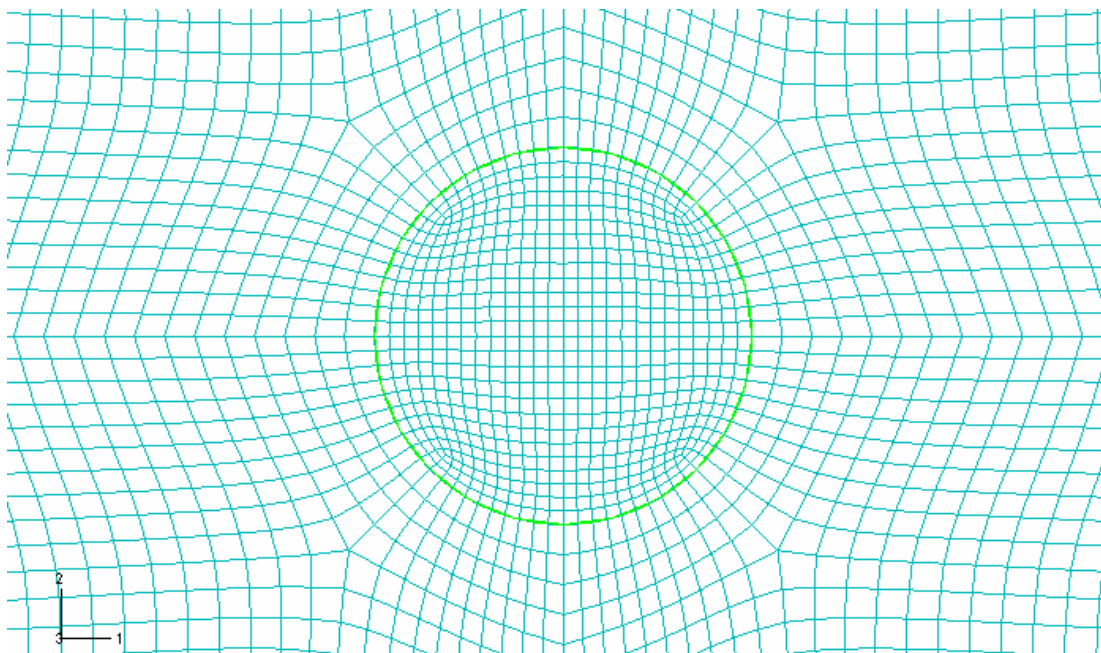


Figure 1.3.2. 2D finite element mesh of dowel/PCC interaction.



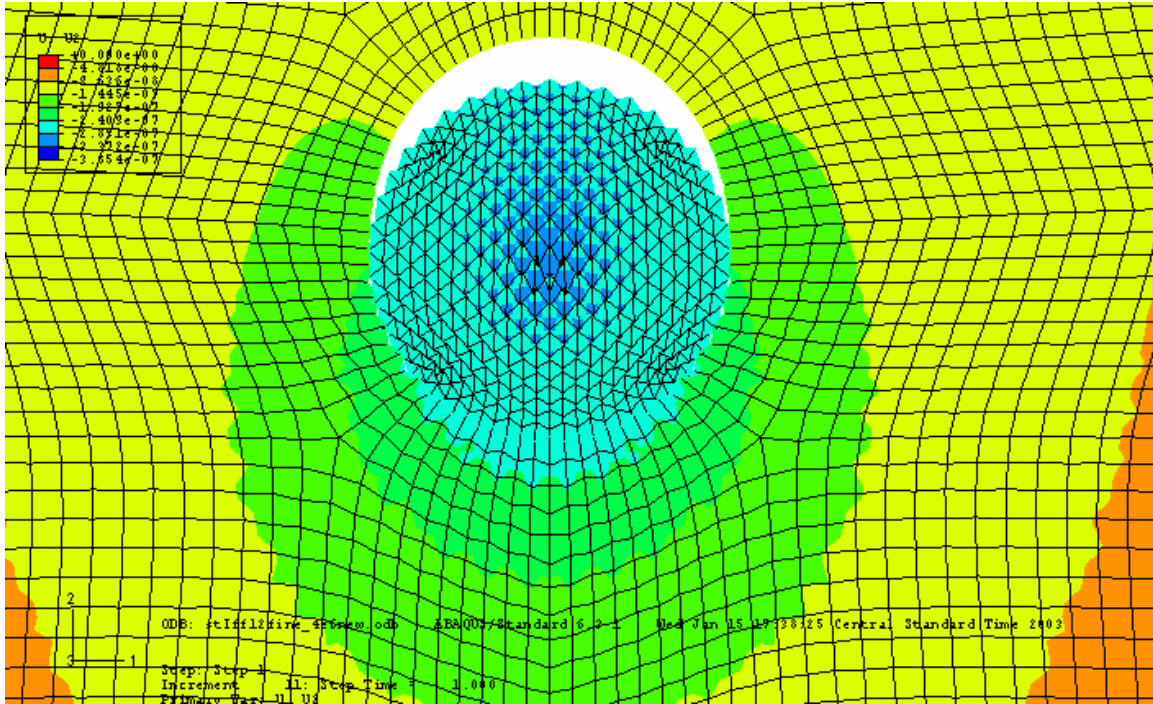


Figure 1.3.5. Typical contours of vertical displacements for a fragment around dowel (deformation scale factor is equal to 1×10^6)

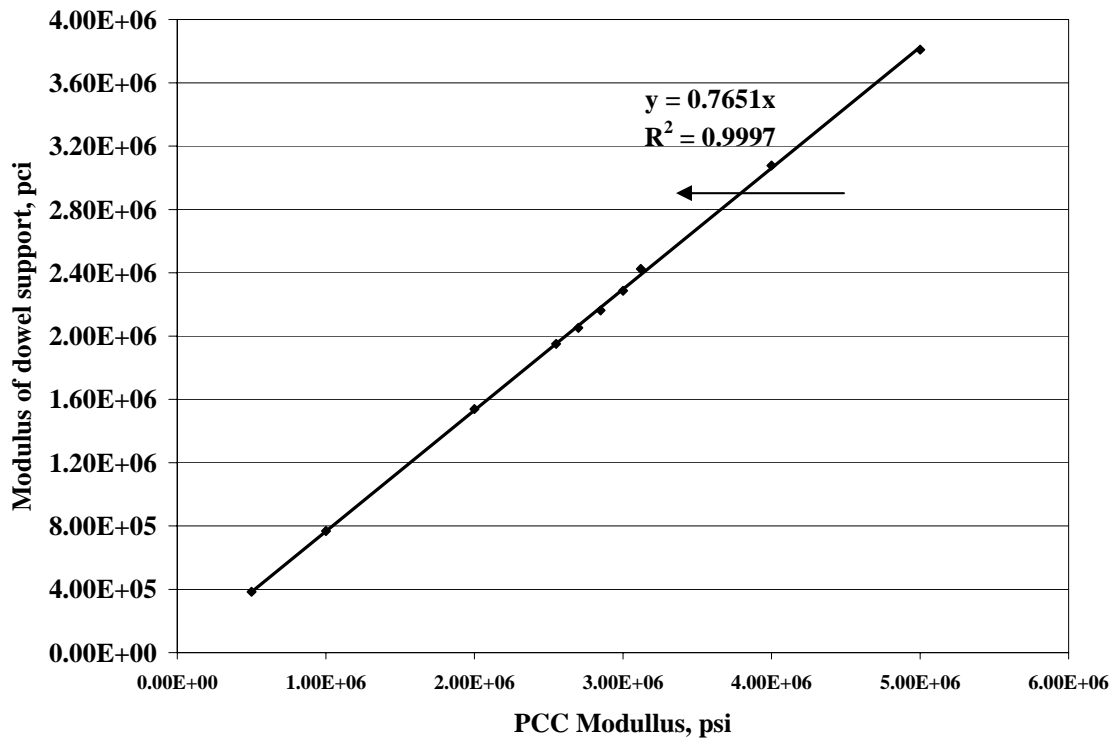


Figure 1.3.6. Modulus of dowel support vs. PCC modulus

A linear regression of the ABAQUS results provided the following model:

$$K = 0.7651 E_c \quad R^2 = 0.9997 \quad \text{Eq. 1.9}$$

This equation is recommended for use in estimating the modulus of dowel support, K, and ultimately the dowel-PCC contact stresses Eqs. 1.2 & 1.5).

1.4 Load Transferred by the Dowel

Another important factor affecting dowel-PCC contact stresses is the maximum load transferred by a single dowel. A simple model for determining of this load was proposed by Frieberg. However, later analysis performed by Guo et al (1996) discovered a deficiency in the Frieberg method.

The force load transferred by any dowel in the joint can be determined using finite element programs such as ILLI-SLAB or ISLAB2000. If Tabatabaie's dowel model is used in the analysis, this force can be calculated using the following equation

$$P_t = D (w_{\text{load}} - w_{\text{unload}}) \quad \text{Eq. 1.10}$$

where : D = dowel shear stiffness
 w_{load} = deflection of loaded side of the joint at the dowel location, in
 w_{unload} = deflection of unloaded side of the joint at the dowel location, in

The dowel shear stiffness is defined as follows:

$$D = 1 / [Z^3(1+\Phi)/(12E_d l_d) + (2+\beta Z)/(2\beta^3 E_d l_d)] \quad \text{Eq 1.11}$$

$$\Phi = [24 (1+\mu_d) l_d] / [A_s Z^2] \quad \text{Eq. 1.12}$$

$$A_s = 0.9 \pi d^2 / 4 \quad \text{Eq. 1.13}$$

Where: μ_d = Poisson's ratio of the dowel bar material
 A_s = cross sectional area of dowel bar in shear

Although the finite element analysis is more accurate than Frieberg's analysis it is

more time consuming and less convenient. To address this limitation, a simplified procedure was developed in this study. This procedure combines simplicity of Frieberg's analysis and accuracy of the finite element modeling. Development of this procedure is presented below.

Khazanovich and Ioannides (1997) provide the following equation for computing the load transferred by the critical dowel:

$$P_c = D \Delta_{\text{free-edge}} (1 - \text{LTE}) / (1 + \text{LTE}) \quad \text{Eq. 1.14}$$

where : LTE = deflection load transfer efficiency, decimal form
 $\Delta_{\text{free-edge}}$ = maximum joint deflection if no dowels exist

Therefore, the maximum load transferred by a dowel can be easily found if the load transfer efficiency and the maximum free edge deflections are known. In this study, simple regression equations based on the results ISLAB2000 analysis were developed to determine these parameters.

1.4.1 Load Transfer Efficiency

According to Ioannides and Korovesis (1992), deflection load transfer efficiency (LTE) of doweled joints depends on the following dimensionless joint stiffness parameter, AGG*, defined as follows:

$$\text{AGG}^* = D / s k l_k \quad \text{Eq. 1.15}$$

where: s = dowel spacing, in
 k = modulus of subgrade reaction (k-value), psi/in
 l_k = dense-liquid radius of relative stiffness, in

The dense-liquid radius of relative stiffness is defined as:

$$l_k = \{ E_c h_c^3 / [12 (1 - \mu_c^2) k] \}^{0.25} \quad \text{Eq. 1.16}$$

Crovetti (1994) proposed the following relationship between the nondimensional joint stiffness and the deflection load transfer efficiency:

$$\text{LTE (\%)} = 100\% / [1 + c_1 \text{ AGG}^{c_2}] \quad \text{Eq. 1.17}$$

Where: LTE(%) = Deflection load transfer efficiency, % = 100% d_u/d_l
 $c_1 = 1.2$
 $c_2 = -0.847$
 d_u = unloaded slab deflection at 12 inches from the center of loading, inches
 d_l = loaded slab deflection at 0 inches from the center of loading, inches

Eq. 1.17 was developed for an FWD-type loading (300 mm circular loading tangent to the joint at mid-slab) with LTE values calculated at positions coincident with FWD deflection sensors (0 and 12 inches from the center of loading). Khazanovich and Gotlif (2003) validated Eq 1.17 for these conditions; however, the load configuration, load position, and location at which LTE should be calculated are different in this WHRP study than those used in Crovetti's analysis and, therefore, additional analysis was conducted to determine the direct applicability of Eq 1.17 for this study.

As it was presented earlier, critical dowels in the right and the left wheelpaths are located at 42 inches from the outer pavement edge and at 6 inches from the center-lane longitudinal edge, respectively, with critical axle load positions at 32 inches from the outer pavement edge and 0 inches from the center-lane longitudinal joint, respectively.

A factorial of ISLAB2000 runs was performed and Crovetti's prediction of deflection load transfer efficiency was compared with the load transfer efficiency calculated directly from the ISLAB2000 deflection output at the location of critical dowels. The following cases were considered:

- PCC thickness – 9 in
- PCC modulus of elasticity 2.55×10^6 psi
- Base thickness – 6 in
- Base modulus of elasticity – 3×10^4 psi
- Longitudinal joint stiffness (AGG factor) – 11,931 psi
- Transverse joints
- Joint type – dowel bars
- Dowel diameter – 1.25 in
- Dowel spacing – 12 in, beginning 6 in off the edges
- Steel modulus of elasticity – 2×10^7 psi
- Poisson's ratio of the dowel bar material – 0.2
- Modulus of dowel support – 1.5, 2.0, 2.5, 3.0, 3.5, and 4.0 Mpsi/in
- Modulus of subgrade reaction – 50, 100, 150, 200, 400, and 1000 psi/in.

The input values for the modulus of subgrade reaction were selected to ensure that the radius of relative stiffness (l_k) varied from 20 inches to over than 40 inches, which covers the typical range of l_k for highway-type PCC pavements. Four loading cases were considered:

- An 18-kip single axle load placed 34 inches from the outer pavement edge (loading position 1)
- A 34-kip tandem axle load placed 34 inches from the outer pavement edge (loading position 1)
- An 18-kip single axle load placed 0 inches from the center-lane longitudinal joint (loading position 2)
- A 34-kip tandem axle load placed 0 inches from the center-lane longitudinal joint (loading position 2)

ISLAB2000 runs were performed and the deflection LTE values (ratios of slab deflections on unloaded and loaded sides of the joints) were calculated for the specified joint locations. For loading position 1 the load transfer efficiency was calculated at 42 in away from the pavement edge, which corresponds to location of the critical dowel in the right wheel path. For loading position 2, the load transfer efficiency was calculated at 6 in away from the longitudinal joint, which corresponds to location of the critical dowel in the

right wheel path. The load transfer efficiencies at these locations were then compared with LTE values calculated using Croveti's equation.

Figures 1.4.1 and 1.4.2 present comparisons of Croveti's and ISLAB2000 LTEs for the critical right wheel path dowel for single and tandem axle loading, respectively. Figures 1.4.3 and 1.4.4 present comparisons of Croveti's and ISLAB2000 LTEs for the critical left wheel path dowel for single and tandem axle loading, respectively. Analysis of these figures shows that Croveti's equation provides relatively good estimates of the joint deflection LTE, but slightly underestimates it for the right wheel path dowel and overestimates it for the left wheel path dowel. This discrepancy may not be significant for other applications, but since the deflection LTE is a crucial parameter for determination of PCC bearing stresses, it was decided to modify Croveti's equation to improve its accuracy for the specific critical axle loadings determined previously.

Analysis of the discrepancies between the ISLAB2000 and Croveti LTE values indicated a dependency on the PCC slab radius of relative stiffness, l_k . Therefore, it was proposed to make adjustments to Eq 1.17 by adjusting the AGG* coefficient (c_1) and exponent (c_2) terms and including an l_k term, where appropriate, resulting in the following general equations:

$$c_1 = a_1 + a_2 l_k + a_3 l_k^2 \quad \text{Eq. 1.18}$$

$$c_2 = -\exp(b_1 + b_2 l_k + b_3 l_k^2) \quad \text{Eq. 1.19}$$

Table 1.4.1 provides appropriate values for the coefficients for Eqs. 1.18 and 1.19 for the four loading cases considered. Figures 1.4.5 through 1.4.8 present comparisons of LTEs obtained from ISLAB2000 and from modified Croveti's equations. As shown, excellent agreement was achieved for all loading cases.

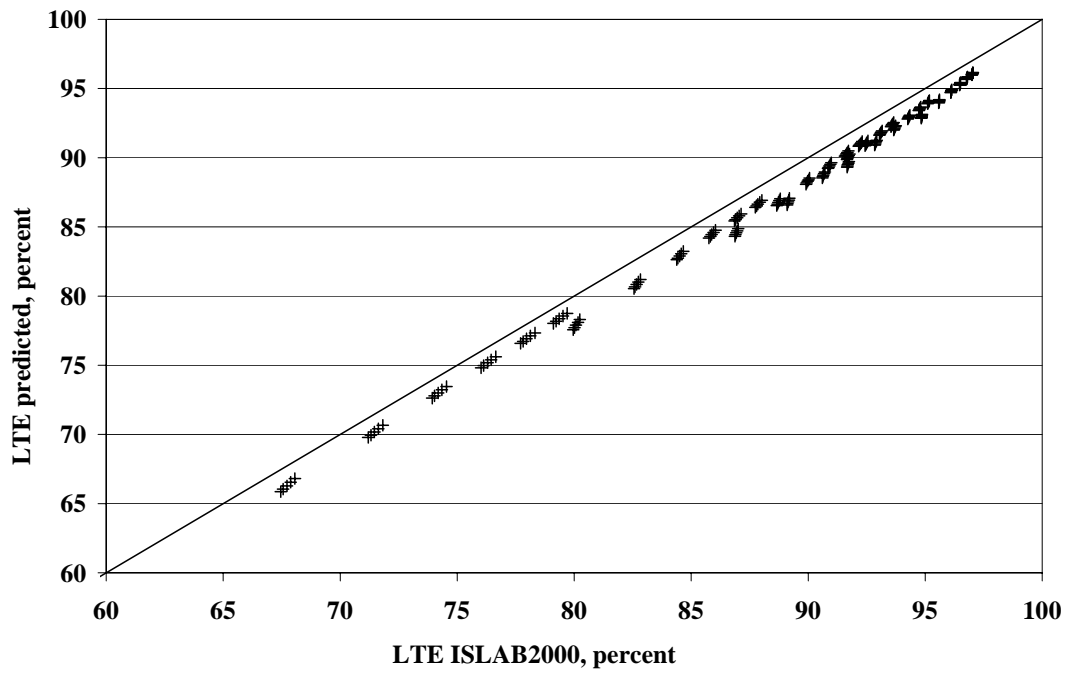


Figure 1.4.1. Comparison of ISLAB2000 LTE and LTE from Croveti's equation.
Single axle loading, right wheel path critical dowel location

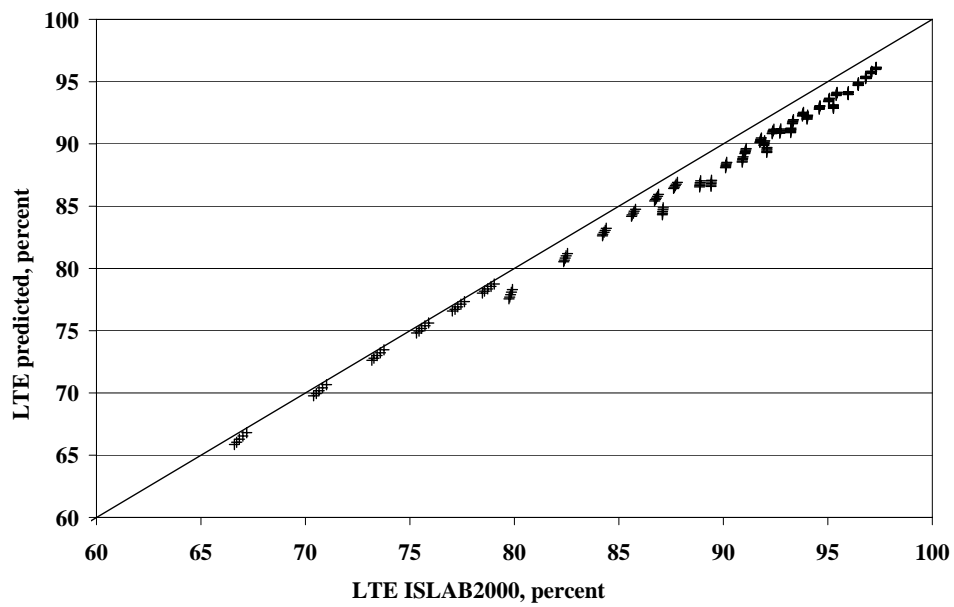


Figure 1.4.2. Comparison of ISLAB2000 LTE and LTE from Croveti's equation.
Tandem axle loading, right wheel path critical dowel location

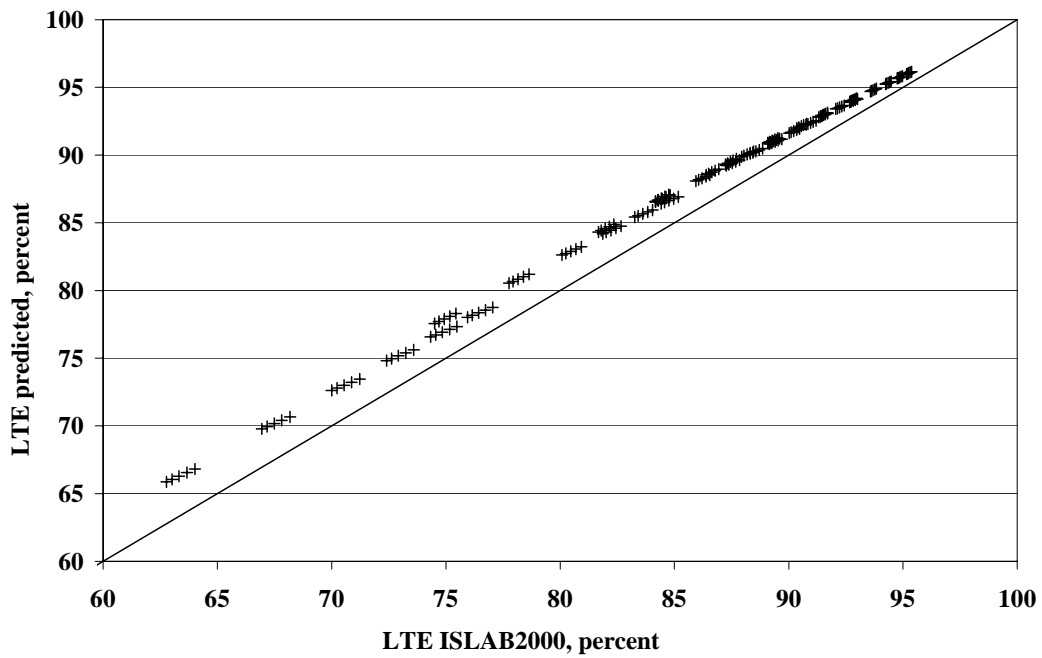


Figure 1.4.3. Comparison of ISLAB2000 LTE and LTE from Croveti's equation.
Single axle loading, left wheel path critical dowel location

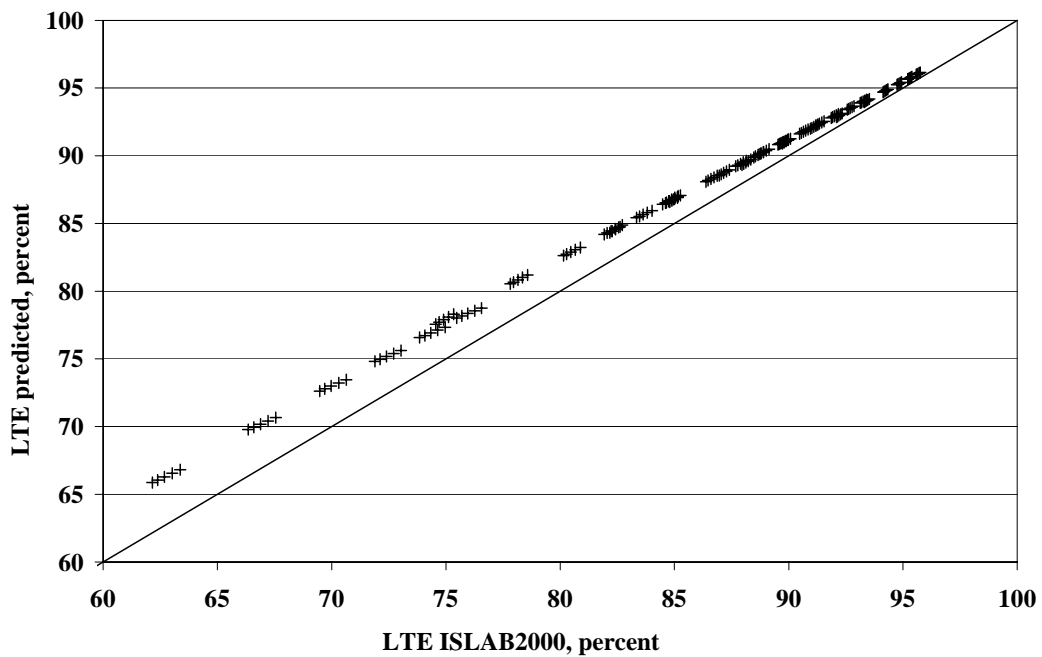


Figure 1.4.4. Comparison of ISLAB2000 LTE and LTE from Croveti's equation.
Tandem axle loading, left wheel path critical dowel location.

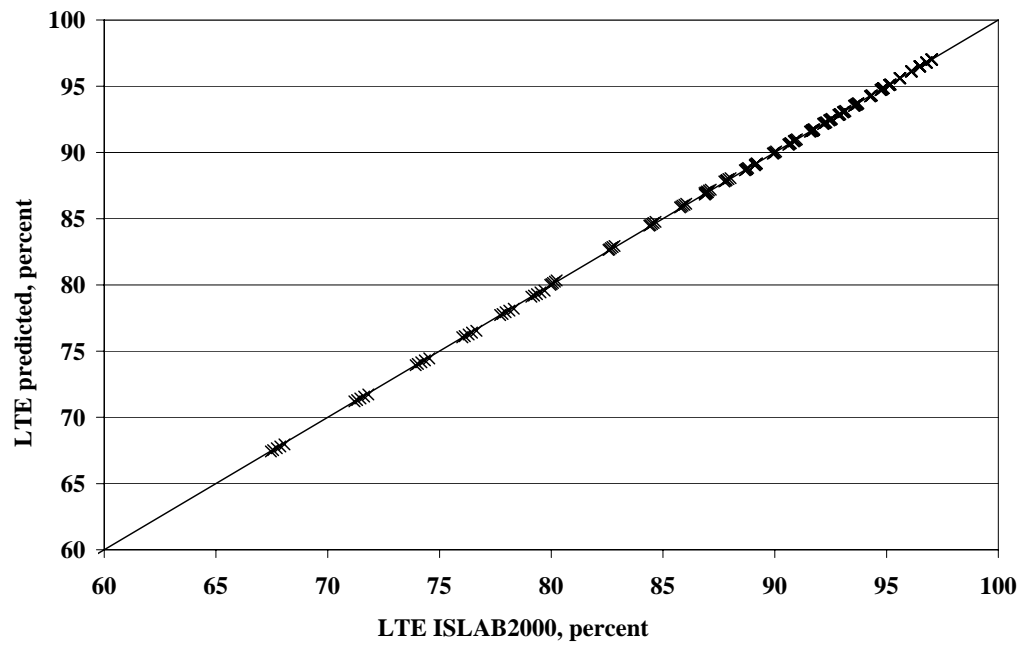


Figure 1.4.5. Comparison of ISLAB2000 LTE and LTE from modified Croveti's equation. Single axle loading, right wheel path critical dowel location

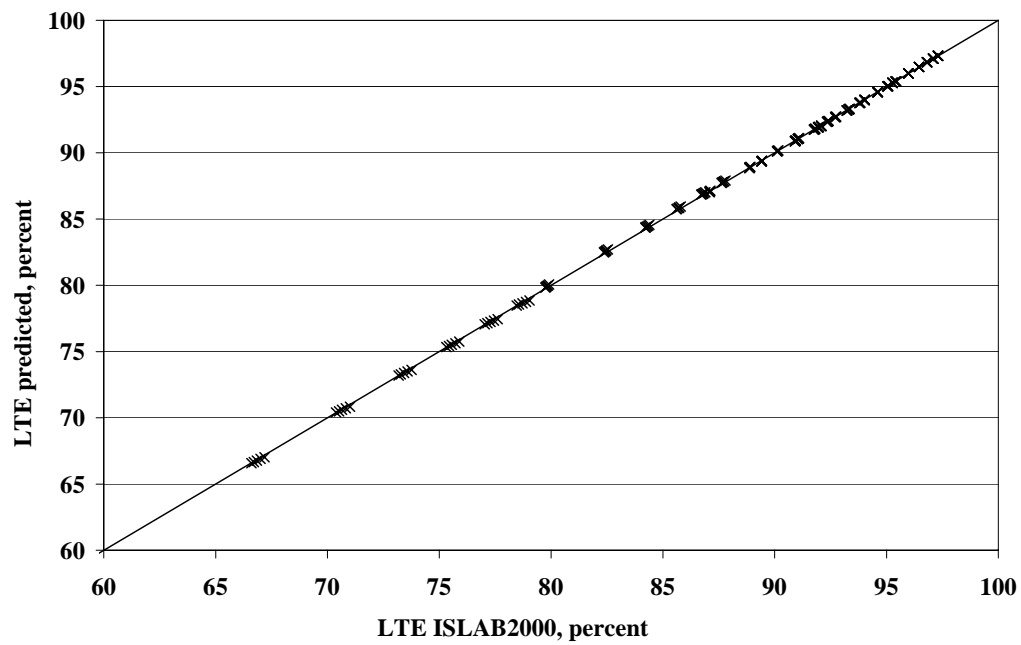


Figure 1.4.6. Comparison of ISLAB2000 LTE and LTE from modified Croveti's equation. Tandem axle loading, right wheel path critical dowel location

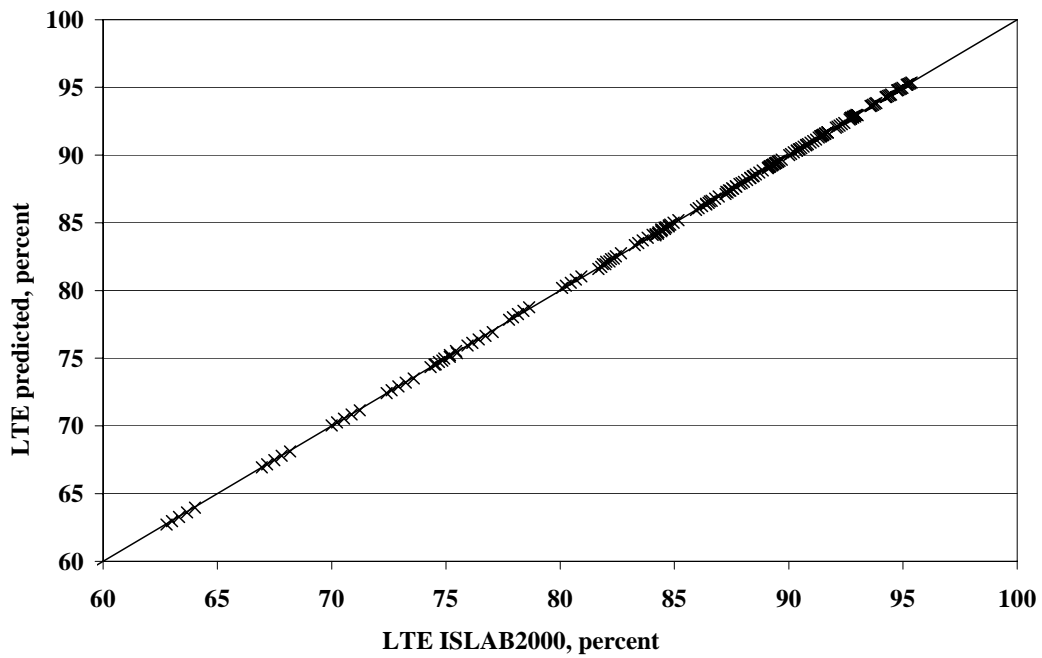


Figure 1.4.7. Comparison of ISLAB2000 LTE and LTE from modified Croveti's equation. Single axle loading, left wheel path critical dowel location

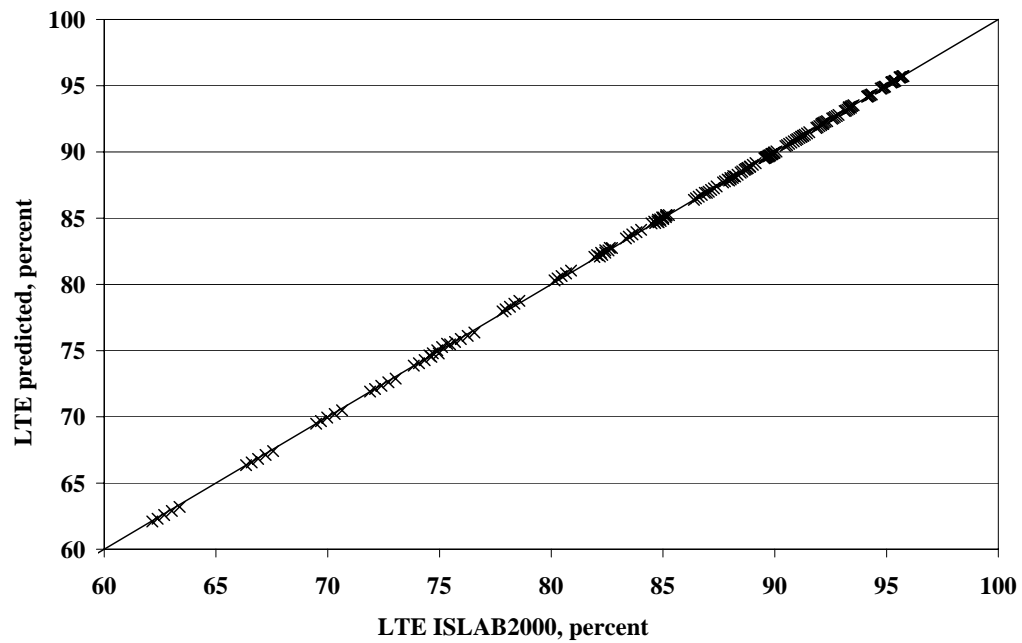


Figure 1.4.8. Comparison of ISLAB2000 LTE and LTE from modified Croveti's equation. Tandem axle loading, left wheel path critical dowel location

Table 1.4.1 Coefficients for Eqs. 1.18 and 1.19

Loading	a ₁	a ₂	a ₃	b ₁	b ₂	b ₃
18k SAL RWP - Pos 1	1.77	-0.0382	0.000322	0.00503	-0.0113	0.000136
34k TAL RWP - Pos 1	1.99	-0.0492	0.000455	-0.00341	-0.0114	0.000156
18k SAL LWP - Pos 2	1.14	0.0168	-0.000175	-0.0442	-0.00596	0.0000823
34k TAL LWP - Pos 2	1.34	0.00846	-0.000153	-0.0615	-0.00463	0.0000634

1.4.2 Maximum Free-edge Deflection

Another very important parameter required for calculation of PCC bearing stresses is free edge deflection, i.e. deflection at the dowel location on the loaded side of the joint if no dowel or aggregate interlock exists in the joint. The following functional form was developed for the free edge deflection:

$$\Delta_{\text{free-edge}} = [P / k l_k^2] [d_1 + d_2 l_k + d_3 l_k^2] \quad \text{Eq. 1.20}$$

where: $\Delta_{\text{free-edge}}$ = free edge deflection, inches
P = total axle load, lbs
d₁, d₂, d₃ = regression coefficients depending on axle type and position.

Several factorials of ISLAB2000 runs were performed and free edge deflections were determined for the left and wheel path dowel locations and corresponding critical loading positions. Table 1.4.2 provides the coefficients for Eq. 1.20 developed through regression analysis.

Table 1.4.2 Coefficients for Eq. 1.20

Loading	d_1	d_2	d_3	R^2
18k SAL RWP - Pos 1	0.0964	0.00353	0.0000603	0.9999
34k TAL RWP - Pos 1	0.0502	0.00039	0.0000876	0.9999
18k SAL LWP - Pos 2	0.138	0.0047	0.0000138	0.9999
34k TAL LWP - Pos 2	0.0602	0.0021	0.0000468	0.9999

Figures 1.4.9 and 1.4.10 present comparisons between calculated and predicted free edge deflections for the right wheel path critical dowel position for the single and tandem axle loadings, respectively. Figures 1.4.11 and 1.4.12 present comparisons between calculated and predicted free edge deflections for the left wheel path critical dowel position for the single and tandem axle loadings, respectively. Excellent correspondence is observed in all cases.

1.4.3 Critical Dowel Load Verification

To demonstrate accuracy of the prediction equations for LTE and maximum deflection, the loads transferred by critical dowels determined from ISLAB2000 analysis were compared with the loads calculated using the prediction equations. As it can be observed from Figure 1.4.13 through 1.4.16, the simplified procedure provides good agreement with ISLAB2000 analysis for both single and tandem axle loading and for right and left wheel path dowels.

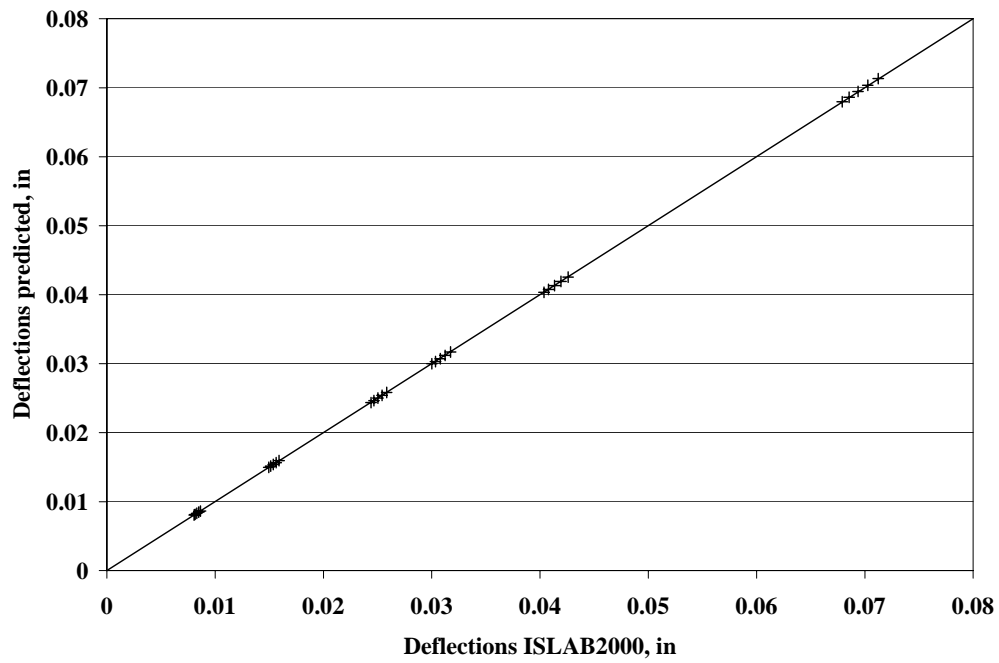


Figure 1.4.9. Comparison of ISLAB2000 and predicted free edge deflections.
Single axle loading, right wheel path critical dowel location

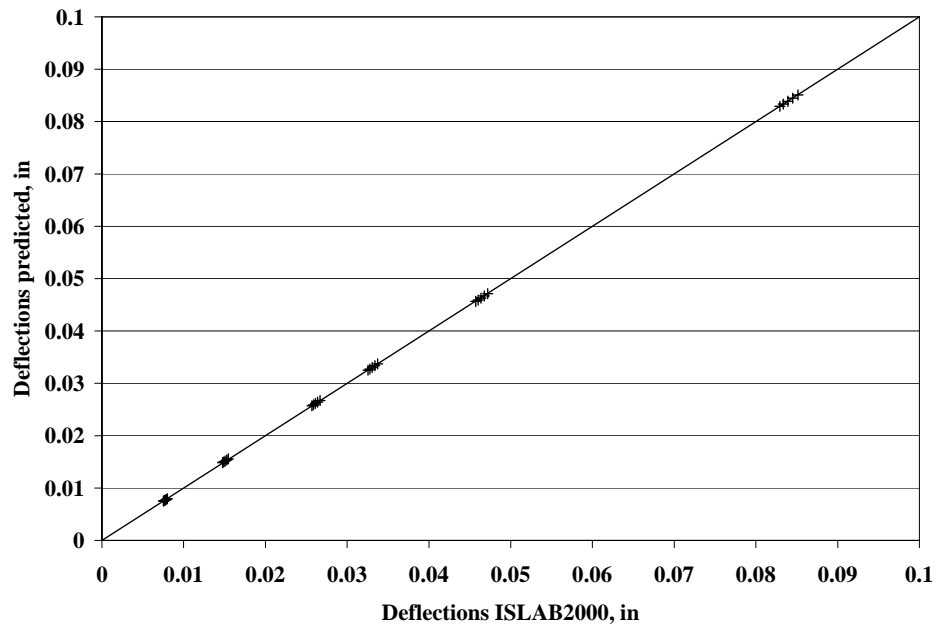


Figure 1.4.10. Comparison of ISLAB2000 and predicted free edge deflections.
Tandem axle loading, right wheel path critical dowel location

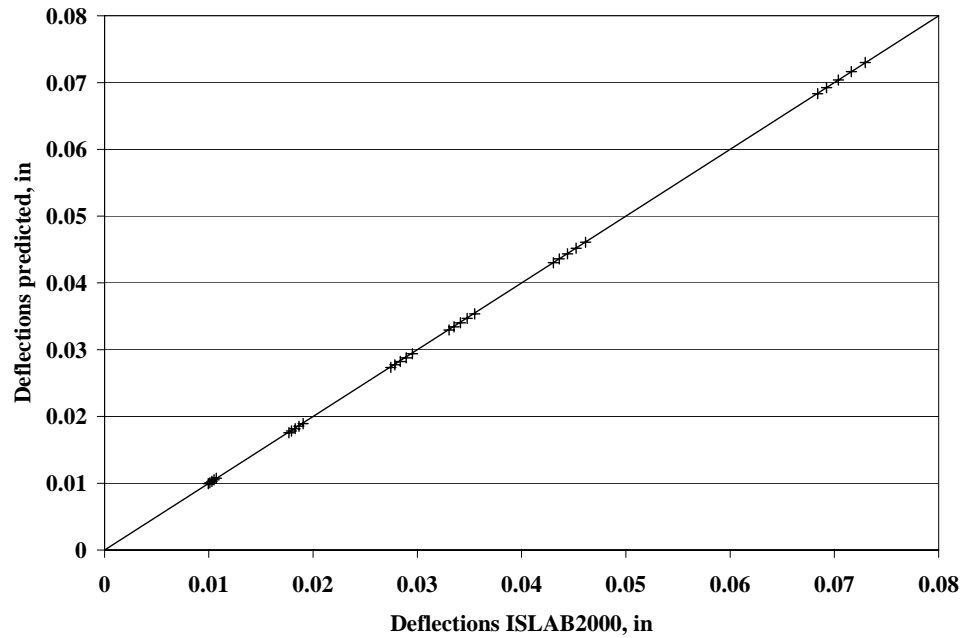


Figure 1.4.11. Comparison of ISLAB2000 and predicted free edge deflections.
Single axle loading, left wheel path critical dowel location

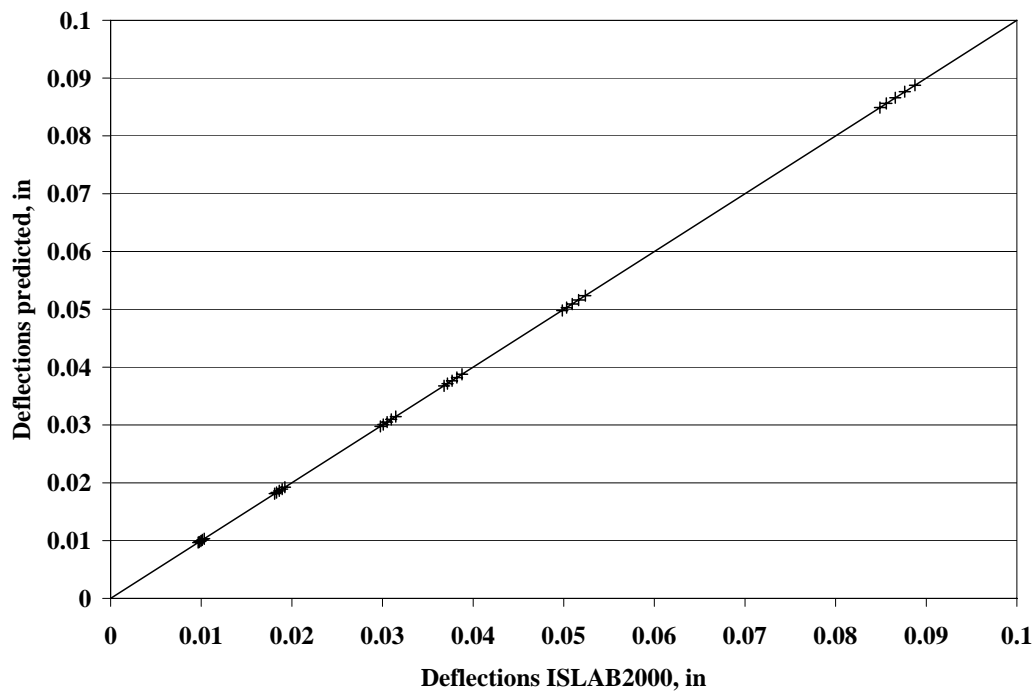


Figure 1.4.12. Comparison of ISLAB2000 and predicted free edge deflections.
Tandem axle loading, left wheel path critical dowel location

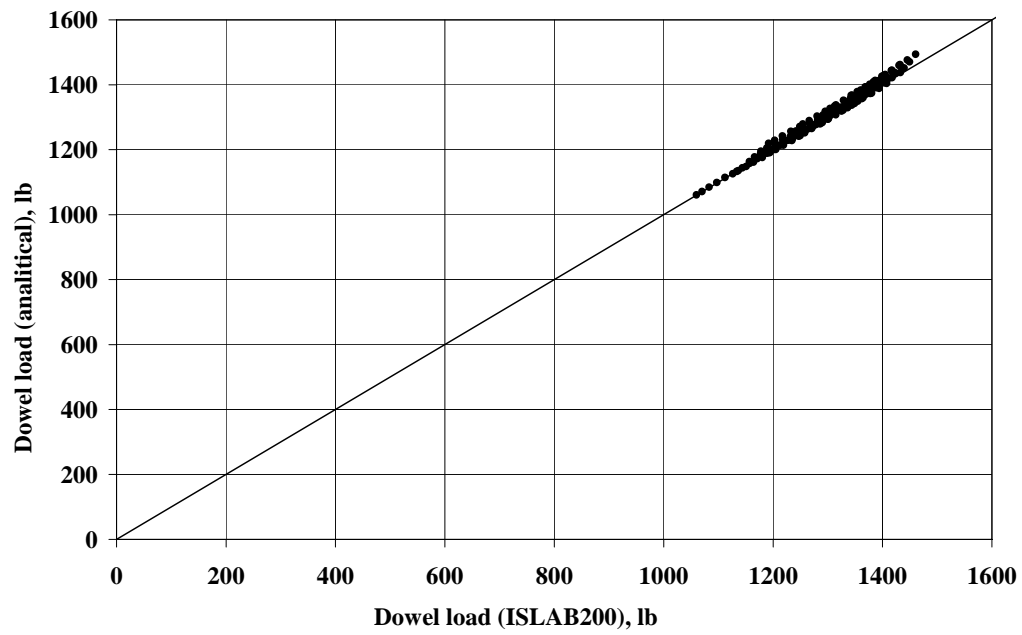


Figure 1.4.13. Total load transferred by a critical dowel, single axle loading, right wheel path dowel

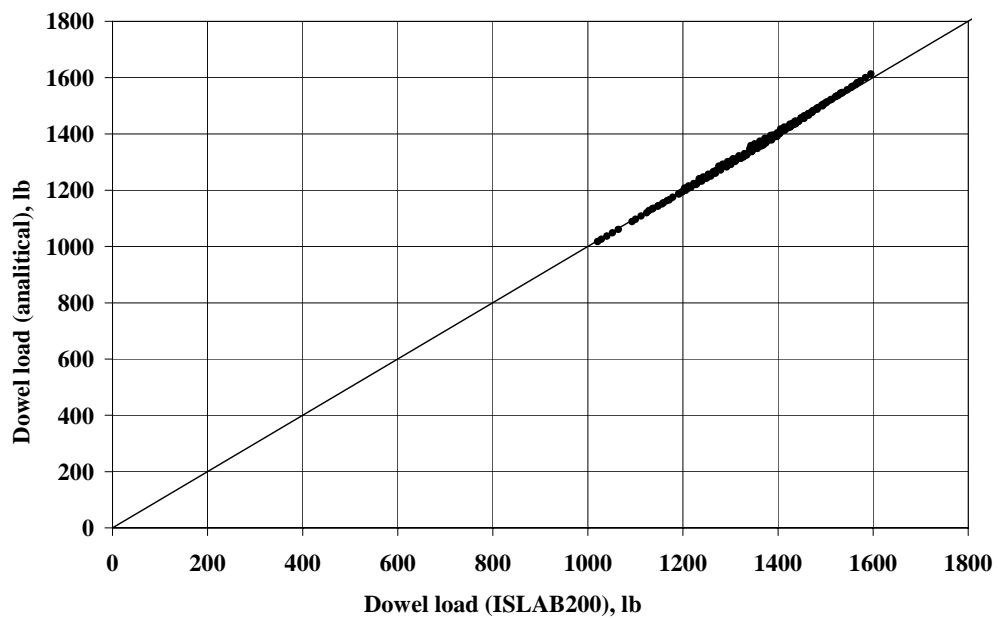


Figure 1.4.14. Total load transferred by a critical dowel, tandem axle loading, right wheel path dowel

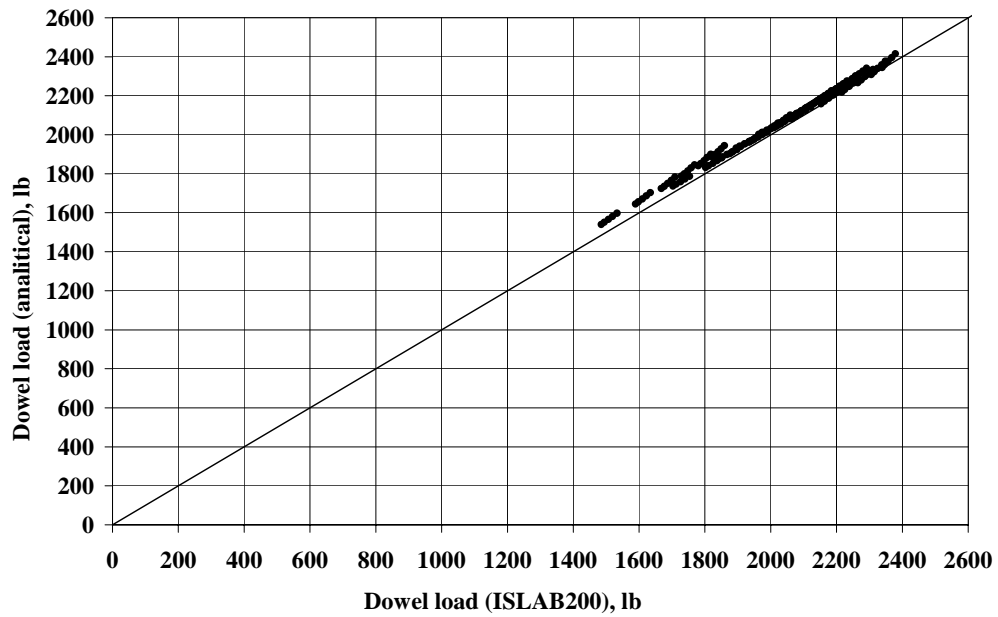


Figure 1.4.15. Total load transferred by a critical dowel, single axle loading, left wheel path dowel

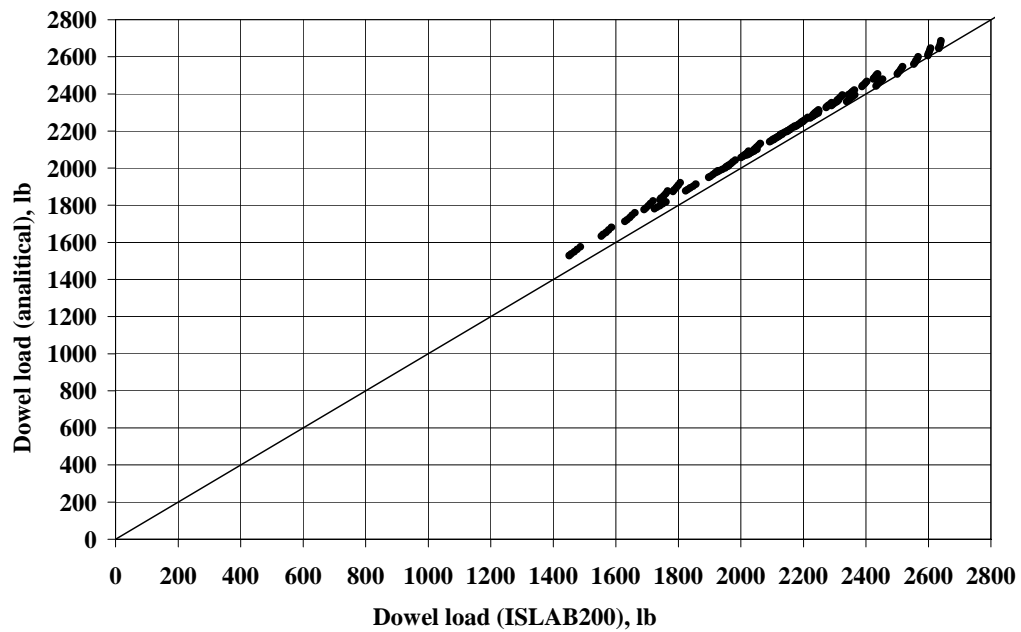


Figure 1.4.16. Total load transferred by a critical dowel, tandem axle loading, left wheel path dowel

1.5 Step-by-Step Analysis Procedure

The previous sections presented derivations for the simplified procedure for determination of the critical dowel loads and PCC bearing stresses. This procedure, which is applicable for a PCC slab-on-grade or a PCC-aggregate base on grade, is summarized below in an easy to use step-by-step format.

Required Input Parameters:

- PCC slab thickness, modulus of elasticity, and Poisson's ratio
- base thickness, modulus of elasticity
- coefficient of subgrade reaction
- dowel diameter, modulus of elasticity, and Poisson's ratio
- dowel spacing
- coefficient of dowel support (if known)
- Axle type (single or tandem) and axle weight
- Dowel location (left or right wheel path)

Analysis Steps:

Step 1. Compute the composite dense-liquid radius of relative stiffness:

$$l_k = \{(E_c h_c^3 + E_b h_b^3) / [12 (1 - \mu_c^2) k]\}^{0.25} \quad \text{Eq. 1.21}$$

where: l_k = composite dense-liquid radius of relative stiffness, inches
 E_c = modulus of elasticity of PCC slab, psi
 h_c = PCC slab thickness, inches
 E_b = modulus of elasticity of aggregate base, psi
 h_b = aggregate base thickness, inches
 μ_c = Poisson's ratio of PCC
 k = modulus of subgrade reaction (k-value), psi/in

Step 2. Determine dowel area in shear and moment inertia:

$$A_s = 0.9 \pi d^2 / 4 \quad \text{Eq. 1.13}$$

$$I_d = 0.9 \pi d^4 / 64 \quad \text{Eq. 1.22}$$

where: A_s = cross sectional area of dowel bar in shear, in²
 d = dowel diameter, inches
 I_d = moment of inertia of dowel, in⁴

Step 3. Estimate the modulus of dowel support::

$$K = 0.7951 E_c \quad \text{Eq. 1.9}$$

Step 4. Compute the relative stiffness of the embedded dowel:

$$\beta = [K d / (4 E_d I_d)]^{0.25} \quad \text{Eq. 1.2}$$

Where: E_d = Dowel bar modulus of elasticity, psi

Step 5. Compute dowel shear stiffness:

$$D = 1 / [Z^3(1+\Phi)/(12E_d I_d) + (2+\beta Z)/(2\beta^3 E_d I_d)] \quad \text{Eq 1.11}$$

$$\Phi = [24 (1+\mu_d) I_d] / [A_s Z^2] \quad \text{Eq. 1.12}$$

$$A_s = 0.9 \pi d^2 / 4 \quad \text{Eq. 1.13}$$

Where: Z = joint opening, inches
 μ_d = Poisson's ratio of the dowel bar material

Step 6. Compute the dimensionless joint stiffness:

$$AGG^* = D / s k I_k \quad \text{Eq. 1.15}$$

where: AGG^* = dimensionless joint stiffness
 s = dowel spacing, in

Step 7. Compute the deflection load transfer efficiency based on load type and location:

$$LTE (\%) = 100\% / [1 + c_1 AGG^{*c2}] \quad \text{Eq. 1.17}$$

Where: $LTE(\%) = \text{Deflection load transfer efficiency, \%} = 100\% d_u/d_l$
 $c_1 = a_1 + a_2 l_k + a_3 l_k^2$
 $c_2 = -\exp(b_1 + b_2 l_k + b_3 l_k^2)$
 $a_1, a_2, a_3, b_1, b_2, b_3 = \text{regression coefficients in Table 1.4.1}$

Eq. 1.18

Eq. 1.19

Table 1.4.1 Coefficients for Eqs. 1.18 and 1.19

Loading	a_1	a_2	a_3	b_1	b_2	b_3
18k SAL R WhP	1.77	-0.0382	0.000322	0.00503	-0.0113	0.000136
34k TAL R WhP	1.99	-0.0492	0.000455	-0.00341	-0.0114	0.000156
18k SAL L WhP	1.14	0.0168	-0.000175	-0.0442	-0.00596	0.0000823
34k TAL L WhP	1.34	0.00846	-0.000153	-0.0615	-0.00463	0.0000634

Step 8. Compute free edge deflection for the specified axle type and dowel position

$$\Delta_{\text{free-edge}} = [P / k l_k^2] [d_1 + d_2 l_k + d_3 l_k^2] \quad \text{Eq. 1.20}$$

where: $\Delta_{\text{free-edge}}$ = free edge deflection, inches
 P = total axle load, lbs
 d_1, d_2, d_3 = regression coefficients in Table 1.4.2

Table 1.4.2 Coefficients for Eq. 1.20

Loading	d_1	d_2	d_3	R^2
18k SAL-R WhP	0.0964	0.00353	0.0000603	0.9999
34k TAL-R WhP	0.0502	0.00039	0.0000876	0.9999
18k SAL-L WhP	0.138	0.0047	0.0000138	0.9999
34k TAL-L WhP	0.0602	0.0021	0.0000468	0.9999

Step 9. Estimate the magnitude of load transferred by the critical dowel:

$$P_c = D \Delta_{\text{free-edge}} (1 - \text{LTE}) / (1 + \text{LTE}) \quad \text{Eq. 1.14}$$

Step 10. Estimate PCC bearing stress under the critical dowel:

$$\sigma_c = [K P_c (2 + \beta Z)] / [4 \beta^3 E_d l_d] \quad \text{Eq. 1.5}$$

1.6 Early Age PCC Bearing Stresses

The procedure summarized in Section 1.5 was applied to investigate the effect of PCC age on PCC bearing stresses. The following pavement structure was analyzed:

- A 9-in PCC slab
- A 6-in aggregate base thickness, modulus of elasticity is equal to 30 ksi.
- Passing lane width – 12 ft
- Truck lane width – 14 ft (striped 2 ft off edge)
- Doweled transverse joints
- Joint type – dowel bars
- Dowel diameter – 1.25 in
- Dowel spacing – 12 in, beginning 6 in off the edges
- Steel modulus of elasticity – 20×10^6 psi
- Poisson's ratio of the dowel bar material – 0.2
- Modulus of dowel support - 500,000 psi/in
- Transverse joint spacing – 15 ft
- Longitudinal joints with joint stiffness 12,000 psi (approximate LTE=70%)

Two levels of subgrade support with modulus of subgrade reaction values equal to 100 and 200 psi/in were considered. An early-age PCC compressive strength gain from 2000 to 3000 psi was considered, with corresponding PCC modulus of elasticity increases estimated using the general ACI equation:

$$E_c = 57,000 f'_c{}^{0.5} \quad \text{Eq. 1.22}$$

where: f'_c = PCC compressive strength, psi

Figures 1.6.1 and 1.6.2 present the values of the bearing stresses under right and left wheel path critical dowels, respectively, for different levels of PCC compressive strength caused by an 18-kip single axle load applied at the corresponding critical locations. Figure 1.6.3 and 1.6.4 present the values of the bearing stresses under right and left wheel path critical dowels, respectively, for different levels of PCC compressive strength caused by a 34-kip tandem axle load applied at the corresponding critical locations. Figures 1.6.1 through 1.6.4 also present allowable bearing stresses determined using the following equation:

$$f_b = f'_c (4 - d) / 3 \quad \text{Eq. 1.23}$$

where: f_b = allowable bearing stress, psi

Analysis of Figures 1.6.1 and 1.6.3 show that if the PCC compressive strength exceeds 2000 psi the right wheel path dowel should sustain either applied load ($f_b > \sigma_c$). Figures 1.6.2 and 1.6.4 show, however, that the critical bearing stresses under the left wheel path dowel may exceed the allowable stresses if the PCC compressive strength is less than 2800 psi. Furthermore, for certain conditions (i.e., soft subgrade $k=100$ psi/in and tandem axle loading) the critical bearing stress exceeds the allowable stress even for the compressive strength equal to 3000 psi.

It should be noted, however, that the analysis presented above is specific to the input parameters selected. Figures 1.6.5 and 1.6.6 illustrate dowel bearing stress ratios under the left wheelpath critical dowel for the 34-kip tandem axle loading.

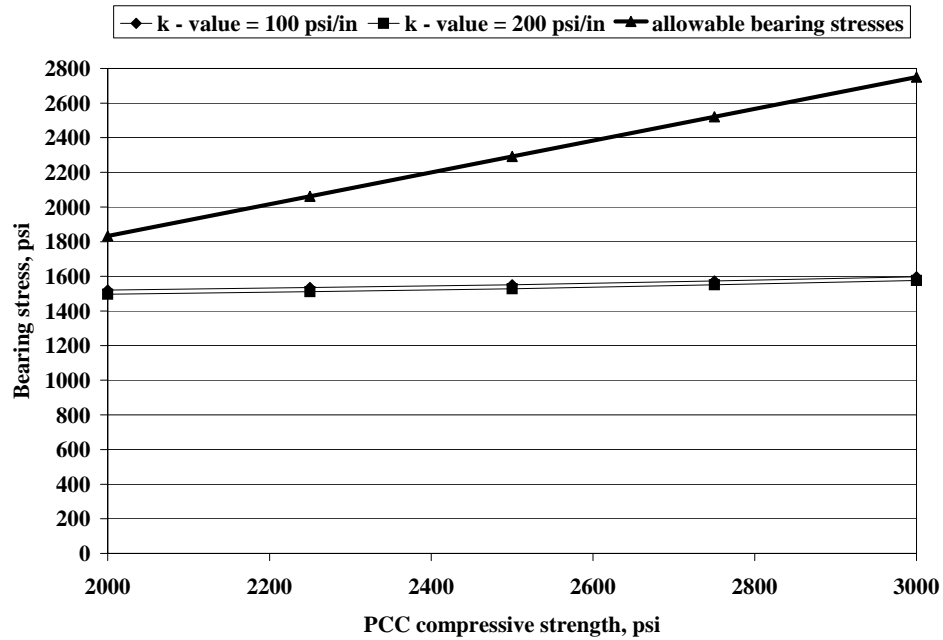


Figure 1.6.1. Bearing stresses vs. PCC strength, single axle loading, right wheel path dowel

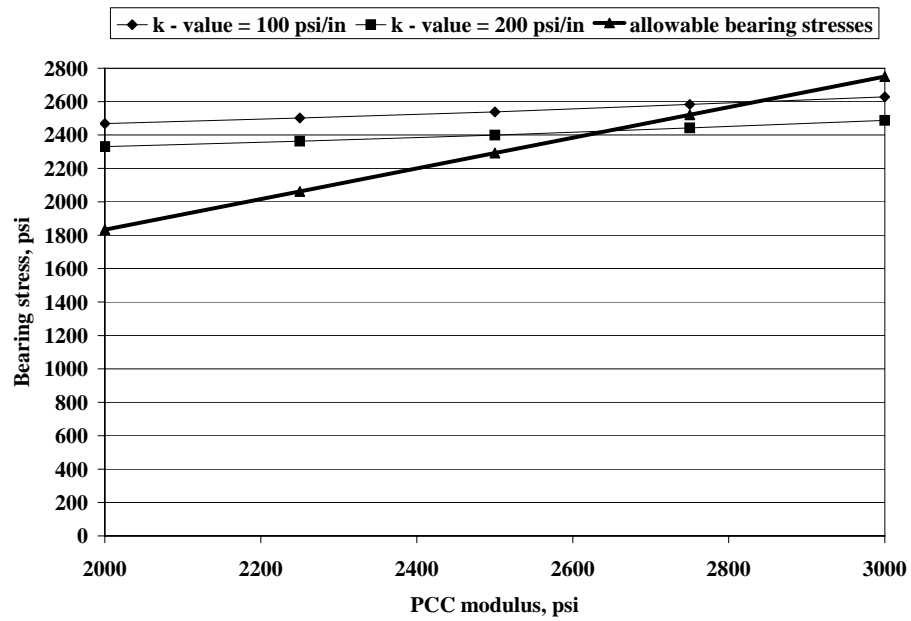


Figure 1.6.2. Bearing stresses vs. PCC strength, single axle loading, left wheel path dowel

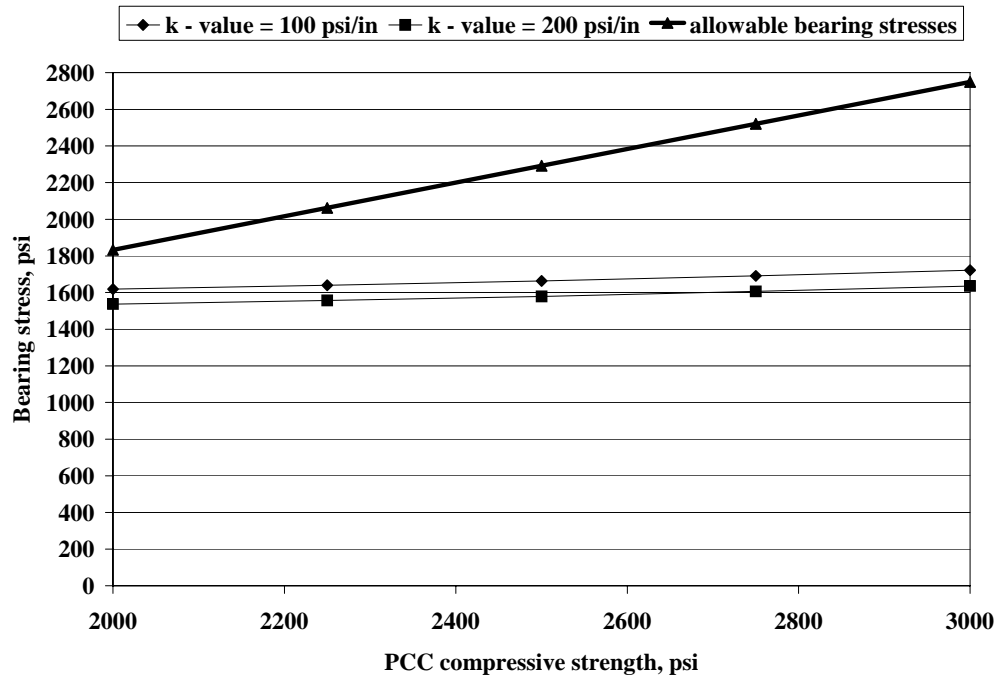


Figure 1.6.3. Bearing stresses vs. PCC strength, tandem axle loading, right wheel path dowel

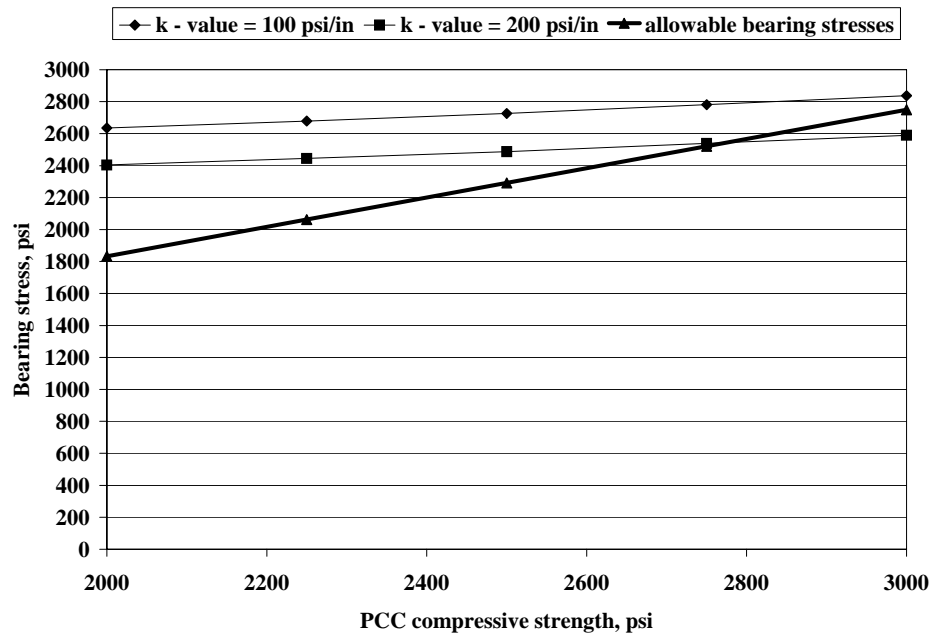


Figure 1.6.4. Bearing stresses vs. PCC strength, tandem axle loading, left wheel path dowel

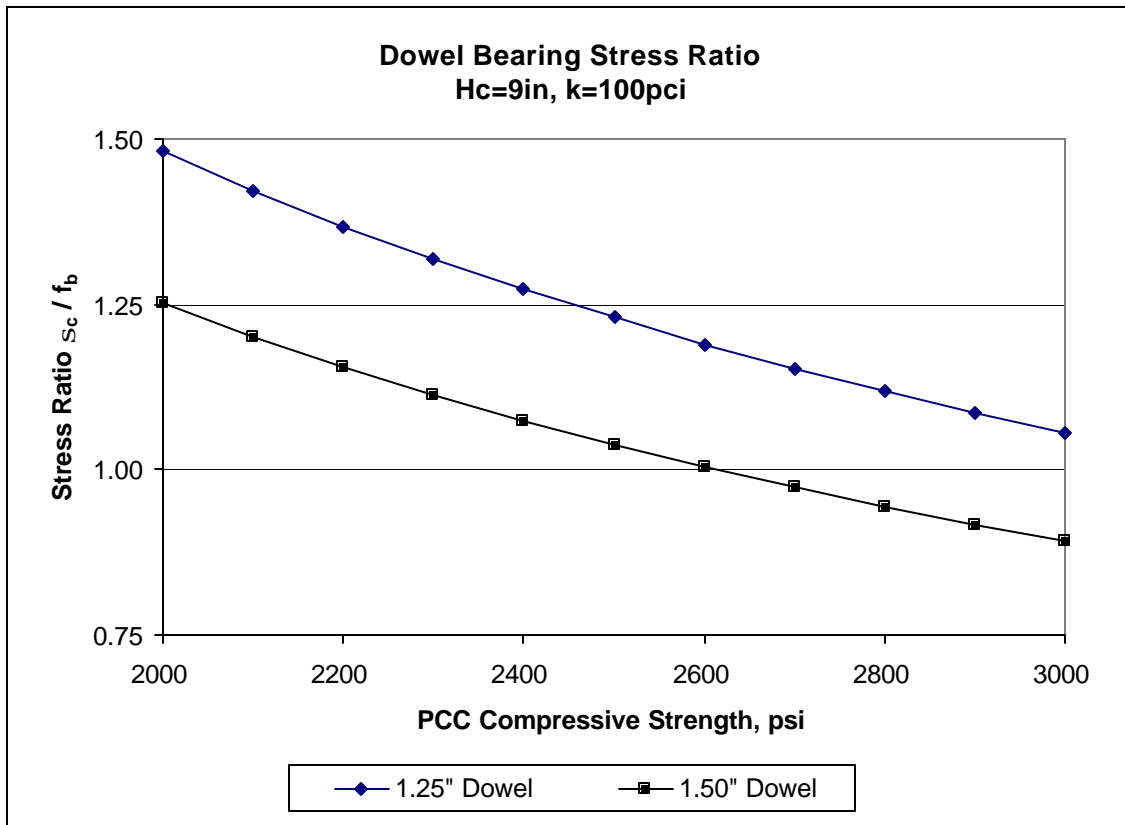


Figure 1.6.5. Dowel Bearing Stress Ratios, 34k TAL, left wheelpath

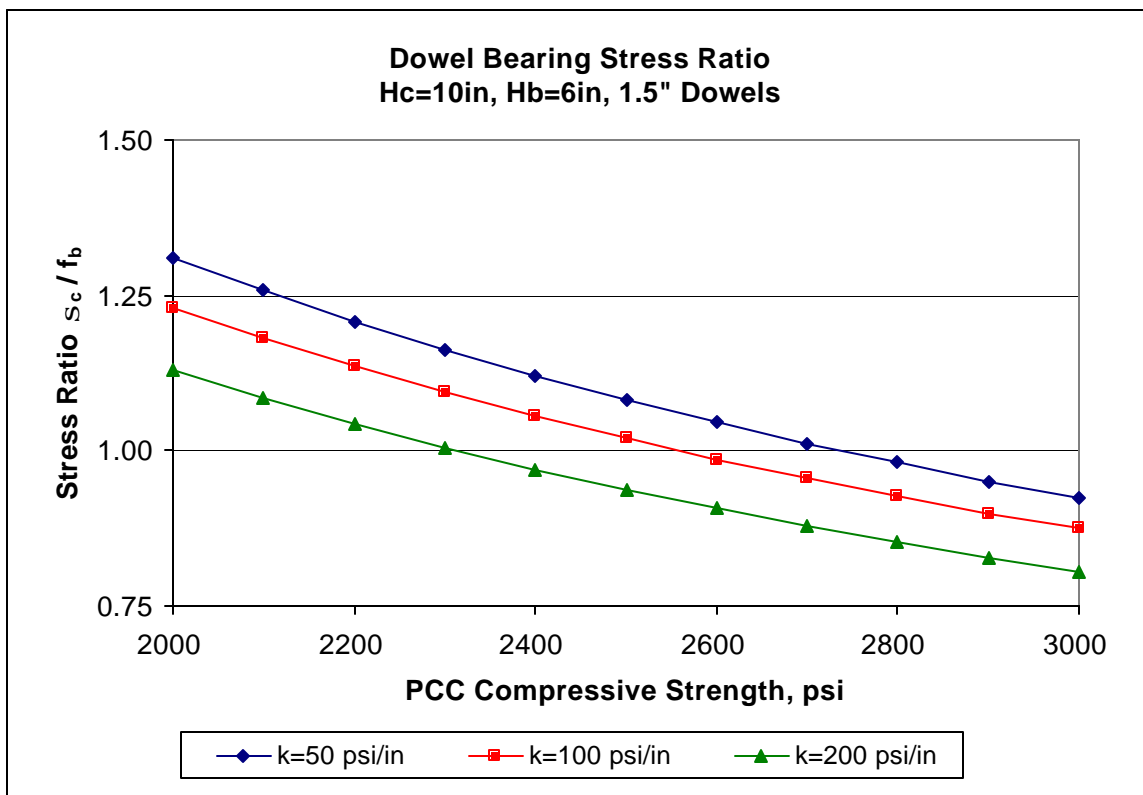


Figure 1.6.6. Dowel Bearing Stress Ratios, 34k TAL, left wheelpath

In Figures 1.6.5 and 1.6.6, the dowel bearing stress ratio, D_{BSR} , is calculated as:

$$D_{BSR} = \sigma_c / f_b \quad \text{Eq. 1.24}$$

As calculated, D_{BSR} values < 1.0 indicate safe dowel bearing stresses, i.e. bearing stress is less than the allowable bearing stress. Figure 1.6.5 indicates a reduced PCC compressive strength requirement from +3000 psi to 2600 psi if dowel bar size is increased to 1.5 inches, which exceeds current WisDOT requirements for a 9 inch PCC slab. Figure 1.6.6 indicates that for the typical WisDOT design conditions of 1.5 inch dowels and a 10 inch PCC slab thickness, minimum PCC compressive strengths ranging from 2300 to 2750 psi are necessary to maintain safe bearing stress ratios for the range of subgrade k-values considered.

1.7 Early Opening Criteria Used by Other States

The early opening criteria used by other States were reviewed and compiled to provide a framework for the criteria used in Wisconsin. Table 1.7.1 provides these criteria which are based on strength measures (flexural or compressive) and/or curing time. As shown the Wisconsin criteria of 3,000 psi minimum compressive strength is the median of all reported compressive strength requirements.

1.8 Summary of Dowel Bearing Stresses

The previous sections have described a method for determining critical bearing stresses in PCC pavements subjected to critical loadings during early age strength gain. The presented results generally support the WisDOT policy of restricting heavy loadings prior to reaching a PCC compressive strength of 3,000 psi for PCC slab thicknesses less than 10 inches where 1.25 inch dowels are specified. For thicker PCC slabs with 1.5 inch

dowels, minimum compressive strengths as low as 2,200 psi may be sufficient to protect the PCC from excessive bearing stresses under embedded dowels, depending on slab thickness, subgrade support value, and axle loading conditions.

The step-by-step analysis described in Section 1.5 provides an efficient method for determining minimum PCC compressive strength requirements to protect the PCC from excessive bearing stresses based on selected design inputs. This process is easily transferable to spreadsheet programs and provides a valuable design and analysis tool for PCC pavement designers.

Table 1.7.1 Early Opening Criteria Used in the U.S.

State	Criteria for Opening to Traffic ⁽¹⁾	Comment
AZ	≥ 3000 CS and 7D	
AR	≥ 3000 CS and 7D	1 D for HES
CA	≥ 550 FS and 10 D	
CO	≥ 3000 CS or 14 D	
CT	≥ 3500 CS	
DE	≥ 3500 CS	
FL	≥ 2400 CS and 14 D	less time if ≥ 550 FS
GA	≥ 2500 CS or 14 D	
HI	≥ 550 FS and 7 D	
ID	≥ 2500 CS	
IL	≥ 3500 CS or 14 D	
IN	≥ 550 FS and 14 D	
IA	≥ 500 FS	
KS	≥ 450 FS or 7 D	
KY	≥ 3625 CS	
LA	≥ 3000 CS or 14 D	
MA	≥ 550 FS and 7 D	≥ 550 FS for High Early Strength
MI	≥ 550 FS and 7 D	
MN	≥ 450 FS or 12 D	
MS	≥ 3500 CS and 28 D	
MO	≥ 3500 CS	
MT	≥ 500 FS	
NE	≥ 3500 CS and 14 D	
NV	≥ 550 FS and 10 D	≥ 550 FS for Type III Cement
NJ	≥ 3000 CS or 9-12 D	9 D May-Oct, 15 D Oct-May
NM	≥ 500 FS or 14 D	
NY	10 - 15 D	10 D Jun-Sep, 15D Sep-May

(1) CS=Compressive Strength, psi; FS =flexural strength, psi, D=days

Table 1.7.1 (Cont.) Early Opening Criteria Used in the U.S.

State	Criteria for Opening to Traffic ⁽¹⁾	Comment
NC	≥ 550 FS	Engineer may reduce time
ND	≥ 500 FS and 7 D	or ≥ 3000 CS and 7 D
OH	≥ 600 FS	
OK	≥ 3000 CS or 14 D	
OR	≥ 4000 CS and 14 D	
PA	≥ 3000 CS and 14 D	≥ 3000 CS and 3 D for High Early Strength
PR	≥ 3000 CS	
RI	≥ 525 FS and 7 D	
SD	≥ 4000 CS	
TN	≥ 3000 CS and 14 D	
UT	≥ 490 FS	
VA	≥ 600 FS or 14 D	
WA	≥ 2500 CS	
WI	≥ 3000 CS or 7 D	3-4 D for High Early Strength
WY	≥ 550 FS or 14 D	

(1) CS=Compressive Strength, psi; FS =flexural strength, psi, D=days

CHAPTER 2 FIELD STUDY

2.1 Introduction

The following sections describe the results of field testing conducted to document the early age strength gain of typical PCC paving mixtures used in Wisconsin. These results were used in conjunction with the laboratory study results presented in Chapter 3 to study the effects of early age loadings on long-term behavior.

The field study portion of this research included the sampling and testing of PCC paving materials used on four selected paving projects constructed in Wisconsin during the 2001-02 construction seasons. Projects were selected based on their availability and suitability for inclusion into this study. Table 2.1.1 provides details of the selected projects.

Table 2.1.1 Project Data

Project ID	Location	Section	Mix Type Coarse Aggregate Type
4015-00-71	STH57 - Fredonia	Rural	FA Gravel
2660-02-70	S. Whitnall Ave - Cudahy	Urban	FA Gravel
2350-05-70	STH 32 - Racine	Urban	FA Limestone
1442-04-71	STH 23 - Fond du Lac	Urban	FA Limestone

For each selected project, representative concrete materials were obtained from trucks delivering mix to the paving site. Sampling locations were selected based on their availability to provide a sufficient work area for the casting and curing of a variety of test specimens, including standard 6 in x 12 in cylinders, 4 in x 8 in cylinders, 4 in x 4 in x 24 in beam specimens, and 12 in x 12 in x 24 in exposed dowel specimens. Test specimens were field cured under exposed conditions similar to those for the pavement they represent. Prevailing air and internal mix temperatures recorded at 10 minute intervals in the test specimens and mainline pavement to provide comparative measures to assess prevailing curing regimes.

2.2 Curing Conditions

As mentioned above, a primary focus of the field study was to develop test specimens that closely matched the mainline pavements with respect to the degree of curing. In traditional quality control applications, concrete cylinders are cast in the field and then cured in enclosed boxes and/or under water, which simulates standard laboratory curing conditions. Exposed curing of test specimens was selected by the researchers to better represent the curing conditions of in-place pavement materials and thus provide a better representation of early age behavior. It is recognized that the pavement mass provides better protection from heat loss that can be obtained with small-sized specimens. However, the degree to which this protective mass affects the actual strength gain of the PCC is uncertain.

It is well documented that the strength gain in PCC is a function of both time and temperature. During standard laboratory curing, the curing temperature is assumed to be equal to the water temperature in which the specimen is immersed and test results are

usually reported as an attained compressive strength after a specified curing time (i.e., 2,500 psi @ 3 days). The maturity concept, which may be defined as either the product of the time and temperature or as an equivalent age at some specified temperature, has been utilized for the estimation of the strength of concrete without the need of physical tests, particularly when the curing regime deviates from standard laboratory conditions, which is typically the case for highway pavements.

During field fabrication of test specimens, multi-depth pavement probes were inserted into test specimens and the mainline pavement to obtain top, middle and bottom temperature measures during curing. A separate air temperature sensor was used to obtain ambient measures at a height of approximately 3 feet above the pavement surface. These measures were used to develop maturity data for the pavement and test specimens.

During initial testing on STH 57-Fredonia, test cylinders were cast and field-cured using two protective methods: surface-applied curing compound and clear plastic bags. The curing compound and plastic bags were obtained from the paving contractor during fabrication. Figures 2.2.1 through 2.2.5 illustrate air, cylinder and pavement temperature measures during the initial 7 days after placement from data recorded at approximately 10 minute intervals. As indicated in Figure 2.2.1, air temperatures approached freezing on three of the first five nights after paving. The cylinder temperature profiles provided in Figures 2.2.2 and 2.2.3 exhibit larger diurnal temperature swings than do the pavement temperature profiles displayed in Figures 2.2.4 and 2.2.5, which indicates the effects of the protective mass of the mainline pavement. Figure 2.2.6 provides the 7-day maturity values for the cylinders and mainline pavement.

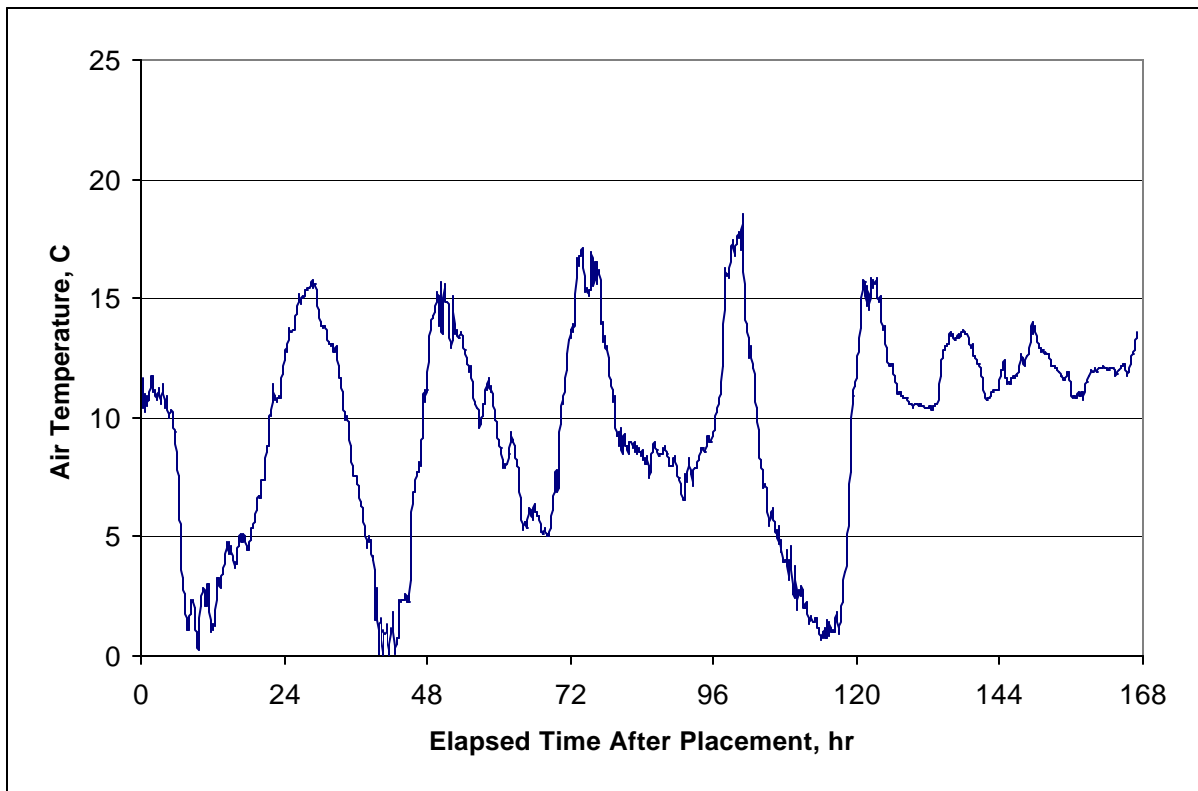


Figure 2.2.1 7-Day Post Paving Temperature Profile, STH 57-Fredonia

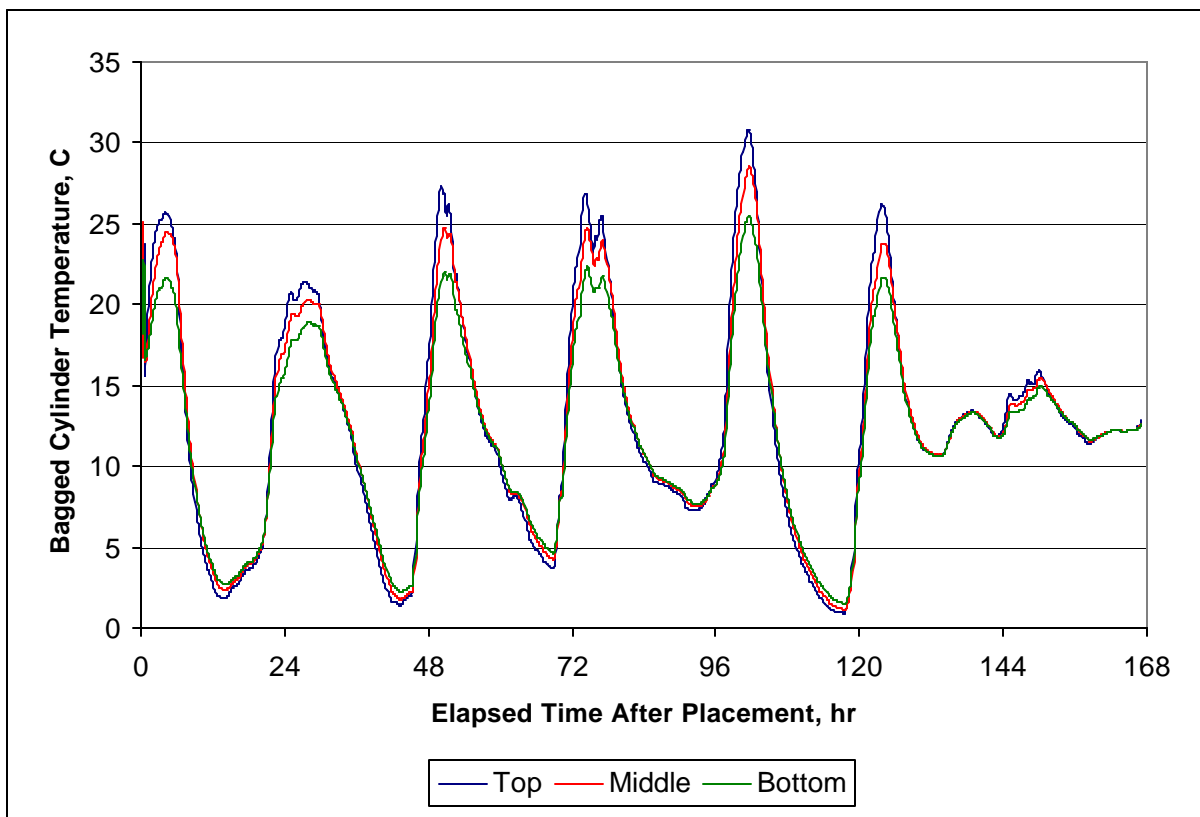


Figure 2.2.2 7-Day Post Paving Temperature Profile, STH 57-Fredonia

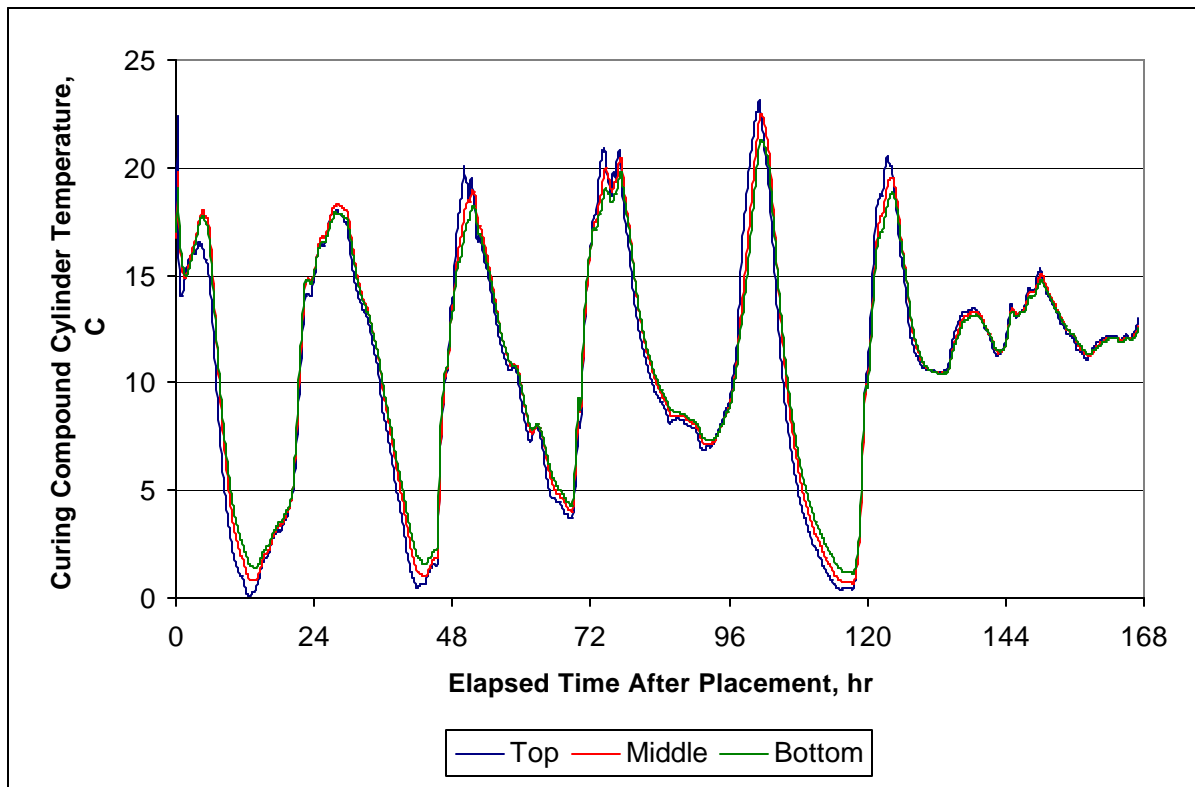


Figure 2.2.3 7-Day Post Paving Temperature Profile, STH 57-Fredonia

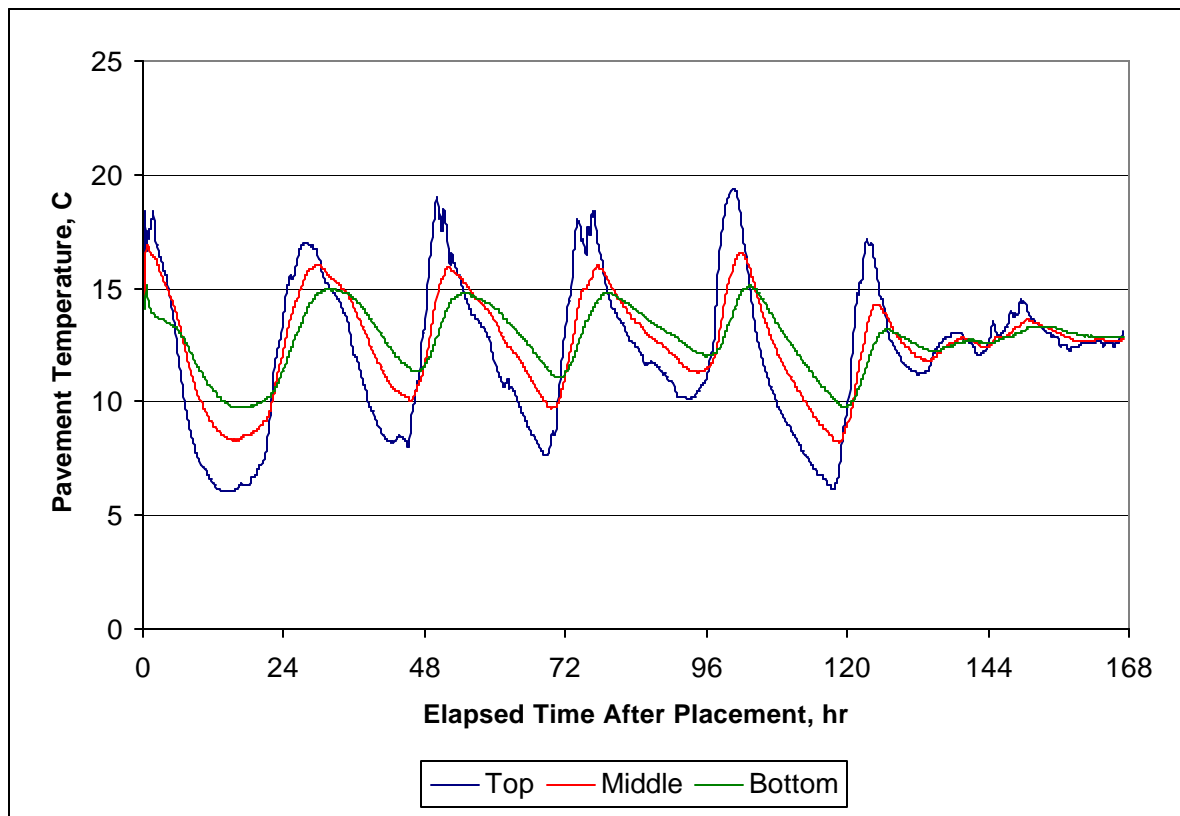


Figure 2.2.4 7-Day Post Paving Temperature Profile, STH 57-Fredonia

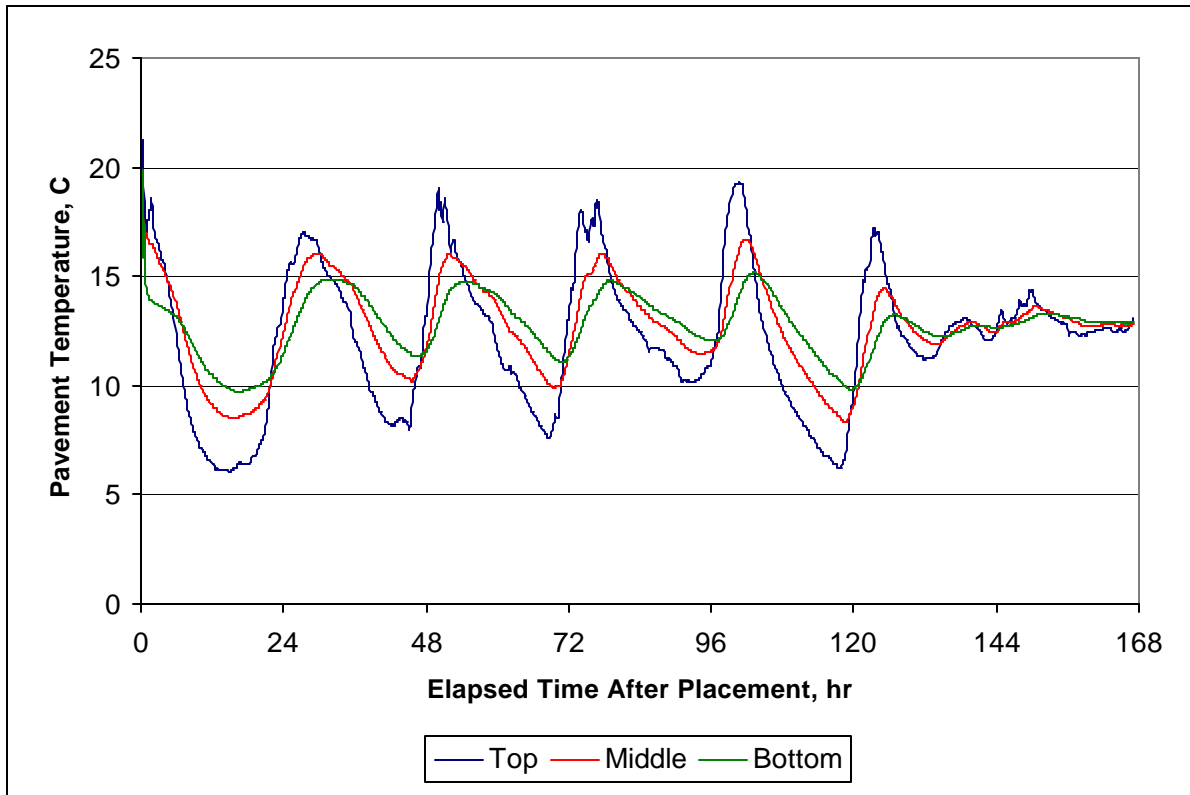


Figure 2.2.5 7-Day Post Paving Temperature Profile, STH 57-Fredonia

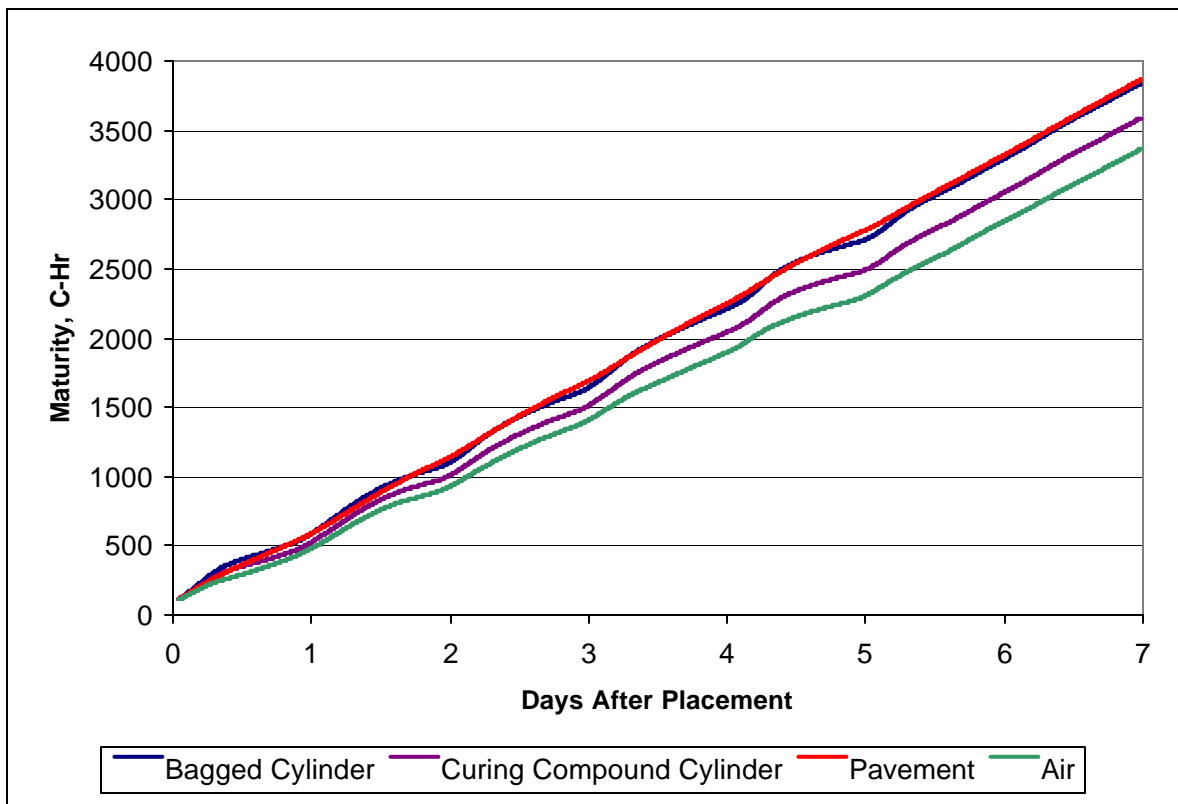


Figure 2.2.6 7-Day Post Paving Maturity Profile, STH 57-Fredonia

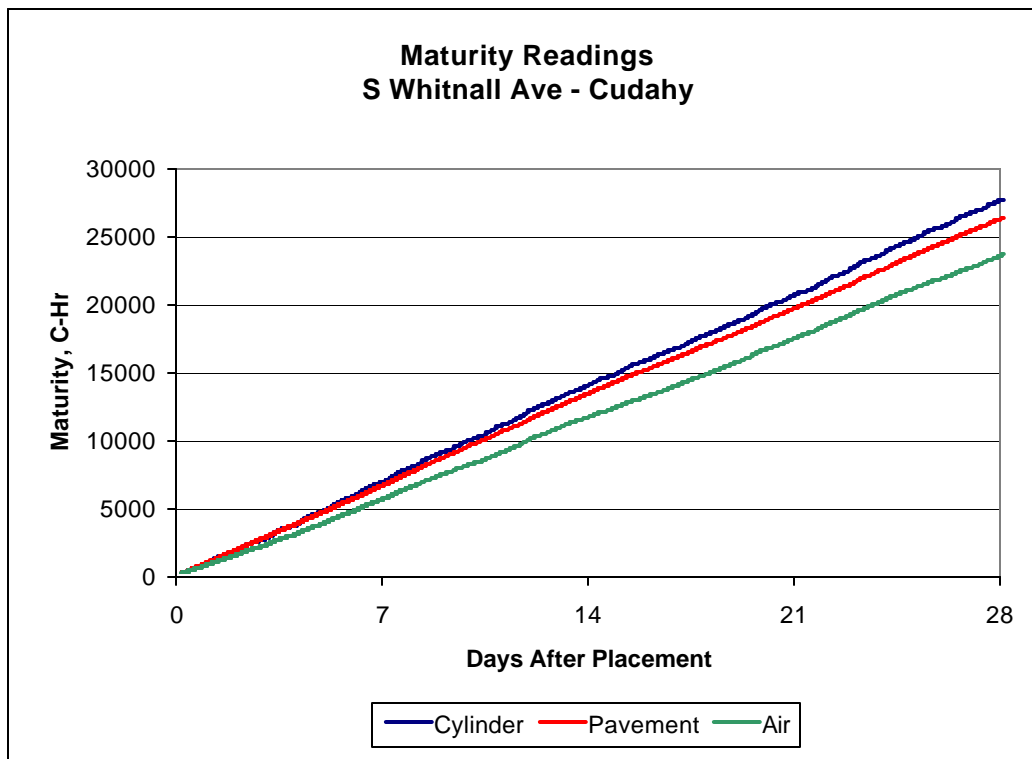
The cylinder and pavement temperature data were used to compute maturity values using the following equation:

$$\text{Maturity} = \sum (T_i + 10) H_i \quad \text{Eq. 2.1}$$

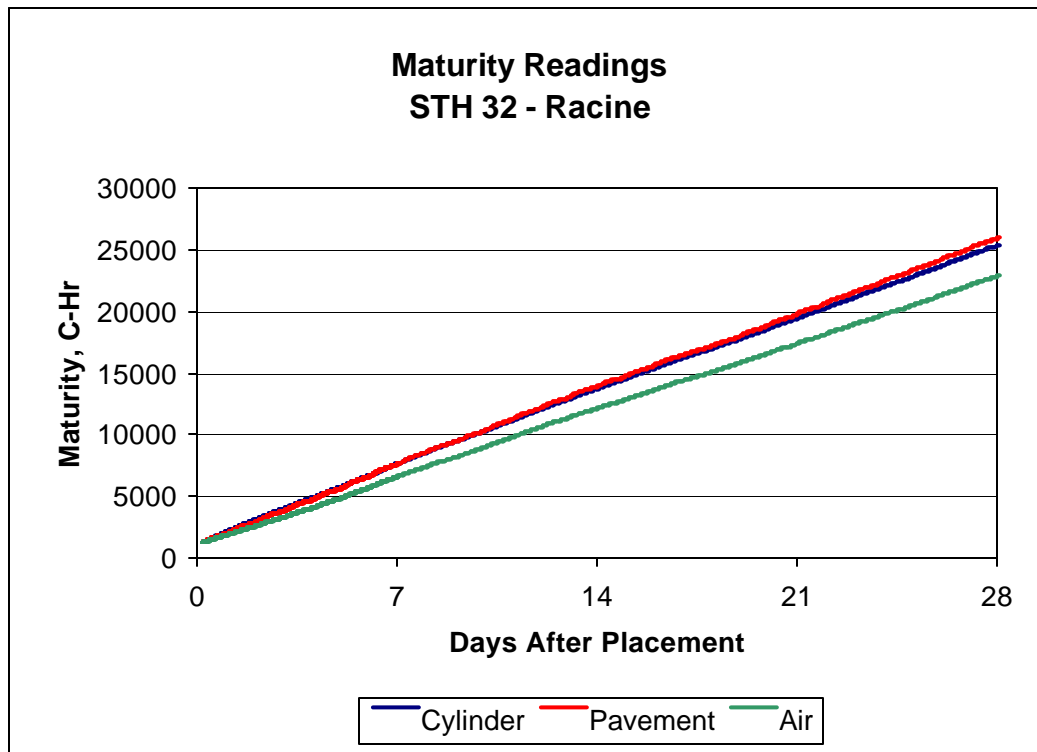
Where: T_i = average temperature reading [(top+mid+bottom)/3] obtained during time increment i , C
 H_i = length of time increment, hr

As shown in Figure 2.2.6, the bagged cylinder closely matches the mainline pavement maturity values while the curing compound cylinder maturity values are approximately 10% lower. Based on these findings, it was deemed justified to utilize field-cured bagged cylinders as representative of the maturity of the mainline pavement. The temperature readings were terminated after seven days of curing due to the rapid and unexpected strength gain of the PCC, as discussed in Chapter 3.

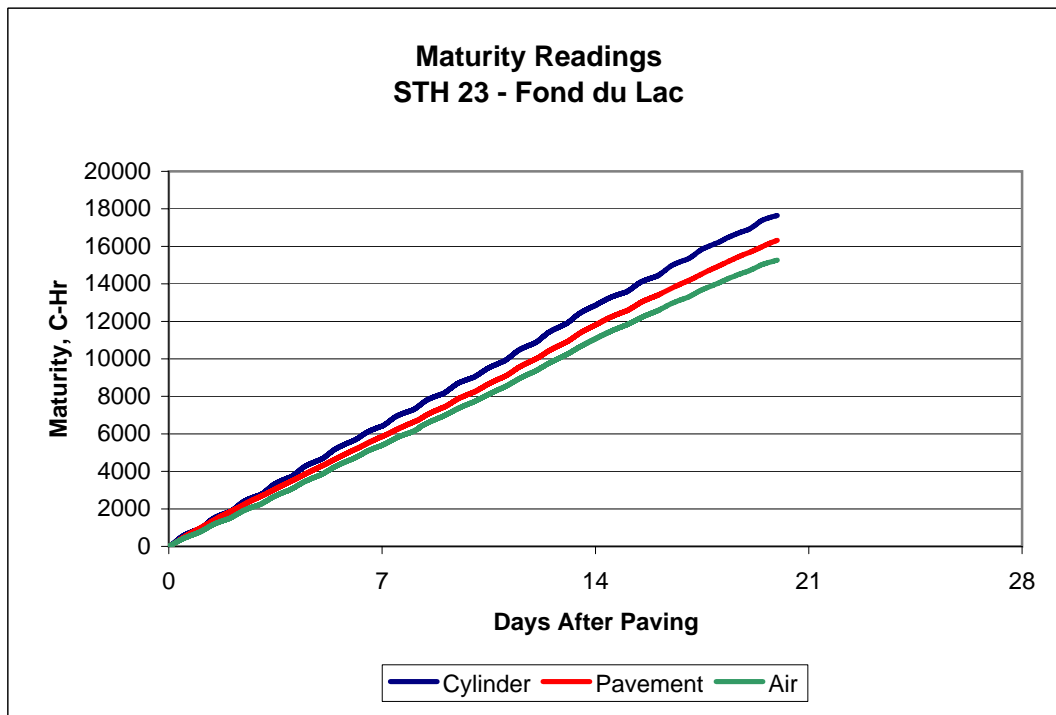
Figures 2.2.7 through 2.2.9 illustrate maturity values for cylinders (1 per project) and mainline pavement for the remaining three paving projects included in this study. As shown, the maturity values for the bagged, field-cured cylinders closely match the mainline pavement values for the Whitnall Ave and STH 32 projects but are approximately 8% higher for the STH 23 project. For all projects, air maturity values are consistently below pavement and cylinder values. It should be noted that the STH 23 temperature probe wires were severed during adjacent construction activities 20 days after paving. The Marquette research staff was not informed of this disruption and did not become aware of it until returning to the job site on day 28 to download the final temperature data. Hence no maturity data is available from day 20 to day 28.



2.2.7: 28-Day post paving Maturity Plot for S Whitnall Ave - Cudahy



2.2.8: 28-Day post paving Maturity Plot for STH 32 - Racine



2.2.9: 20-Day post paving Maturity Plot for STH 23 - Fond du Lac

2.3 Summary

Temperature readings obtained with multi-depth probes placed within the mainline pavement and fabricated test cylinders indicate that the maturity of the mainline pavement is closely matched by field-cured cylinders protected by a clear plastic bag. This bag results in a terrarium effect which helps prevent moisture loss and maintains cylinder temperatures. Based on these findings, it is inferred that strength measures obtained from these field-cured cylinders generally represent those that would be obtained from cylinders cored from the mainline pavement. The use of the maturity concept for predicting the in-place strength of mainline pavements is presented in Chapter 3.

CHAPTER 3 LABORATORY STUDY

3.1 Introduction

Laboratory testing was conducted on all fabricated specimens to develop relations between strength measures and maturity. Two randomly selected concrete cylinders were tested in compression at selected times of curing to develop early-age strength gain characteristics. Single randomly selected beam specimens were tested in flexure (third-point loading) to provide comparative strength measures. The average compressive and flexural strengths obtained at the various stages of curing were used in combination with prevailing curing temperatures to develop maturity relations for each mixture tested.

Single randomly selected exposed dowel specimens were also tested in conjunction with compression and flexural testing by applying a short-term cyclic load to the exposed dowel. After initial loading, the exposed dowel specimens were allowed to field cure for the full 28 days. After full curing, static loading of the exposed dowel was conducted to determine relative dowel/concrete displacements and concrete surrounding the dowel in the compression zone was examined for evidence of cracking.

3.2 Compression Test Results

Standard cylinder compression tests were typically performed at Marquette University using a 400-kip Forney compression tester. The primary focus of this testing was to develop information on the early-age strength gain of the PCC and to identify appropriate testing times for the exposed dowel specimens, i.e. when the PCC compressive strength would be in the range of 2,000 to 3,000 psi. This target early-age

strength range was selected based on the dowel-concrete bearing stress analysis presented in Chapter 1.

Initial testing was conducted approximately 24 hours after placement to establish baseline strength values. Based on these baseline values, subsequent test times were estimated to yield compressive strength values within the desired range.

3.2.1 STH 57 - Fredonia

Sampling and specimen fabrication was conducted mid-day on Wednesday, October 17, 2001 in conjunction with normal paving operations. Air temperatures at the time of sampling were approximately 11C (52F) with mix temperatures at placement of approximately 17 C (63F). Air temperatures remained relatively steady during daylight hours, after which they steadily declined to a night time low near freezing (Figure 2.2.1). Mainline and cylinder temperatures also showed significant overnight declines (Figures 2.2.2 and 2.2.4). An initial cylinder compression test was conducted on Thursday, October 18th, 28 hours after placement using contractor test equipment available in the field. This initial test yielded a compressive strength of 338 psi, and due to this low value, no other strength tests were obtained. A second compression test was conducted on Friday, October 19th, 48.5 hours after placement, again using contractor test equipment, yielding a compressive strength of 1,360 psi. Based on these initial strength measures, a reported 3-day strength of 1,876 psi under laboratory curing conditions, and projected weekend temperatures similar to those prevailing since placement, it was decided to suspend compression testing until Monday, October 22nd.

Subsequent compression tests were conducted at Marquette University on October 22nd, 120 hours after placement. Tests results from two randomly selected specimens

yielded compressive strengths of 4,530 and 4,228 psi, significantly greater than expected based on the prevailing temperatures and the mix design data provided by the contractor which, under standard laboratory curing conditions indicated projected compressive strengths of 1876, 2847 and 4291 psi at 3, 7 and 28 days, respectively. Subsequent cylinder testing conducted at Marquette confirmed the higher than expected compressive strength values and indicated that the target early-age strength range was consumed during the weekend. Figure 3.2.1 provides comparative compressive strength results vs curing days for this mixture as measured by Marquette staff and as reported by GeoTest in their 08/14/01 report of laboratory trial batch. As shown, consistently higher strength values were obtained during tests conducted at Marquette using materials obtained during paving.

The increased strength results noted from the Marquette testing were discussed with the paving contractor and it was indicated that a change in the mix design, which increased the dosage of water reducer, most likely led to the increased strengths. As paving was already completed for this project phase, the opportunity to re-do the sampling and testing was lost. Instead, sufficient material samples were obtained from the on-site batch plant to allow for the lab mixing and casting of additional specimens to better define the early-age strength gain. Concrete cylinders were cast using both 4 in x 8 in and 6 in x 12 in cylinders molds to test the suitability of the smaller cylinders for estimating concrete strength gain. Figure 3.2.2 provides compressive strength results for the lab and field specimens. As shown, the laboratory mix results are slightly higher than comparable field results and no significant differences exist between test results for the 4x8 and 6x12 specimens.

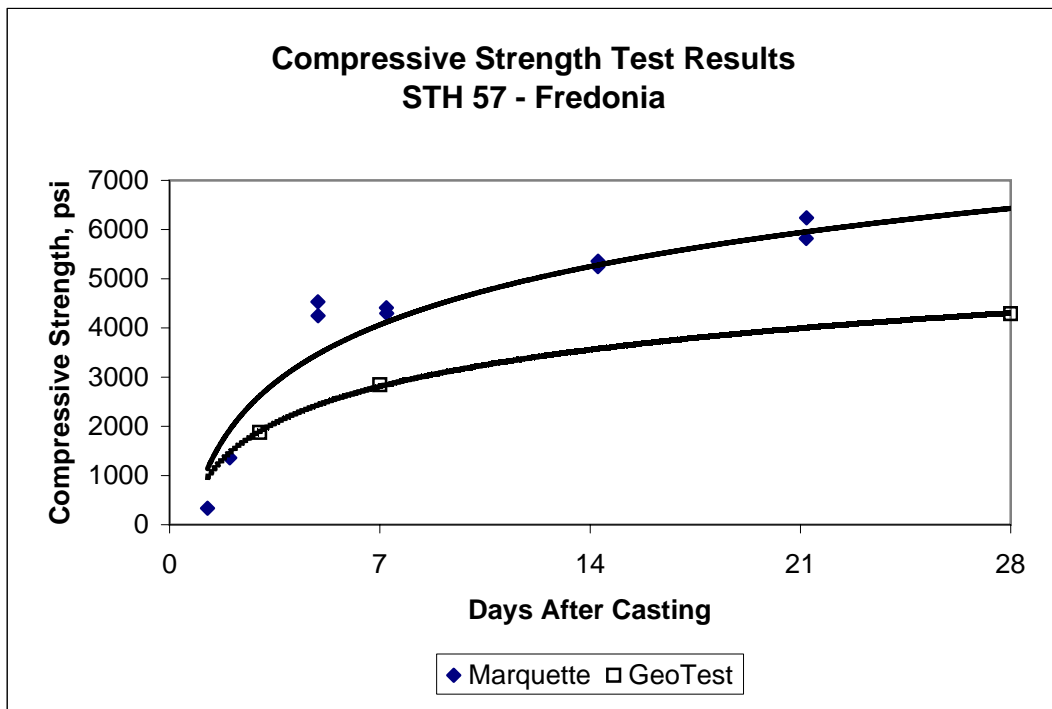


Figure 3.2.1: Comparative Compressive Strength Results, STH 57 - Fredonia

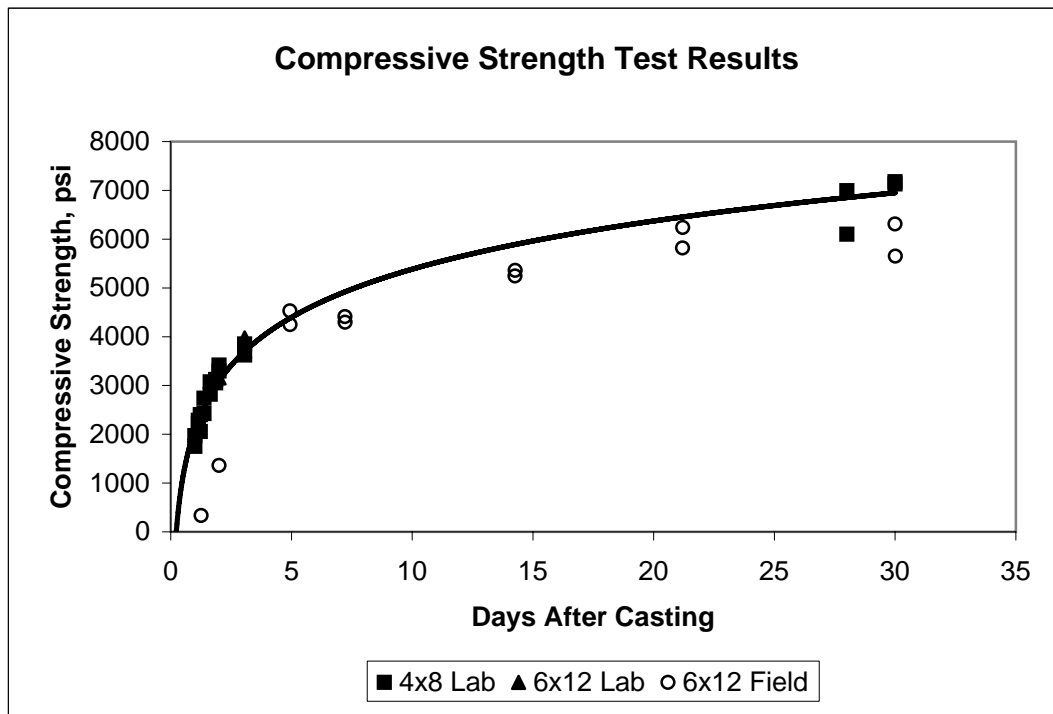


Figure 3.2.2: Comparative Compressive Strength Results, STH 57 - Fredonia

3.2.2 South Whitnall Avenue - Cudahy

Sampling and specimen fabrication was conducted late-morning on Thursday, June 27, 2002 in conjunction with normal paving operations. Air temperatures at the time of sampling were approximately 22C (72F) with mix temperatures at placement of approximately 27 C (81F). Air temperatures remained relatively steady throughout the daylight hours, dropping to a low of approximately 19C (66F) during the first evening. Daytime high continually increased during the next 7 days after placement, reaching a high of approximately 36C (97F) on day 7. Nighttime lows ranged from 12C (54F) to 23C (73F) during this period.

Initial 6in x 12 in cylinder compression tests were conducted on Friday, June 28th, 24 hours after placement, yielding an average compressive strength of 1158 psi. Subsequent compression tests were performed at post-placement times of 28, 35, 45, 53, 70 and 94 hours after placement to define the early-age strength gain. A final set of compression tests were performed 28 days after placement. Figure 3.2.3 provides a plot of the strength gain for this mixture.

3.2.3 STH 32 - Racine

Sampling and specimen fabrication were conducted late-morning on Monday, August 5, 2002 in conjunction with normal paving operations. Air temperatures at the time of sampling were approximately 26C (79F) with mix temperatures at placement of approximately 33C (91F). Air temperatures rose to 27C (81F) during the morning hours and then steady declined throughout the day, dropping to a low of approximately 18C (64F) during the first evening. Daytime high continually increased during the next 7 days after placement, reaching a high of approximately 37C (99F) on day 7. Nighttime lows ranged

from 13C (55F) to 20C (68F) during this period.

Initial 4 in x 8 in cylinder compression tests were conducted on Tuesday, August 6th, 25 hours after placement, yielding an average compressive strength of 2082 psi. Subsequent compression tests were performed at post-placement times of 30, 47, 52, and 72 hours after placement to define the early-age strength gain. Additional compression tests were performed at 7, 14 and 29 days after placement to define the longer-term strength gain. Figure 3.2.4 provides a plot of the strength gain for this mixture.

3.2.4 STH 23 - Fond du Lac

Sampling and specimen fabrication were completed during the morning of Tuesday, August 27, 2002 in conjunction with normal paving operations. Air temperatures at the time of sampling were approximately 22C (72F) with mix temperatures at placement of approximately 23C (73F). Air temperatures rose to a high of 30C (86F) during daylight hours, dropping to a low of approximately 15C (59F) during the first evening. Daytime highs ranged from 28C (82F) to 33C (91F) during the next 7 days after placement, with nighttime lows ranging from 12C (54F) to 17C (63F) during this period.

Initial 4 in x 8 in cylinder compression tests were conducted on Wednesday, August 28th, 27.5 hours after placement, yielding an average compressive strength of 1628 psi. Subsequent compression tests were performed at post-placement times of 35.5, 50, 59, 72, 82.5, 96, 121.5 and 169.5 hours after placement to define the early-age strength gain. The larger number of test times resulted due to the slower strength gain of this mixture. Additional compression tests were performed at 13 and 29 days after placement to define the longer-term strength gain. Figure 3.2.5 provides a plot of the strength gain for this mixture.

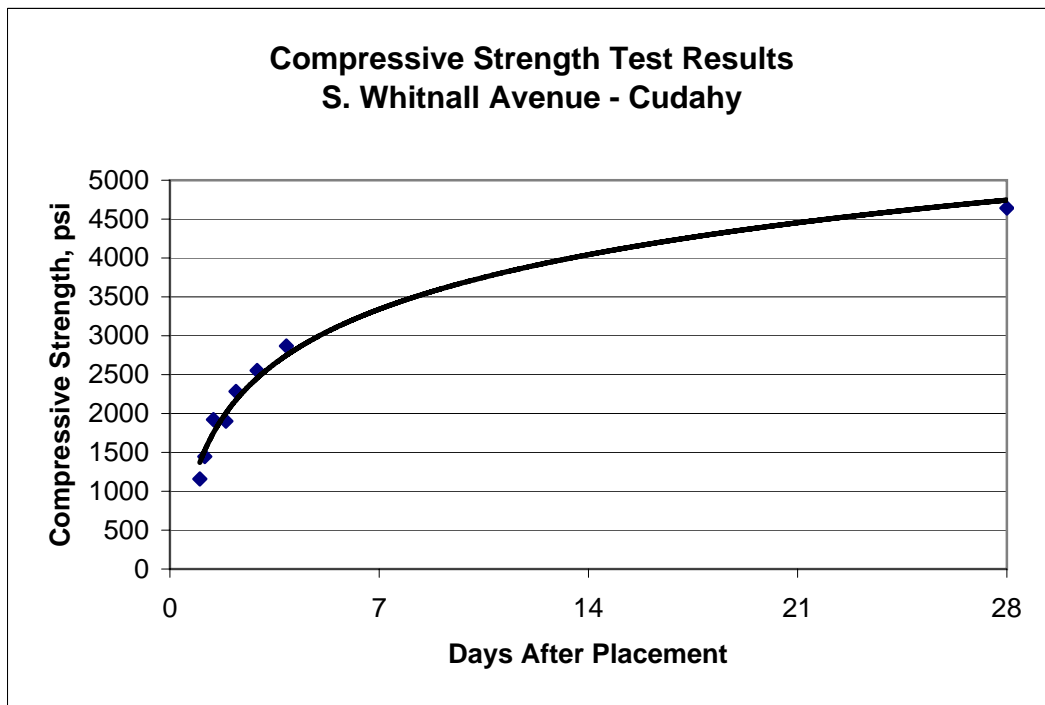


Figure 3.2.3: Compressive Strength Results, S Whitnall Ave - Cudahy

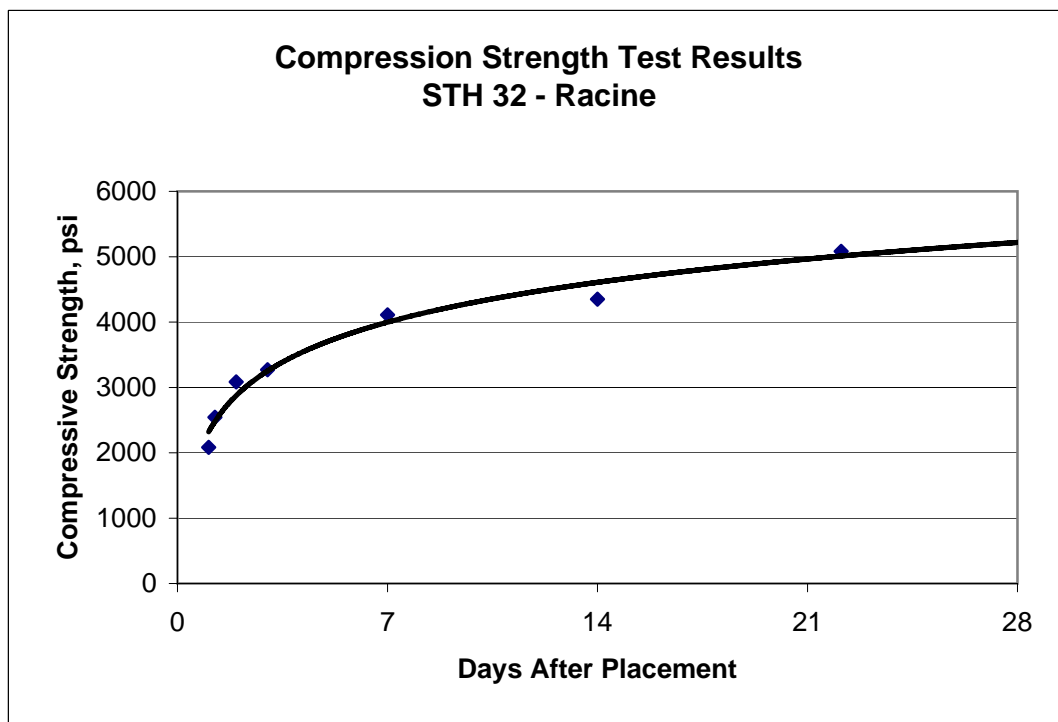


Figure 3.2.4: Compressive Strength Results, STH 32 - Racine

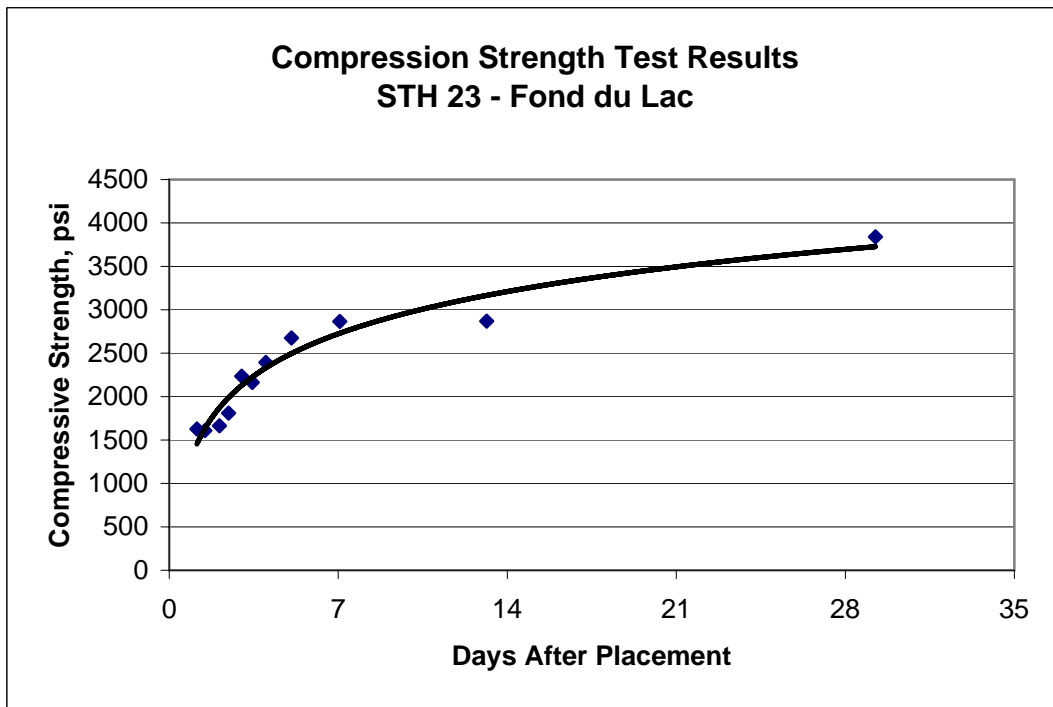


Figure 3.2.5: Compressive Strength Results, STH 23 - Fond du Lac

3.2.5 Maturity Readings

The field air and bagged cylinder temperature data collected from all projects were utilized to develop compressive strength versus maturity data. For this analysis, maturity was calculated using the Nurse-Saul expression:

$$M(t) = \sum (T_a - T_o) \Delta t \quad \text{Eq. 3.1}$$

Where: $M(t)$ = maturity at age t , C-Hr
 T_a = average temperature during recorded time interval, C
 T_o = datum temperature = -10C
 Δt = time interval, hr

Air and bagged concrete cylinder maturity values were computed by Eq. 3.1 using recorded average ambient air temperatures and average cylinder temperatures, respectively.

Figures 3.2.6 and 3.2.7 provide measured compressive strengths versus air and bagged cylinder maturity values, respectively, for all project data. As shown, data from each project follow expected log-linear trends but due to the various mix designs and 28-day compressive strengths, each project follows a different trend line, as expected.

The maturity trend lines developed for each project were used to estimate respective 28-day compressive strengths based on standard laboratory curing conditions, which equates to a maturity value of 20,832 C-Hr [$28 \times 24 \times (21 + 10) = 20,832$]. For each project, the measured compressive strengths and estimated 28-Day strengths were then used to compute the %28-Day Strength. These values were then plotted versus the recorded air and bagged cylinder maturity values. Figures 3.2.8 and 3.2.9 provide combined maturity plots based on air and bagged cylinder maturity values, respectively.

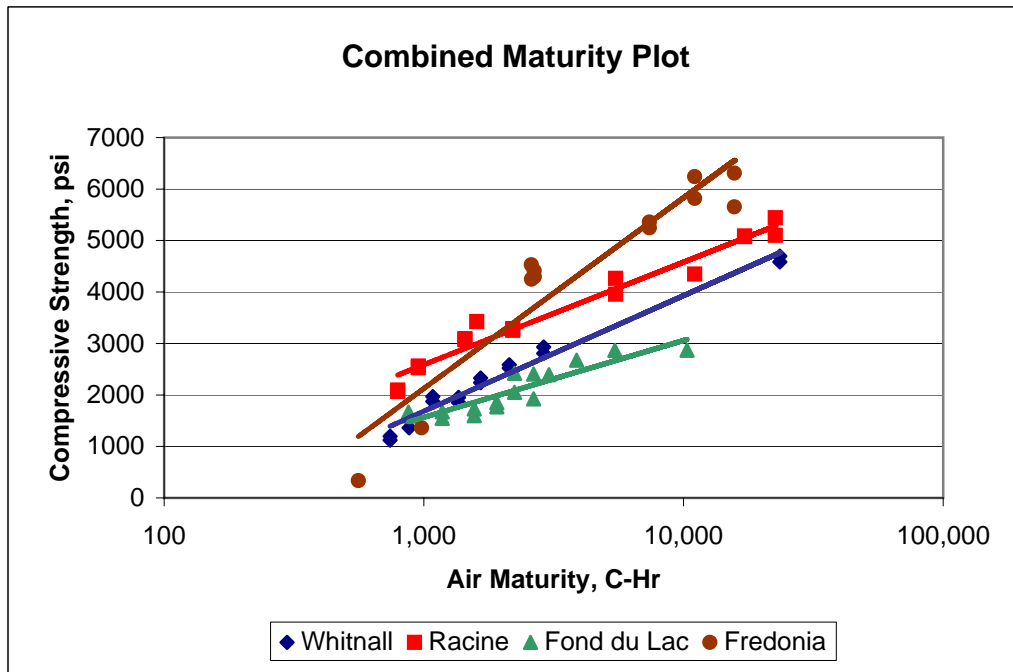


Figure 3.2.6: Project Maturity Plots Using Air Temperatures

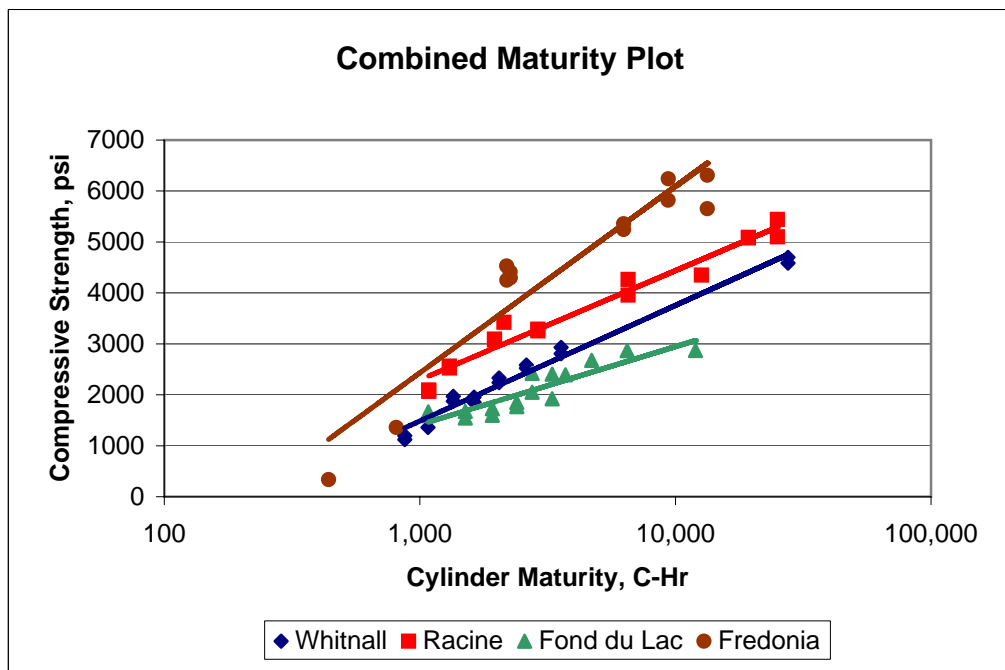


Figure 3.2.7: Project Maturity Plots Using Bagged Cylinder Temperatures

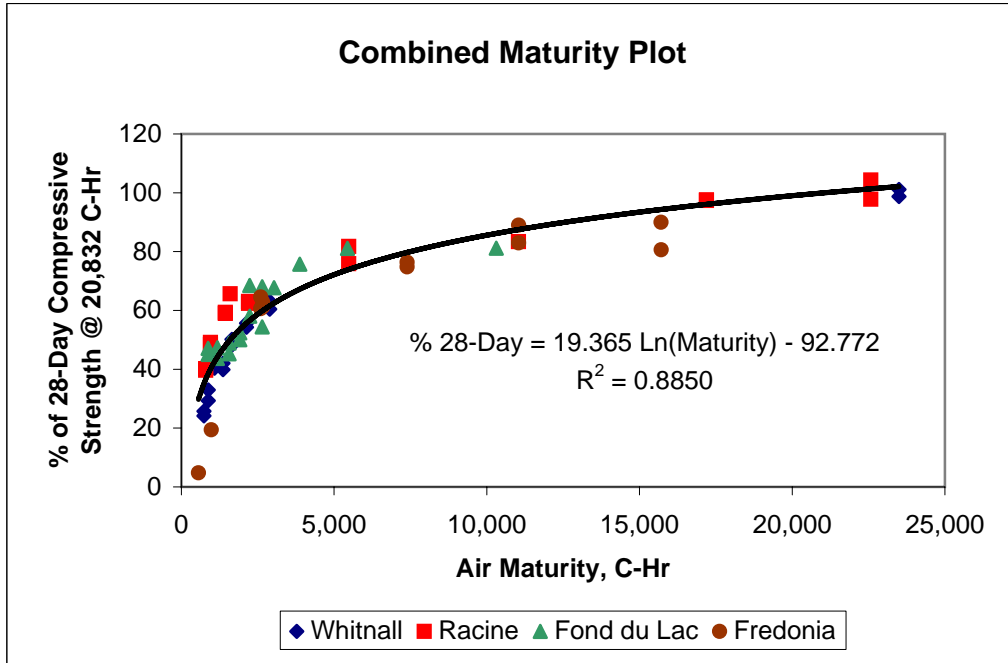


Figure 3.2.8: Combined Maturity Plot Using Air Temperatures

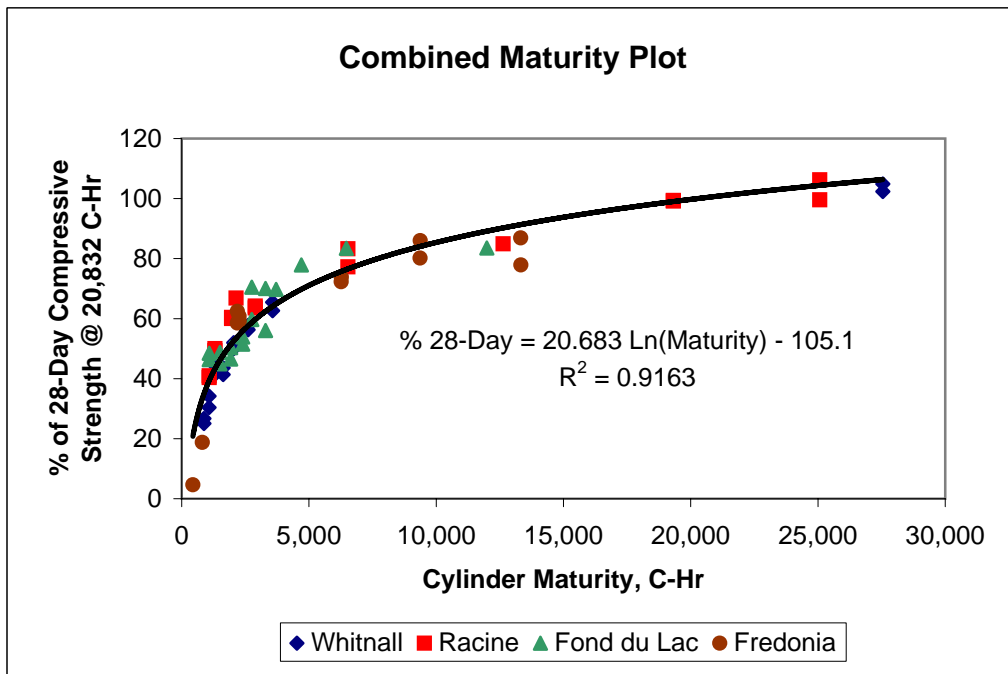


Figure 3.2.9: Combined Maturity Plot Using Bagged Cylinder Temperatures

As shown, all project data come together to form a single trend line even though they each have very different 28-Day strengths. Better agreement (higher R^2) is noted for the trend line using bagged cylinder maturity readings, which are essentially equal to mainline pavement maturity readings.

The trend lines developed for each project were also used to estimate respective 7-day compressive strengths based on standard laboratory curing conditions, which equates to a maturity value of 5,208 C-Hr [$7 \times 24 \times (21 + 10) = 5,208$]. For each project, the measured compressive strengths and estimated 7-Day strengths were used to compute the %7-Day Strength. These values were then plotted versus the recorded air and bagged cylinder maturity values as shown in Figures 3.2.10 and 3.2.11. As indicated, all project data again come together to form a single trend line even though they each have very different 28-Day strengths. Better agreement (higher R^2) is noted for the %7-Day trend lines as compared to the %28-Day trend lines and for bagged cylinder maturity values as compared to air maturity values.

Figures 3.2.8 through 3.2.11 illustrate the value of the maturity concept for predicting concrete strength at early ages based on 28-Day or 7-Day compression strengths measured in the lab. For practical use, approved mix designs can be used to establish representative 7-Day or 28-Day compressive strengths. Target strength requirements can then be used to compute the desired %7-Day or %28-Day strength and the required maturity value. Bagged cylinder and/or pavement temperature readings can then be used to establish cumulative maturity values, which can be used to provide better indications of when the pavement has reached its desired strength. Confirmatory compression strength tests can then be conducted for verification.

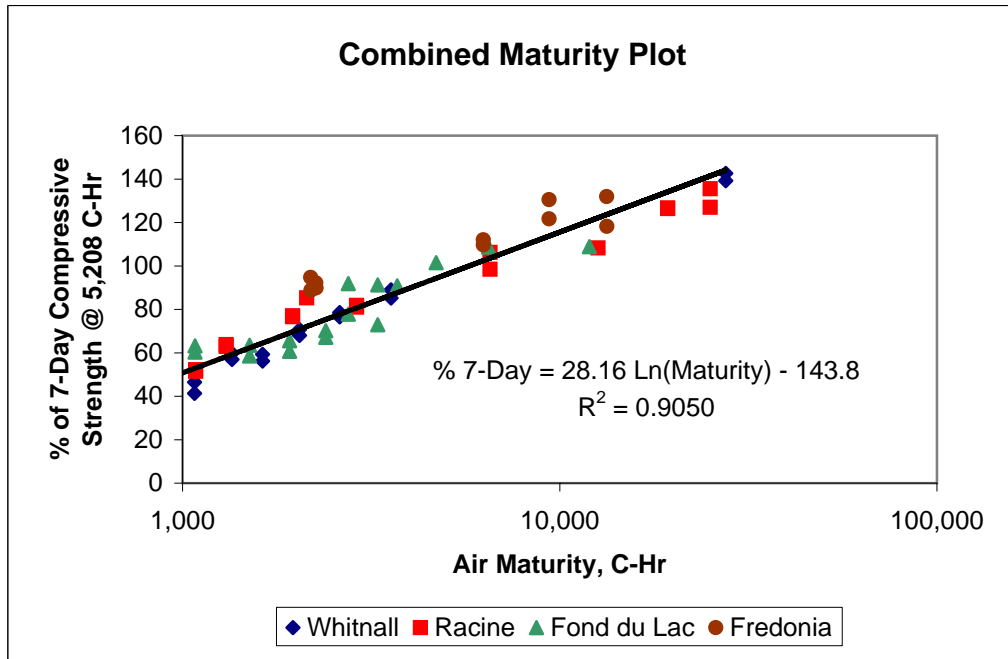


Figure 3.2.10: Combined Maturity Plot Using Air Temperatures

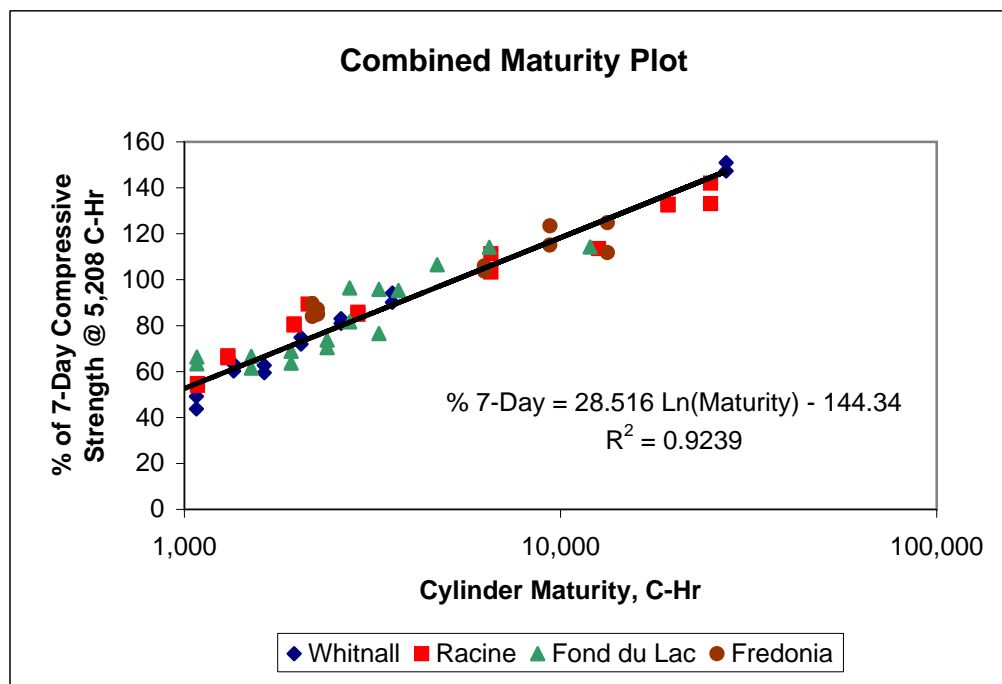


Figure 3.2.11: Combined Maturity Plot Using Bagged Cylinder Temperatures

3.3 Flexural Testing

Third-point loading tests were used to determine the flexural strength of 6in x 6in x 21in cast beam specimens using a portable beam tester. Figure 3.3.1 provides a photo of this equipment. The primary focus of this testing was to develop/validate relations for predicting early age flexural strength from standard compressive strength tests.

For normal weight concretes, a number of relations between flexural and compressive strengths have been proposed as indicated by the following:

$$f'_r / f'_c = 0.11 \text{ to } 0.23 \quad \text{Eq. 3.2}$$

$$f'_r = 8 (f'_c)^{1/2} \text{ to } 10 (f'_c)^{1/2} \quad \text{Eq. 3.3}$$

$$f'_r = 2.3 (f'_c)^{2/3} \quad \text{Eq. 3.4}$$

Figures 3.3.2 through 3.3.4 illustrate the results of comparative flexural and compressive strengths obtained from all projects included in this research using the general form of the relations described by Eqns. 3.2 through 3.4 (i.e., linear with zero intercept). The combined data for this project agree with each equation form, with the highest correlation to the $(f'_c)^{2/3}$ function (Figure 3.3.4). The comparative strength data was also analyzed based on coarse aggregate type. The following relations, based on the limited project data, suggest that a slightly higher flexural strength (assuming equal compressive strength) may be anticipated for mixtures utilizing gravel coarse aggregates.

All Data:	$f'_r = 2.344 (f'_c)^{2/3}$	$R^2=0.8756$	Eq. 3.5
-----------	-----------------------------	--------------	---------

Gravels (Fredonia, Whitnall)	$f'_r = 2.381 (f'_c)^{2/3}$	$R^2=0.8675$	Eq. 3.6
------------------------------	-----------------------------	--------------	---------

Limestone (Racine, Fond du Lac):	$f'_r = 2.303 (f'_c)^{2/3}$	$R^2=0.8941$	Eq. 3.7
----------------------------------	-----------------------------	--------------	---------



Figure 3.3.1: Portable Beam Tester

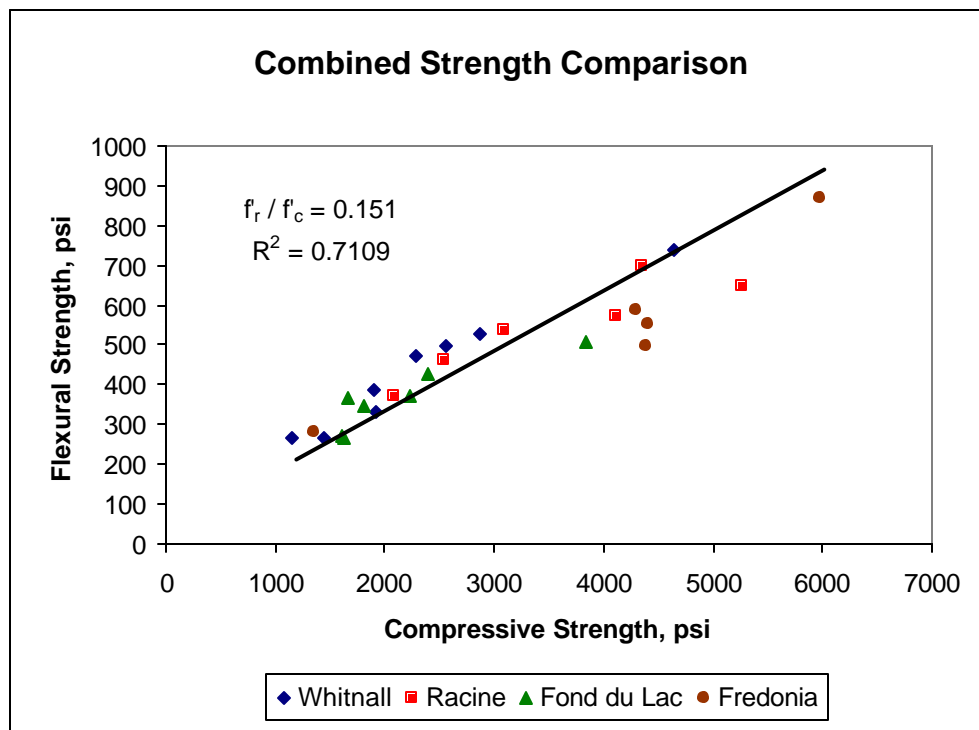


Figure 3.3.2: Comparative Plot of Flexural vs Compressive Strength

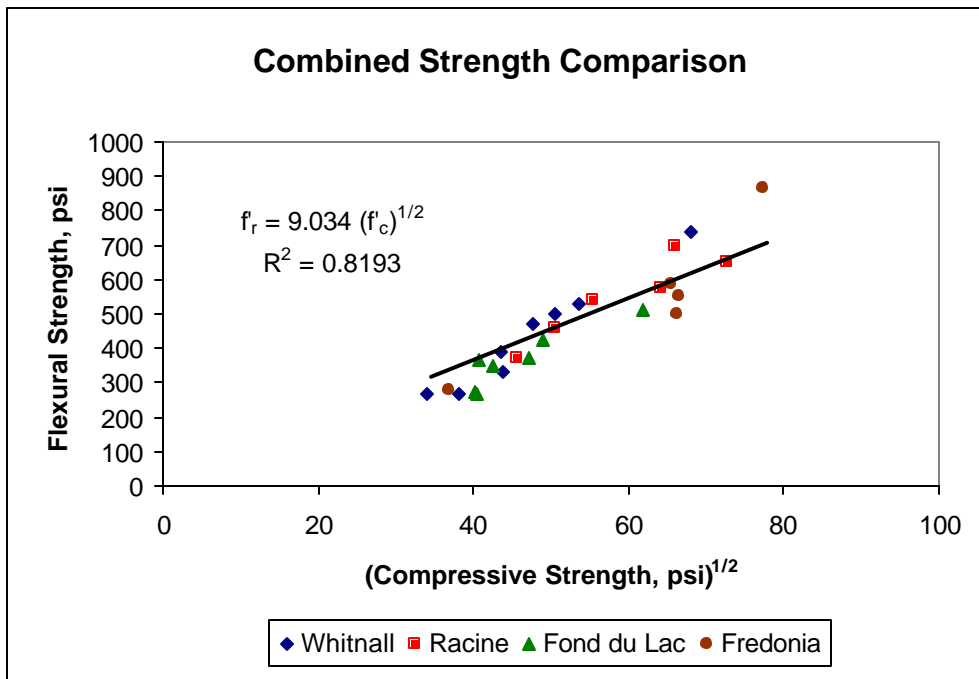


Figure 3.3.3: Comparative Plot of Flexural vs Compressive Strength

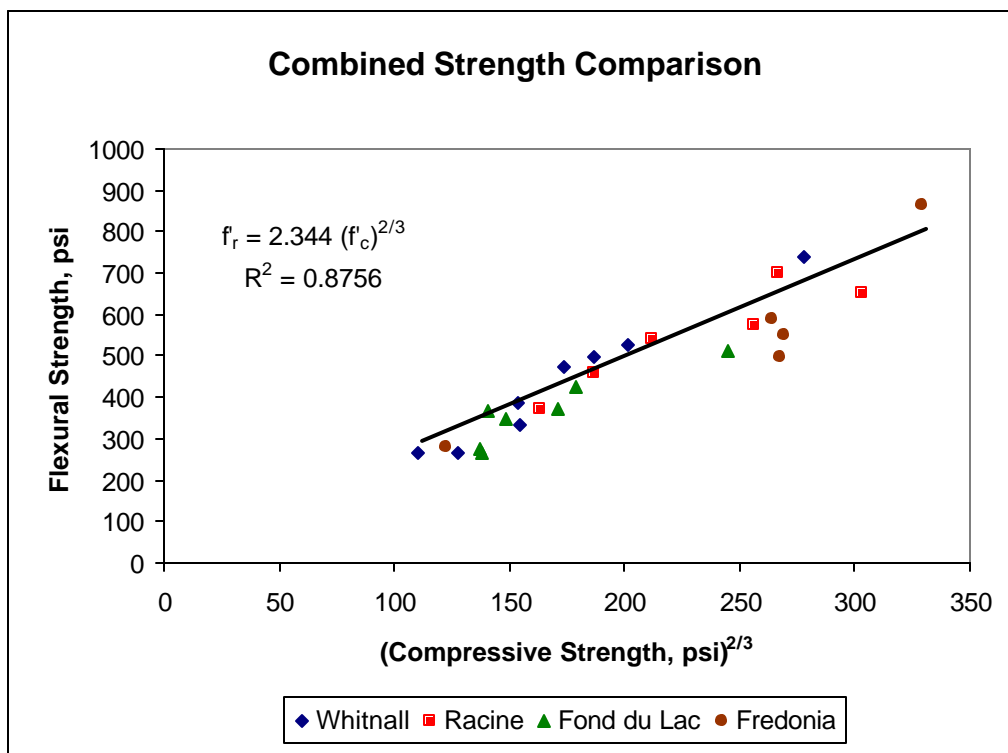


Figure 3.3.4: Comparative Plot of Flexural vs Compressive Strength

3.4 Exposed Dowel Specimens

Exposed dowel loading tests were conducted to determine the impacts of early-age loadings. Specimens were cast during paving using materials (concrete and dowels) obtained from the paving contractor. The primary focus of this testing was to investigate the impacts of early-age loadings on the longer-term behavior of doweled joints. It was hypothesized that early-age loadings may result in dowel-concrete bearing stresses which exceed allowable values (as computed by Eq 1.23), potentially reducing the load transfer capacity of the joint and compromising long-term pavement performance. Distress of this type would likely go unnoticed during construction as deflection testing is not part of acceptance criteria and no associated surface cracking may be present to warrant corrective measures.

Based on the results of the bearing stress analysis presented in Chapter 1, a test sequence which included 5 cycles of a 2,000 lb load positioned approximately mid-length of the exposed dowel section was deemed appropriate. Test loads were applied using a 5-kip load ram coupled to the hand pump of the portable beam tester. Randomly selected specimens were targeted for testing during early-age strength gain, as quantified by measured cylinder compression strengths in the range of 2,000 to 3,000 psi. After completion of the test loadings, the exposed dowel specimens were then allowed to field cure to 28-days. After full curing, the dowels were reloaded with the dowel displacement at the concrete interface recorded during loading.

3.4.1 STH 57 - Fredonia

During paving operations on STH 57 - Fredonia, exposed dowel specimens were cast in a wooden mold fabricated at Marquette University which allowed for the group casting of

seven 6in x 6in x 24 inch concrete specimens, with dowels positioned at mid-height of the 6in x 6 in face and embedded in the concrete for half of their length. Figure 3.4.1 provides a photo of an exposed dowel specimen positioned for initial load testing.

Initial testing of the STH 57 - Fredonia exposed dowel bar specimens was conducted during the first weekend after paving in conjunction with modulus of rupture testing. As discussed in Section 3.2.1, compression testing was not conducted during this first weekend due to low strength values measured up to 2 days after placement. Because of the portability of the flexural and exposed dowel testing equipment, it was decided to conduct these two tests over the weekend and return to standard comparative testing (compression, flexural, exposed dowel) during the following week when compression strengths were expected in the range of 2,000 to 3,000 psi. Randomly selected beam and exposed dowel specimens (2 each) were transported to the residence of a Marquette staff member and tested at ages of 71.5 and 95 hours.

During testing of the first exposed dowel specimen ($f'_r = 400$ psi) initial cracking was observed at a load of 900 lb and complete failure occurred at 1,800 lb. During testing of the second specimen ($f'_r = 440$ psi) initial cracking was observed at a load of 1,800 lb and complete failure occurred at 2,000 lb. The typical cracking pattern of both specimen failures is shown in Figure 3.4.2. As shown, this cracking pattern is similar to that observed along I-90/94 near Wisconsin Dells, which is the subject of current extensive study.



Figure 3.4.1: 6x6x24 Exposed Dowel Test Specimen Prepared for Initial Testing



Figure 3.4.2: Cracked 6x6x24 Exposed Dowel Specimen

A third exposed dowel specimen was tested in conjunction with compression and flexural testing at an age of 122 hours after placement. Average compression and flexural strengths were measured at 4,353 and 500 psi, respectively, at the time of exposed dowel bar loading. No cracking was observed in this specimen after the application of the five, 2,000 lb dowel loads. At the time of this testing, it was apparent that the early-age target compressive strength window of 2,000 to 3,000 had unexpectedly closed. Two additional exposed dowel specimens were subsequently tested after 170 hours of curing to provide additional informational data.

Using compression and flexural strength results for this mix, the following mix specific correlation equation was developed:

$$f'_r = 2.248 f'_c^{2/3} \quad R^2 = 0.8365 \quad \text{Eq. 3.8}$$

Based on measured flexural strengths of 400 and 440 psi at 71.5 and 95 hours, respectively, compression strengths at the time of initial exposed dowel bar testing were back-estimated at 3,559 and 4,106 psi. As these values are well in excess of the required opening strength of 3,000 psi, the specimen failures noted during testing were deemed to be the result of insufficient material cover on the dowels. Subsequent exposed dowel bar specimens were fabricated using a face height equal to the pavement thickness, a face width of 12 in, and a depth of 12 in. Figure 3.4.3 provides a photo of a test specimen constructed with these modified dimensions.

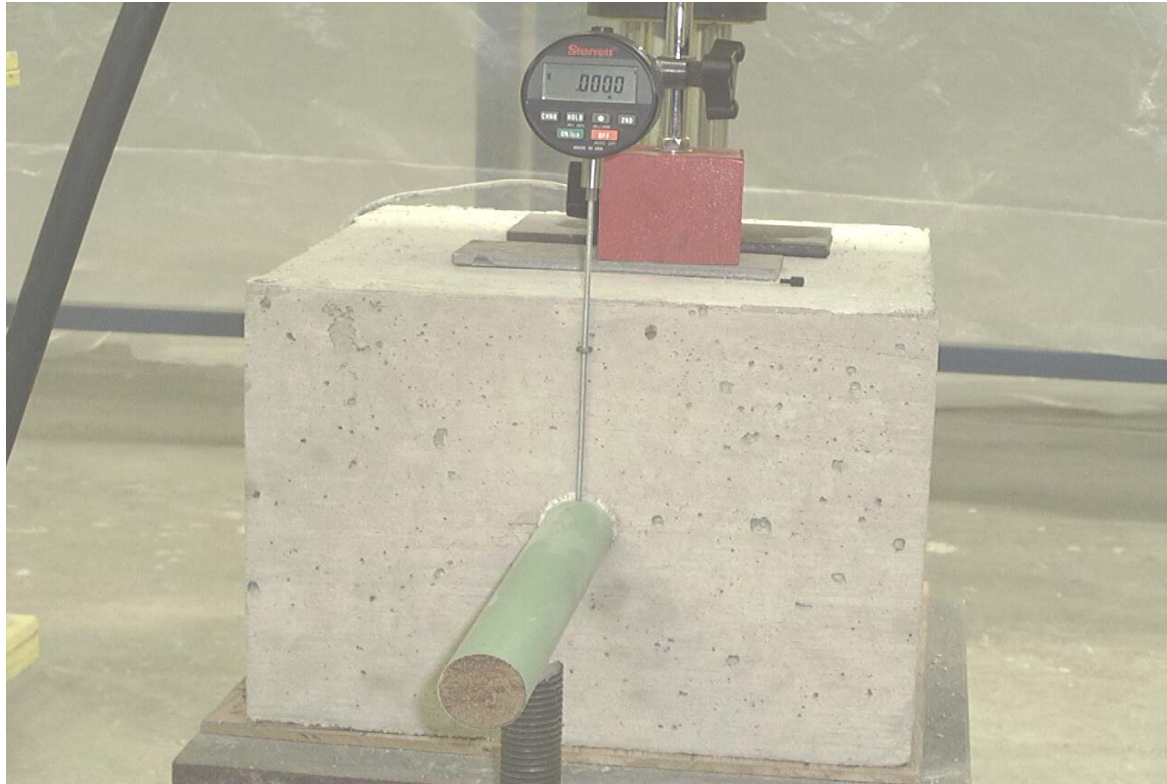


Fig 3.4.3 9x12x12 Exposed Dowel Specimen

Five additional 9in x 12in x 12in exposed dowel bar specimens were fabricated using representative paving materials transported to, and mixed at Marquette University. Initial dowel bar loadings were conducted at compressive strengths ranging from 1,500 to 3,000 psi and no specimen failure occurred during these early-age tests. These results indicate that the specimen failures during the initial test series at higher compressive strengths were due to inadequate specimen size. Subsequent dowel testing was conducted after 28 days of curing for each specimen. Table 3.4.1 provides pertinent data on all initial exposed dowel bar testing completed for the STH 57 - Fredonia project.

Table 3.4.1: STH 57 Exposed Dowel Bar Data

Specimen ID	Flexural Strength ⁽¹⁾	Compressive Strength ⁽²⁾	Comment
SP6	400	3559 ⁽³⁾	Initial cracking at 900 lb (1 st load) Failure at 2,000 lb (1 st load)
SP3	440	4106 ⁽³⁾	Initial cracking at 1800 lb (1 st load) Failure at 2,000 lb (5 th load)
SP2	500	4353	Failure after 5 th 2,000 lb loads
SP4	553	4545	No cracking observed
SP5	553	4545	Initial cracking at 1620 lb (3 rd load) No failure after 5 th 2,000 lb loads
SP1	867	5981	No cracking observed
SP8	867	5981	No cracking observed
D1	345 ⁽⁴⁾	1900	No cracking observed
D2	345 ⁽⁴⁾	1900	No cracking observed
D3	377 ⁽⁴⁾	2175	No cracking observed
D4	468 ⁽⁴⁾	3000	No cracking observed
D5	295 ⁽⁴⁾	1500	No cracking observed

⁽¹⁾ Flexural strength determined on companion 6x6x21 beam specimens

⁽²⁾ Compressive strength determined on companion 6x12 cylinders

⁽³⁾ Compressive strength estimated from flexural strength

⁽⁴⁾ Flexural strength estimated from compressive strength

Figures 3.4.4 and 3.4.5 provide dowel-PCC interface deflections versus load for the tests conducted after 28 days of curing. Legend values indicate specimen designation and compressive strength at original loading (in parenthesis). Dowel deflection testing on the uncracked 6x6x24 specimens, illustrated in Figure 3.4.4, provide erratic results with specimen SP8, which had the highest compressive strength at original loading, showing the

highest deflection response at 28 days. Subsequent testing on the 9x12x12 specimens, illustrated in Figure 3.4.5, indicate generally increasing deflection for specimens originally loaded at lower compressive strengths. Again, however, there is erratic behavior in the trends with specimen D4 (highest strength at initial loading) having higher deflections than specimens D2 and D3, which had substantially lower strengths at initial loading. No interfacial cracking was observed for any of these test specimens after the completion of dowel deflection testing.

3.4.2 South Whitnall Avenue - Cudahy

Five exposed dowel bar specimens were fabricated during placement using a specimen size of 10 in x 12 in x 12 in. Based on the results observed during STH 57 - Fredonia testing, the target strength window was expanded to include lower early age strengths. Table 3.4.2 provides relevant specimen data for S Whitnall Avenue specimens.

Table 3.4.2 S Whitnall Avenue Exposed Dowel Bar Data

Specimen ID	Flexural Strength ⁽¹⁾	Compressive Strength ⁽²⁾	Comment
W1	267	1158	No cracking observed
W2	267	1446	No cracking observed
W3	333	1922	No cracking observed
W4	473	2284	No cracking observed
W5	527	2870	No cracking observed

⁽¹⁾ Flexural strength determined on companion 6x6x21 beam specimens

⁽²⁾ Compressive strength determined on companion 4x8 cylinders

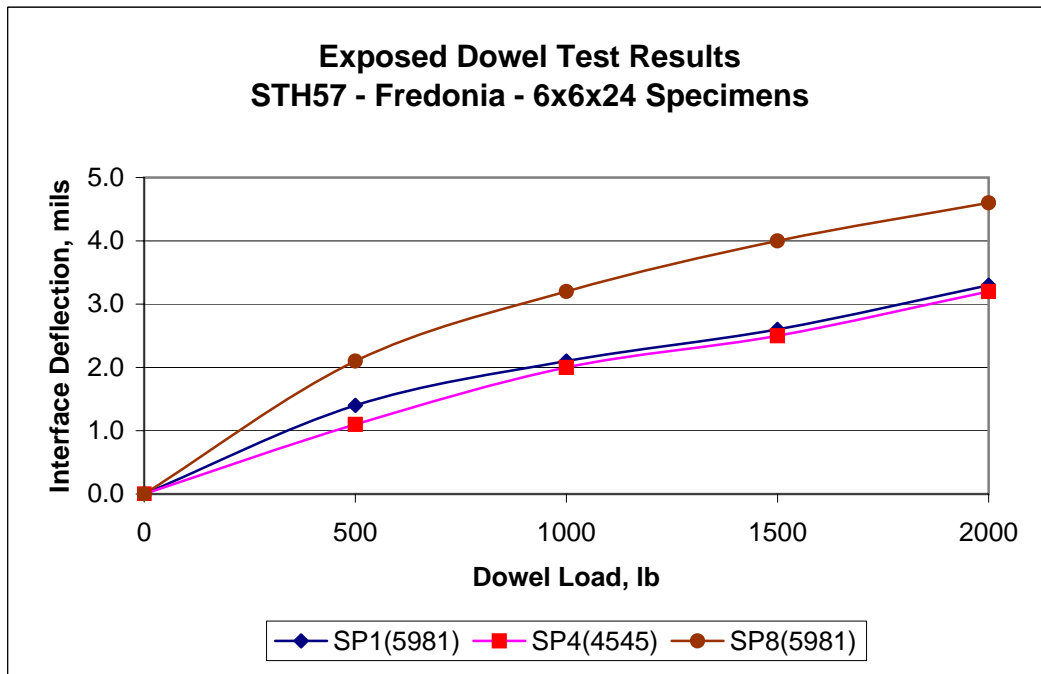


Figure 3.4.4: Exposed Dowel Deflection Results - STH 57 - Fredonia

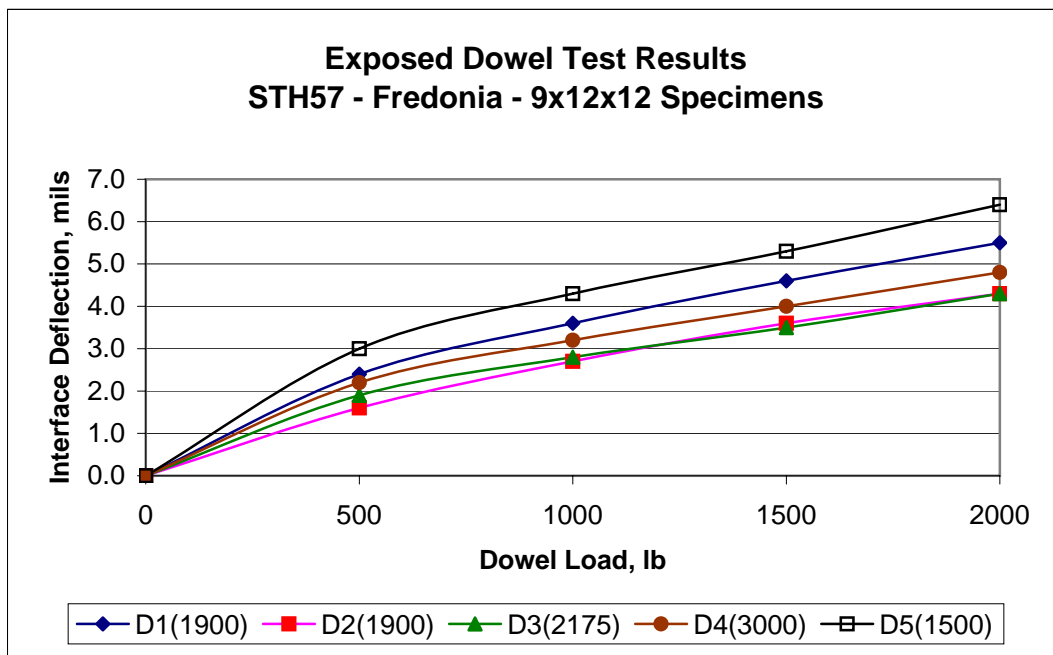


Figure 3.4.5: Exposed Dowel Deflection Results - STH 57 - Fredonia

Figure 3.4.6 provides dowel-PCC interface deflections versus dowel load for all tests conducted after 28 days of curing. As shown, interface deflections generally increase with decreasing strength at initial loading, but again there is erratic behavior with specimen W4 having deflections similar to those measured for specimens W1 and W2, each of which had significantly lower compressive strengths at initial loading.

3.4.3 STH 32 - Racine

Four exposed dowel bar specimens were fabricated during placement using a specimen size of 10 in x 12 in x 12 in. Table 3.4.3 provides relevant data for STH 32 - Racine specimens.

Table 3.4.3 STH 32 - Racine Exposed Dowel Bar Data

Specimen ID	Flexural Strength ⁽¹⁾	Compressive Strength ⁽²⁾	Comment
R1	373	2082	No cracking observed
R2	460	2544	No cracking observed
R3	540	3084	No cracking observed
R4	540	3084	No cracking observed

⁽¹⁾ Flexural strength determined on companion 6x6x21 beam specimens

⁽²⁾ Compressive strength determined on companion 4x8 cylinders

Figure 3.4.7 provides dowel-PCC interface deflections versus dowel load for all tests conducted after 28 days of curing. As shown, interface deflections show erratic behavior with specimen R3 (highest strength at initial loading) having deflections similar to those measured for specimen R1 (lowest strength at initial loading).

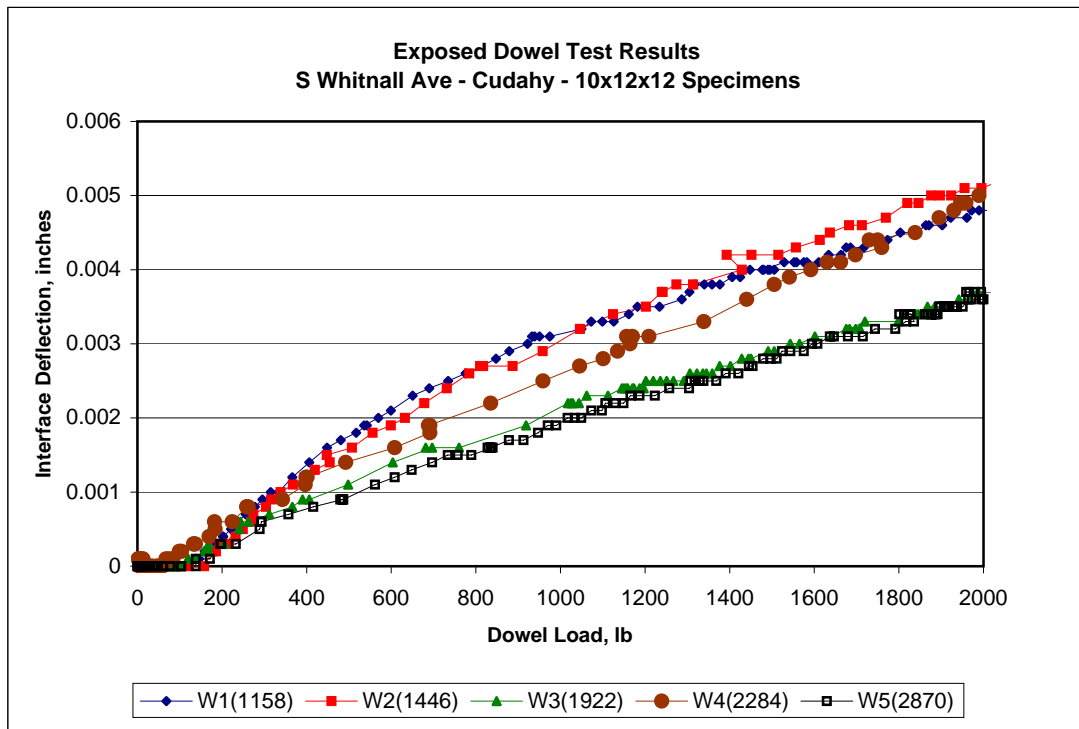


Figure 3.4.6: Exposed Dowel Deflection Results - S Whitnall ave - Cudahy

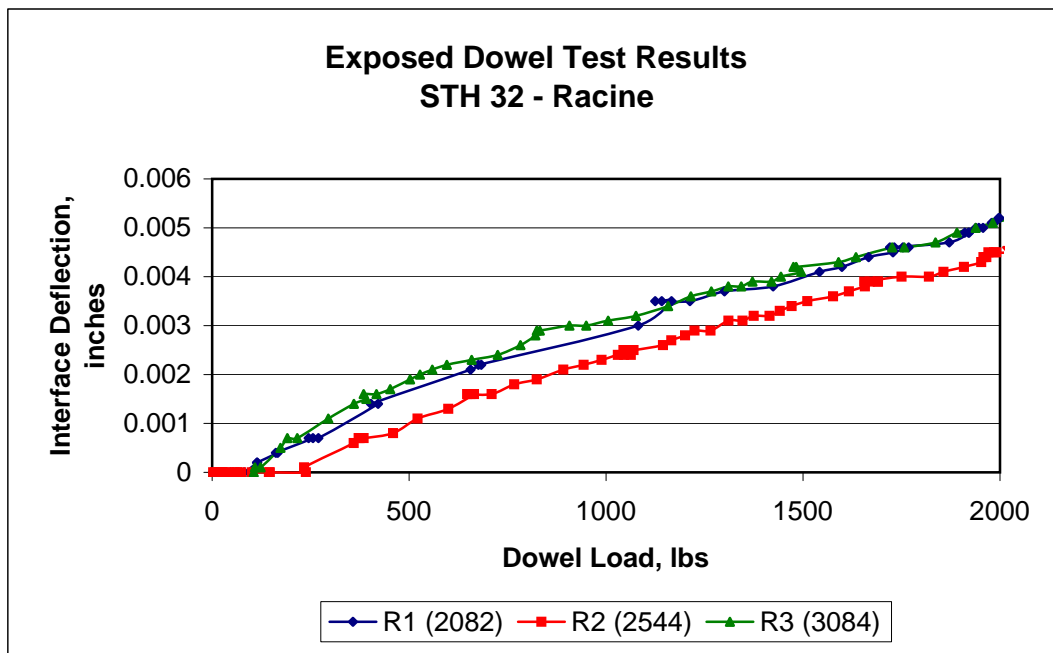


Figure 3.4.7: Exposed Dowel Deflection Results - STH 32 - Racine

3.4.4 STH 23 - Fond du Lac

Five exposed dowel bar specimens were fabricated during placement using a specimen size of 10 in x 12 in x 12 in. Table 3.4.4 provides relevant data for STH 23 - Fond du Lac specimens. Figure 3.4.8 provides dowel-PCC interface deflections versus dowel load for all tests conducted after 28 days of curing.

Table 3.4.4 STH 23 - Fond du Lac Exposed Dowel Bar Data

Specimen ID	Flexural Strength ⁽¹⁾	Compressive Strength ⁽²⁾	Comment
F1	267	1628	No cracking observed
F2	373	2235	No cracking observed
F3	427	2394	No cracking observed
F4	452 ⁽³⁾	2675	No cracking observed
F5	473 ⁽³⁾	2869	No cracking observed

⁽¹⁾ Flexural strength determined on companion 6x6x21 beam specimens

⁽²⁾ Compressive strength determined on companion 4x8 cylinders

⁽³⁾ Flexural strength estimated from compressive strength

As shown in Figure 3.4.8, interface deflections show erratic behavior with specimen F3 (middle strength at initial loading) having the greatest deflections and specimen F5 (highest strength at initial testing) having deflection results similar to those measured for specimen F1 (lowest strength at initial loading).

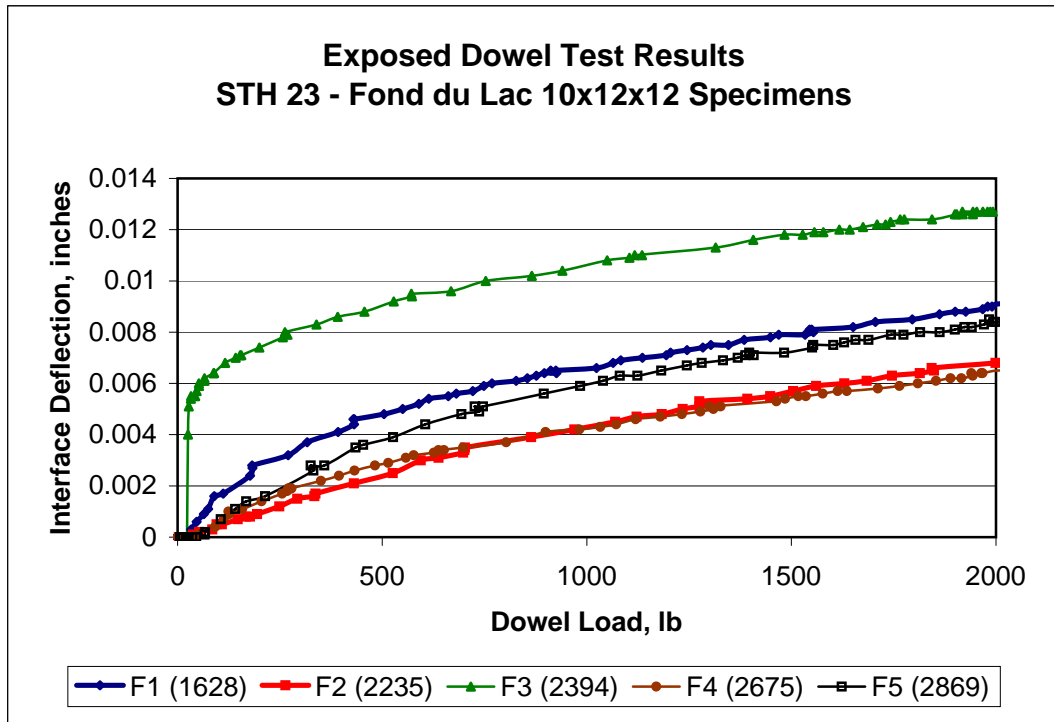


Figure 3.4.8: Exposed Dowel Deflection Results - STH 23 - Fond du Lac

3.5 Summary of Laboratory Testing

This chapter has provided the results of strength test conducted on various specimens fabricated from sampled paving materials. Good correlations between measured cylinder compressive strengths and computed maturity values were developed and are consistent with those reported in the literature. These correlations provide a useful means for estimating early age strength gain based on 7-Day or 28-Day laboratory test results and may be used to determine when required strength testing should be performed to ensure a specified minimum compressive strength has been attained.

Good correlations were also developed between the flexural and compressive strength of fabricated specimens. These correlations provide a useful means for predicting flexural strength based on simple cylinder strength testing at any age up to 28 days. The flexural strength of the PCC is directly related to the fatigue resistance of the slab to load induced longitudinal and transverse cracking.

Generally poor correlations were observed from the results of the exposed dowel bar load tests. These tests were envisioned to provide a useful indicator for minimum strength requirements to guard against PCC compression failures in the dowel embedment zone due to early-age loading. Based on the tests performed at various early-age strengths, no evidence of compression zone failures were observed. Furthermore, relations between PCC-dowel interface deflections and early-age strength at initial loading were poorly defined. More research in this area is needed if practical guidelines for test protocol and acceptance criteria are desired.

CHAPTER 4

SUMMARY AND RECOMMENDATIONS

This report presents the results of a detailed stress analysis and field and laboratory test program which investigated the early-age strength gain for selected PCC paving mixtures used in Wisconsin as well as the effects of early-age loading on doweled pavement joints. A detailed stress analysis is presented which provides an easy-to-use procedure for predicting critical dowel-PCC interface stresses. These stresses may be used in conjunction with allowable bearing stresses to establish minimum compressive strength requirements for opening to traffic based on pavement design parameters, including PCC, base, subgrade and dowel material properties.

Materials sampled from four Wisconsin paving projects were used to fabricate cylinder, beam and exposed dowel specimens. Multi-depth temperature probes were also installed in the mainline pavement and test cylinders to obtain maturity readings up to 28 days after placement. Cylinder compression strength data were used in conjunction with maturity values to validate correlations between compressive strength and PCC maturity. Specific equations for predicting early-age PCC compressive strength from 7-Day or 28-Day laboratory test results were developed for the tested Wisconsin mixtures based on maturity readings. These equations provide a practical means for establishing appropriate times for quality assurance testing. The best correlation was observed for estimating the %7-Day early-age strength based on maturity readings of field-cured bagged cylinders.

Comparative cylinder compressive and beam flexural strength tests were used to validate relations between these two important strength measures. These equations provide a practical means for estimating the early-age PCC flexural strength based on simple

cylinder compression tests. Using data from the four Wisconsin mixtures tested at ages up to 28 days after placement, the best correlation was observed between flexural strength and compressive strength raised to the $2/3$ power.

Exposed dowel load and deflection tests were used to investigate the effects of early-age loading on the PCC immediately surrounding the dowel. These tests, conducted on specimens with early-age compressive strengths ranging from 1,158 to 3,000 psi, were envisioned to provide confirmatory readings of the detrimental effects of early-age loadings on the load transfer capacity of doweled PCC joints. However, the test results proved inconclusive with no apparent trends in the data. More research in this area is needed to develop appropriate testing protocol and practical guidelines for implementation.

Based on the research effort documented in this report, the following recommendations are provided:

- (1) For doweled PCC pavements using 1.25 inch dowels, the required minimum opening compressive strength requirement of 3,000 psi should be maintained to protect against excessive dowel-PCC bearing stresses under heavy truck loadings. Based on the current WisDOT specifications as detailed in Section 14-10-10 of the Facilities Development Manual, this would include all PCC pavements with constructed thickness of 9.5 inches or less.
- (2) For doweled PCC pavements using 1.50 inch dowels, minimum opening compressive strength requirements to protect against excessive dowel-PCC bearing stresses may be reduced based on key pavement design inputs including slab thickness and subgrade k-value. Based on the current WisDOT specifications as detailed in Section 14-10-10 of the Facilities Development Manual, this would include

all PCC pavements with a constructed thickness of 10 inches or greater. Minimum compressive ranging from 2,300 to 2,750 psi were found adequate for a 10 inch PCC slab resting on an a 6 inch aggregate based over subgrade k-values ranging from 200 to 50 psi/in, respectively.

(3) Maturity readings from bagged test cylinders, cured in the field alongside the mainline pavement, may be used to provide an indication of the strength gain of the pavement based on 7-Day or 28-Day laboratory strength measures. For practical implementation, the 7-Day laboratory strength measure may be more appropriate to allow for test cylinders to be cast with available paving materials combined at the specified PCC job-mix proportions.

REFERENCES

- Crovetti, J.A. (1994). "Evaluation of Jointed Concrete Pavement Systems Incorporating Open-Graded Permeable Bases," Ph.D. Dissertation, University of Illinois at Urbana-Champaign.
- Friberg, B. F. (1940). "Design of Dowels in Transverse Joints of Concrete Pavements," Transactions, ASCE. Volume 105.
- Guo H, J.A. Sherwood, and M.B. Snyder (1996). "Component Dowel-Bar Model for Load-Transfer Systems in PCC Pavements," Journal of Transportation Engineering, Vol. 121, pp. 289-298.
- Ioannides, A.M., and G.T. Korovesis (1992). "Analysis and Design of Doweled Slab-On-Grade Pavement Systems." Journal of Transportation Engineering, ASCE, Vol. 118, No. 6, New York, NY, pp. 745-768.
- Khazanovich, L., H.T. Yu, S. Rao, K. Galasova, E. Shats, and R. Jones. (2000). ISLAB2000—Finite Element Analysis Program for Rigid and Composite Pavements. User's Guide. Champaign, IL: ERES Consultants.
- Nishizawa, T., Fukuda, T., and Matsusino, S., A Refined Model of Dowel Joints for Concrete Pavement Using FEM, Proceedings of 4th International Conference on Concrete Pavement Design and Rehabilitation, Purdue University, pp.735-745, 1989
- Timoshenko, S. and J.M. Lessels, "Applied Elasticity", Westinghouse Technical Night School Press, Pennsylvania, 1925.